LA-7616-PR

Progress Report

Nuclear Safeguards Research and Development

Program Status Report

May—August 1978

University of California

LOS ALAMOS SCIENTIFIC LABORATORY

Post Office Box 1663 Los Alamos, New Mexico 87545

The four most recent reports in this series, unclassified, are LA-6849-PR, LA-7030-PR, LA-7211-PR, and LA-7439-PR.

This work was supported by the US Department of Energy, Office of Safeguards and Security.

LA-7616-PR
Progress Report
UC-15
Issued: April 1979

Nuclear Safeguards Research and Development

Program Status Report

May—August 1978

Samuel D. Gardner, Editor

Manuscript completed: December 1978
Issued: April 1979

NUCLEAR SAFEGUARDS RESEARCH AND DEVELOPMENT

Program Status Report

May—August 1978

Samuel D. Gardner, Editor

ABSTRACT

This report presents the status of the Nuclear Safeguards Research and Development program pursued by LASL Safeguards Groups Q-1, Q-2, Q-3, and Q-4. Topics covered include nondestructive assay technology development and applications, international safeguards, perimeter safeguards and surveillance, concepts and subsystems development (e.g., DYMAC program), integrated safeguards systems, training courses, and technology transfer.

Salient features of the program and technical progress during the current reporting period are outlined in the Executive Summary.

CONTENTS

NUCLEAR SAFEGUARDS RESEARCH AND DEVELOPMENT

EXECUTIVE SUMMARY

G. Robert Keepin
Associate Division Leader for Safeguards Affairs

and

William H. Chambers
Associate Division Leader for Safeguards Operations

The Nuclear Safeguards Program at LASL encompasses four technical groups: Q-1, Safeguards Technology, International Safeguards and Training; Q-2, Detection, Surveillance, Verification, and Recovery; Q-3, Safeguards Subsystems Development and Evaluation; and Q-4, Integrated Safeguards Systems and Technology Transfer. This program status report is divided into four parts, one for each of the safeguards technical groups; each part begins with a brief overview of the group's function and major programmatic efforts. Although the work of the four safeguards groups is closely interrelated, these program status reports are structured so that each group contribution can, if necessary, be read independently of the others.

In an ongoing program of improved nondestructive methods for verifying spent fuel burnup, we are evaluating correlations of spent fuel gamma-ray emission with reactor history and fuel cooling periods. The method is being developed using measurements on spent fuel at LASL's Omega West Reactor (a materials testing reactor). When completed, it will be the basis of a similar analysis of spent fuel from boiling water and pressurized water reactors. A statistical analysis of previous measurements from the Omega West Reactor shows that certain combinations of gamma-ray line emissions correlate well with burnup and cooling times. Further data, taken from the Big Rock Point Nuclear Plant (a boiling water reactor) and the Zion Generating Station (a pressurized water reactor), are being analyzed. In an associated effort, we are investigating techniques for precise and rapid measurements of gamma-ray and neutron activity along the axis of fuel rods. Successful use of a gas chamber incorporating multiwire gas counter techniques promises a significant reduction in time required to measure axial profiles.

As a part of neutron-assay technique development, data handling for the ^{252}Cf Shuffler was automated by integrating it with an LSI-11 microcomputer system. In addition, the high-level neutron coincidence counter technology was transferred to commercial instrumentation suppliers, as evidenced by the purchase request of nine of the systems for IAEA and Laboratory use. The potential advantages of methane over ^{4}He for use in proportional counters led to an evaluation of a methane proportional counter as a fast-neutron detector. The evaluation showed that in a high gamma background the methane neutron counting efficiency is about four times that of ^{4}He for pressures up to 5 atm. However, above this pressure the response (per unit pressure) falls off. This high-pressure saturation is not yet completely understood. As a continuation of the study, a series of low-gamma background counting efficiency measurements is being made.

Under our program for improving gamma- and x-ray assay techniques, a method for uranium-solution assay by transmission-corrected x-ray fluorescence is being extended to low-concentration (<20 g/ℓ) plutonium or uranium solutions. The low counting rates in earlier work have been improved so that precisions of $<1\%$ were achieved in 500-s counting intervals for uranium concentrations of 1-20 g/ℓ. Further optimization of this technique is planned. Raygun, a "hands-off" computer code for rapid analysis of high-resolution gamma-ray spectra, is also being evaluated for its applicability to spent fuel data. Test runs with Zion and Big Rock Point spent fuel data are planned.

A number of instrumentation field tests were carried out, including calibration and testing of a Shuffler for the Savannah River Plant, testing of the earthquake resistance of another Shuffler for the Idaho Chemical Processing Plant, evaluation and calibration of neutron coincidence counters with IAEA personnel, and an evaluation of fuel-pin scanners for HEDL.

A proposed technique of combined neutron coincidence and singles measurements is being studied for use in a gas centrifuge plant to verify uranium enrichment of material in alumina traps. It was tested with well-characterized UF_6 samples and found to be generally suitable for alerting a safeguards inspector to high-enrichment uranium-fluorine compounds although it will not give a direct quantitative measure of enrichments above about 20%.

An extended study was begun on the effectiveness of vehicle SNM monitoring, centered around a test-bed gate monitor to be constructed on-site. The optimum configuration for the gamma and neutron detectors was established and the gate monitor was designed; construction is to start soon. In an assessment of commercial, hand-held SNM monitors, the effect of detector thickness on detection sensitivity was determined for two optional NaI(Tℓ) crystal thicknesses. In connection with safeguards for Sandia Laboratories' Fast Critical Assembly, we assisted in their acquisition of ^{3}He proportional counters, the design of a passive neutron detector for their personnel portal monitor, and in their evaluation of material pass-through monitors.

The tunnel neutron detector, proposed for large-vehicle portal monitoring at the CTF (Centrifuge Test Facility), has been evaluated experimentally in scale-model systems and with full-scale Monte Carlo calculations. The tunnel is to detect passive neutrons emitted from UF_6 in feed, tails, or product carried in cars, trucks, boxcars, or other carriers that exit via the CTF vehicle portal. Detailed measurements on scale-model systems indicate excellent sensitivity to UF_6 in large transport vehicles. Concurrent Monte Carlo calculations are in excellent agreement with the scale-model measurements.

Our DYMAC system has been keeping pace with the progressive occupation of the Plutonium Facility. CMB-11 had occupied ~50% of the facility at the end of August 1978, with DYMAC servicing all processing sections. The major activity during the May-August period was the installation of DYMAC instruments and software at the new facility. Included were thermal neutron counters, electronic balances, fast-neutron coincidence counters, pressure transducers, and segmented gamma scanners. We are also investigating bar-code labels for containers of radioactive materials. These labels are machine-readable and can significantly reduce the radiation exposure to individuals inventorying storage vaults. The DYMAC computer programming team has also made the material control system faster and more responsive. The computer has been squeezed for logical space, so the logical structure of the data base was reorganized and the applications program restructured to decrease response time. A second Eclipse C330 computer arriving in October will relieve the pressure on computer time.

At the request of the Arms Control and Disarmament Agency, we are looking at safeguards strategies for commercial-scale enrichment facilities that will use laser isotope separation methods. The study uses reference-facility designs developed in NASAP (Nonproliferation Alternative System Assessment Program). In another of a series of alternative fuel cycle studies, we are evaluating coconversion of coprocessed uranium-plutonium nitrate systems. Concept development for reprocessing thorium-uranium fuels is also being pursued; draft reports were prepared on materials management aspects of this fuel cycle and on applicable safeguards analytical techniques.

To get a clearer grasp of the realities and potentialities of international safeguards and nuclear proliferation, we initiated a study of international safeguards of a light water reactor fuel reprocessing plant. The baseline facility will be a combination of the AGNS (Allied-General Nuclear Services) reprocessing facility and a plutonium nitrate-to-oxide conversion plant designed by Savannah River. The study will be pursued jointly by the Los Alamos and Sandia Laboratories.

A method is being developed for identifying optimum diversion strategies, which will allow identification of worst-case detection probabilities, independent of the diversion method. A series of simulation modules for security characteristics were

developed and a decision framework established to analyze risks. A broad definition for operational reliability was developed that included areas affecting timeliness of job completion, such as software failures, operator error, and machine loading. System-reliability simulation and analysis applied to the DYMAC system in our Plutonium Facility showed it to be a robust system from a reliability viewpoint and amenable to upgrading for future growth, when and if justified.

The problem of obtaining improved estimates of in-process inventories in various types of fuel reprocessing contactors is being pursued with General Atomic and Clemson University. Their results will provide the technical base for our contactor model development.

In our continuing commitment to training and technology transfer, the LASL safeguards staff has trained, briefed, and transmitted technical design information and data to representatives from various US nuclear industry and contractor facilities, as well as domestic, foreign government, and international agencies.

PART I

SAFEGUARDS TECHNOLOGY, INTERNATIONAL SAFEGUARDS AND TRAINING

GROUP Q-1

Roddy B. Walton, Group Leader

H. O. Menlove, Alternate Group Leader

Group Q-1 is responsible for the development and application of a broad range of measurement techniques for the NDA (nondestructive assay) of fissionable materials in the many physical and chemical forms found in the nuclear fuel cycle. Specific applications of NDA technology currently under development by Group Q-1 include: plutonium process materials at DOE facilities, highly enriched uranium, enrichment process materials, and spent fuel reprocessing. Prototype instruments for these applications are developed, calibrated, and tested in operating plant environments. The Group Q-1 NDA technology program provides technical support to material control demonstration systems, such as DYMAC (dynamic materials control), and a base of measurement technology for integrated safeguards system studies.

To implement the transfer of NDA technology to various types of plants and facilities in the nuclear community, Group Q-1 is a major contributor to the DOE Safeguards and Technology Training Program, which is offered to safeguards inspectors (both domestic and international) and qualified government and industry personnel. Additional Q-1 efforts to facilitate technology transfer include briefing, consultations, and issuance of design documentation, operations manuals, interlaboratory assay comparisons, and consensus standards.

A major Q-1 effort is technical assistance to IAEA international safeguards. This effort includes development of portable NDA instrumentation to address specific inspection situations, as well as associated calibration and evaluation of this instrumentation, and personnel training.

I. SPENT FUEL ASSAY

A. Omega West Exercise (J. R. Phillips, S. T. Hsue, K. Kaieda, E. G. Medina, and T. R. Bement*)

Gamma-ray data obtained from September and January spent fuel measurements at the LASL (Los Alamos Scientific Laboratory) Omega West Reactor (a materials testing reactor) were analyzed to determine correlation between the declared burnup and declared cooling times and the selected nondestructively measured isotopic and ratio distributions. Fifty-three variables for the September exercise and 34 for the January exercise were investigated by simple correlation analysis, cluster analysis, and principal component analysis to determine which measured variables provided the most significant correlations with declared burnups and cooling times.

In previous gamma-ray techniques only one variable was used to estimate the correlations. However, cluster analysis indicated that the linear combination of two or three variables can predict the highest percentage of variation in each data set. The primary value of this analysis was the grouping of variables in clusters from which representatives could be selected on the basis of individual precisions. Similar combinations of variables appeared independently in each of the two data sets. We made stepwise regression analyses with these

*Group S-1.

TABLE I

NONDESTRUCTIVE MEASUREMENTS MADE AT BIG ROCK POINT NUCLEAR PLANT, MAY 15-26, 1978

Fuel Assembly	Declared Burnup (MWD/ton)	Discharge Date	Be(γ,n) Chamber	Fission Chamber	Gas Chamber	Germanium Detector
BRP-1	4 356	1-76	X	X	X	X
BRP-2	8 883	6-74		X	X	X
BRP-3	12 459	1-76	X		X	X
BRP-4	13 332	1-76		X	X	X
BRP-5	14 652	1-76	X		X	X
BRP-6	15 264	1-76		X	X	X
BRP-7	16 233	7-77	X		X	X
BRP-8	16 658	1-76	X		X	X
BRP-9	17 122	1-76		X	X	X
BRP-10	17 814	1-76	X		X	X
BRP-11	18 804	7-77	X	X	X	X

representatives to determine variation in burnup indicated by various data sets.

The principal component analysis technique identified the number of dimensions required to represent each data set geometrically. Although more than 30 variables were involved in each analysis, five or six of them could explain >99% of the variation. These results were based on small sample sizes of 10 fuel assemblies for September and 8 fuel assemblies for January. These analyses showed that linear combinations of ^{134}Cs (605 keV) and ^{134}Cs/^{137}Cs (605 keV/662 keV) explain >99% of the variation in ^{137}Cs activity for the September and the January exercises. A linear combination of two variables, ^{134}Cs/^{137}Cs (605 keV/662 keV) and ^{154}Eu/^{144}Pr (1275 keV/2186 keV), is a good predictor of cooling times. Together the two variables explain 79% of the variations in the September data and 95% of the variations in the January data.

A formal report will be issued after additional evaluation of these two sets of data is completed. These results will form the basis for evaluation of the BRP (Big Rock Point) and Zion data.

B. Big Rock Point Exercise (J. R. Phillips, S. T. Hsue, D. M. Lee, K. Kaieda, E. G. Medina, S. E. Beach, and J. K. Halbig)

Results from nondestructive gamma-ray and neutron measurements made on 11 BWR (boiling water reactor) assemblies having average burnups from 4356 to 18 804 MWD/ton are listed in Table I. From the four measurements we were able to define the relative axial profile of the irradiated assemblies (the germanium data were used to correlate the relationships between individual assemblies).

The assay of fuel assemblies requires two measurements: (1) relative axial burnup profile and (2) specific measurement of burnup. The relative axial profile is necessary not only to ensure that sections of fuel have not been removed but to generate a function for integrating the total exposure on the basis of one or two precise measurements at specified positions. We are investigating techniques to measure the axial profile quickly—techniques that can be coupled with more time-consuming burnup analyses at a few locations. The Be (γ,n)

chamber, fission chamber, and gas chamber are used principally for profile measurements. The germanium detector and fission chamber are being evaluated for the more precise measurements.

The Be(γ,n) detector consists of a small ^{235}U fission chamber encircled by (1) a beryllium annulus to produce photoneutrons and (2) a polyethylene annulus to thermalize the neutrons. Because the photoneutron threshold for beryllium is >1.66 MeV, the detector is sensitive only to high-energy gamma photons. Also, because the fission chamber is sensitive only to neutrons, the detector can operate in areas of high gamma-ray background.

For the fission chamber measurements, the relative neutron flux profiles were measured (in an unshielded chamber) as a function of axial position. Curium-242 and ^{244}Cm isotopes contribute most of the neutron fluxes measured in BWR assemblies.

The gas chamber, described more fully in Sec. I-E, provides a quick, precise method of measuring the relative axial profile of the gross gamma activity.

Complete gamma-ray spectra were collected at specified axial positions for correlation with the radiation found by the other three techniques. The specific gamma activities for all prominent gamma rays were calculated and will be analyzed to determine the correlations of specific isotopes and/or ratios with the declared burnup values and cooling times of the individual assemblies.

C. Zion Generating Station Exercise (J. R. Phillips, S. T. Hsue, D. M. Lee, K. Kaieda, S. E. Beach, J. K. Halbig, and E. Dermendjiev*)

Nondestructive measurements similar to those made for the BRP exercise are given in Table II for 14 irradiated PWR (pressurized water reactor) assemblies with declared burnups ranging from 16 604 to 32 185 MWD/ton. The CdTe detector (used for the Zion exercise but not for BRP) was operated in the current mode because the high

*IAEA participant.

TABLE II

NONDESTRUCTIVE MEASUREMENTS PERFORMED AT ZION GENERATING STATION, JUNE 12-21, 1978

Fuel Assembly	Declared Burnup (MWD/ton)	Discharge Date	Be(γ,n) Chamber	Fission Chamber	Gas Chamber	Germanium Detector	CdTe Detector
Z-1	16 604	3-5-76			X	X	X
Z-2	17 404	1-7-77	X	X	X	X	X
Z-3	17 776	3-5-76	X	X	X	X	X
Z-4	18 279	1-7-77	X	X		X	
Z-5	18 723	3-5-76			X	X	X
Z-6	19 826	1-7-77			X	X	
Z-7	19 913	1-7-77			X	X	X
Z-8	20 066	1-7-77	X	X		X	
Z-9	20 252	1-7-77	X	X		X	
Z-10	30 947	9-9-77			X	X	X
Z-11	31 850	9-9-77			X	X	X
Z-12	31 851	9-9-77	X	X	X	X	X
Z-13	32 094	9-9-77			X	X	X
Z-14	32 185	9-9-77	X	X	X	X	X

gamma activity precluded use of the pulse mode. Results were similar to those obtained with the gas chamber in the integration mode. Preliminary analysis of the results has begun.

D. Passive Neutron Assay of Spent Fuel Assemblies (S. T. Hsue, K. Kaieda, J. E. Stewart, and J. K. Halbig)

In Ref. 1, pp. 5-6, we reported a Monte Carlo calculation of passive neutron assay of a spent PWR assembly. We concluded that the neutron multiplication factor is constant as the burnups vary (between 13 000 to 27 000 MWD/MTU) and that the neutron counting can detect signals from the interior rows of fuel pins. Some results from two separate neutron measurements made at the BRP and Zion power plants are presented here.

At BRP, we measured the neutron response as the detector-to-assembly distance was increased. The detector, a fission chamber containing 58 mg ^{235}U deposit, was submerged in a tube at approximately the midplane of an assembly. The spent fuel assembly, BRP-10, has a declared burnup of 17 814 MWD/MTU and a cooling time of 2.5 yr. The results, together with the calculated values for thermal neutrons (6 to 9% precision), are shown in Fig. 1. For thermal neutrons, the measured diffusion length of 4.3 cm agrees with the calculation. In general, the passive thermal-neutron counting rate decreases by an order of magnitude when the detector-assembly distance is increased by 10 cm. In comparison, the ionization chamber signal decreases by a factor of 10 when the distance is increased by 30 cm; thus, the thermal-neutron detectors have a shorter range than the ionization chamber. We also conclude that the number of neutrons from the (γ,n) reaction on water (or other low-Z material in the pool) is negligible compared with that emitted from the spent fuel.

Next we tried to correlate the fission chamber counting rate at midassembly with the declared burnup of different assemblies. A cooling time correlation was not made. Figure 2 shows the correlation for five BRP assemblies; Fig. 3 shows the correlation for nine Zion assemblies. All the fission chamber counting rates are proportional to burnup raised to the 3.39 power—an agreement that is surprising because BRP is a BWR and Zion is a PWR and may have different actinide buildups. This agreement may be fortuitous, but the results indicate that passive neutron counting is a useful technique and can complement the gamma assay of spent fuel.

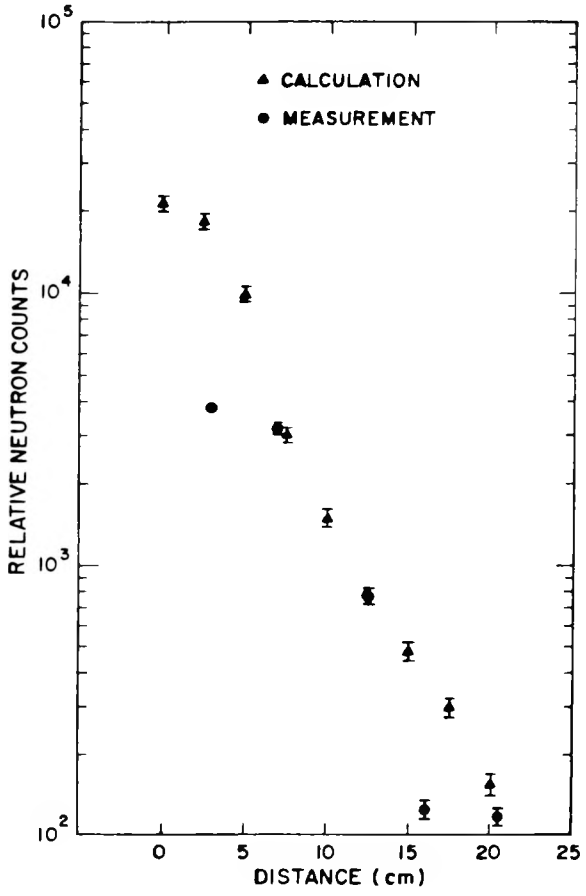

Fig. 1.
Comparison of measured and calculated relative thermal-neutron response as a function of increasing detector-to-assembly distance.

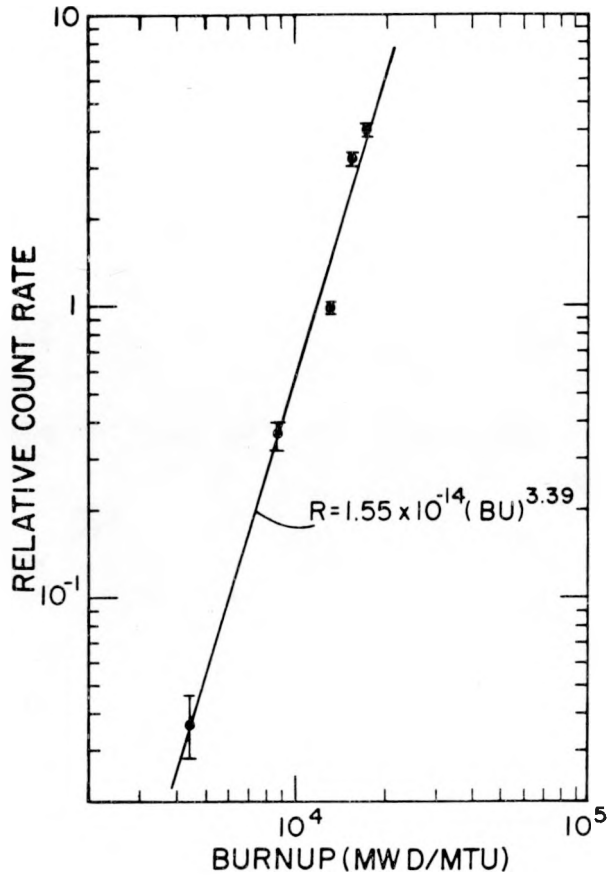

Fig. 2.
Relative fission chamber response vs burnup for five BRP reactor spent fuel assemblies.

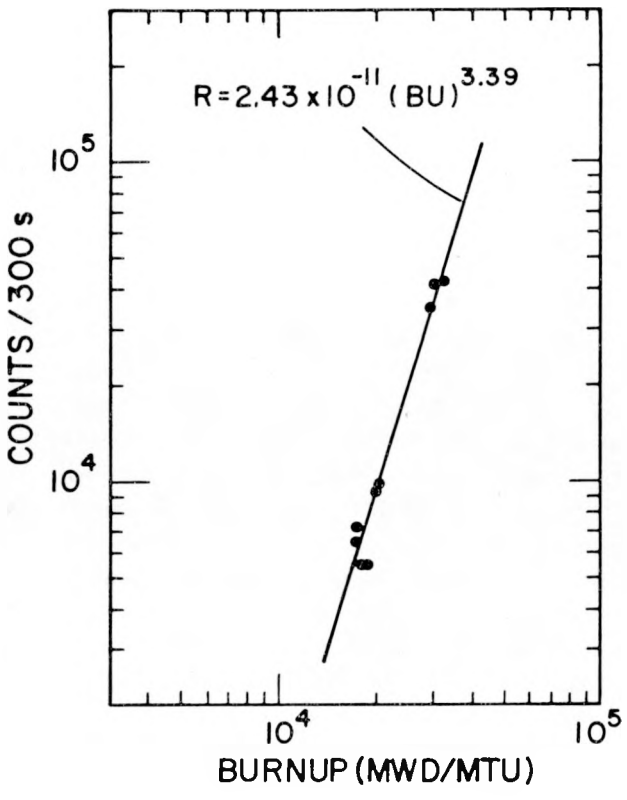

Fig. 3.
Relative fission chamber response vs burnup for nine Zion reactor spent fuel assemblies. Error bars are smaller than the data points.

E. Gas Chamber Techniques for Measuring Activity Profiles of Spent Fuel Assemblies (D. M. Lee, J. R. Phillips, S. T. Hsue, K. Kaieda, T. Van Lyssel, E. G. Medina, S. Beach, J. K. Halbig, and E. Dermendjiev*)

Measurement of the axial profile of irradiated fuel assemblies normally has been performed by scanning the assembly with an intrinsic germanium detector, collecting the fission-product gamma spectra, and analyzing the data. One hour or more is required for scanning each assembly, depending on the number of points taken for each profile. The gamma profiles obtained are proportional to the axial neutron flux $\phi_n(\vec{r})$ in the reactor; therefore each profile is proportional to the number of fissions that have occurred. The profiles most commonly used are the activity distributions of ^{137}Cs, $^{134}Cs/^{137}Cs$, and ^{144}Pr. Disadvantages of this method of measuring profiles include the need for a collimator for the germanium detector and the need for a way to move the fuel element past the collimator tube. Also, with the vast number of spent fuel assemblies in a typical spent fuel pond, a faster technique for obtaining axial profile measurements is highly desirable.

For many years, multiwire gas counter techniques have been used successfully at high-energy and medium-energy particle accelerator laboratories throughout the world for particle track or beam profile information.[2] The position sensitivity of these counters ranges from a few centimeters to a few tenths of a millimeter. Multiple wires permit two-dimensional information to be recorded without complicated mechanical scanning systems.[3] These

*IAEA participant.

counters employ both pulse counting and current-measurement techniques, the latter normally used in the ionization region. The simplicity and portability of these devices suggest their application to the rapid measurement of the axial gamma profile of irradiated fuel assemblies. Consequently, we examined PWR and BWR spent fuel assemblies by current-measurement techniques to take advantage of the high radiation fields associated with irradiated fuel assemblies.

The electronics for all of these measurements are shown in Fig. 4, which shows a gas chamber (current source) connected to a current-to-voltage amplifier, followed by a digital voltmeter. The system was designed to operate at the 100 x 10^{-12} A level, with a noise level of 1 x 10^{-12} A. Typical current levels obtained during the exercises varied from 10^{-9} A to 5 x 10^{-8} A, so electronics noise was not a significant problem.

A different detector design was used for each exercise mainly to maximize the signals. The gas chamber for the BWR exercise is shown in Fig. 5. The active area was 3.8 cm x 6.25 cm. The anode wires were 20-m gold-plated tungsten wire at a 1.25-cm wire-to-wire spacing. The voltage characteristic of this chamber is shown in Fig. 6. The plateau corresponds to the ionization region (gas gain = unity), with the proportional region extending beyond ~1000 V. The proportional region can be used when dose levels are low and electronic noise becomes a problem. In all cases the chamber was operated at 300 V (in the ionization mode). A typical profile measured by the gas chamber is shown in Fig. 7. Also plotted is the profile from a Be(γ,n) detector. The Be(γ,n) detector responds primarily to the axial distribution of ^{144}Pr and should be representative of the recent power profile distribution. The agreement is excellent. Because the gas chamber is an integrating device, it is sensitive to all of the fission-product gamma rays—those that are proportional to $\phi_n(\vec{r})$ and $\phi_n^2(\vec{r})$. Those gamma rays with the greatest yield that are proportional to $\phi_n(\vec{r})$ are ^{137}Cs, ^{95}Zr, ^{95}Nb, and ^{144}Pr and those gamma rays that are proportional to $\phi_n^2(\vec{r})$ are ^{134}Cs and ^{106}Ru. The excellent agreement in Fig. 7 indicates that the gas chamber is predominantly sensitive to gamma rays that are proportional to $\phi_n(\vec{r})$ and is supported by theoretical arguments in a private communication from P. Rinard.

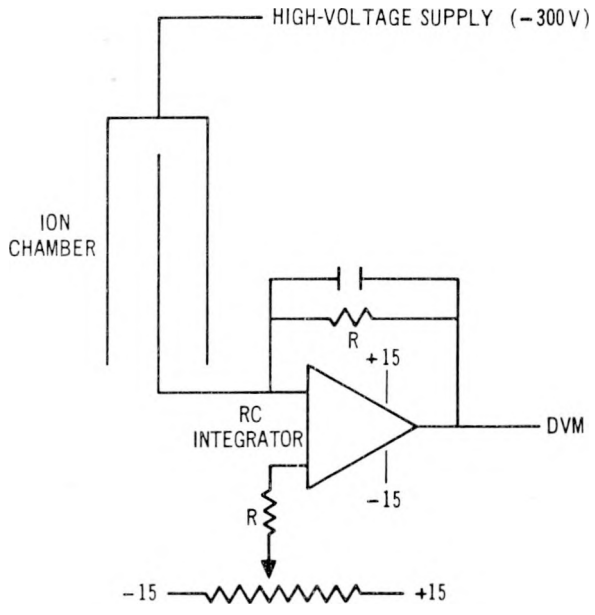

Fig. 4.
Test electronics for gas chamber.

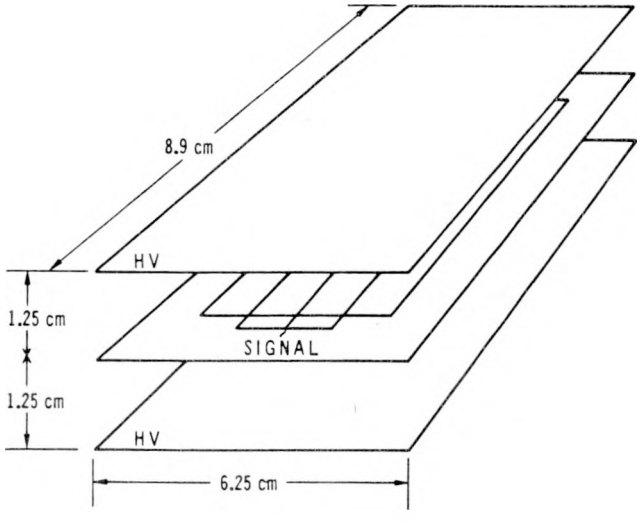

Fig. 5.
Schematic of gas chamber used for BWR irradiated fuel examination.

Figure 8 illustrates the response of different filling gases. A high-Z gas (xenon) and low-Z gas (helium) were examined. Although the magnitude of the current signal was greater for xenon and lower for helium when compared with the air filling, the profiles showed no significant differences. Because

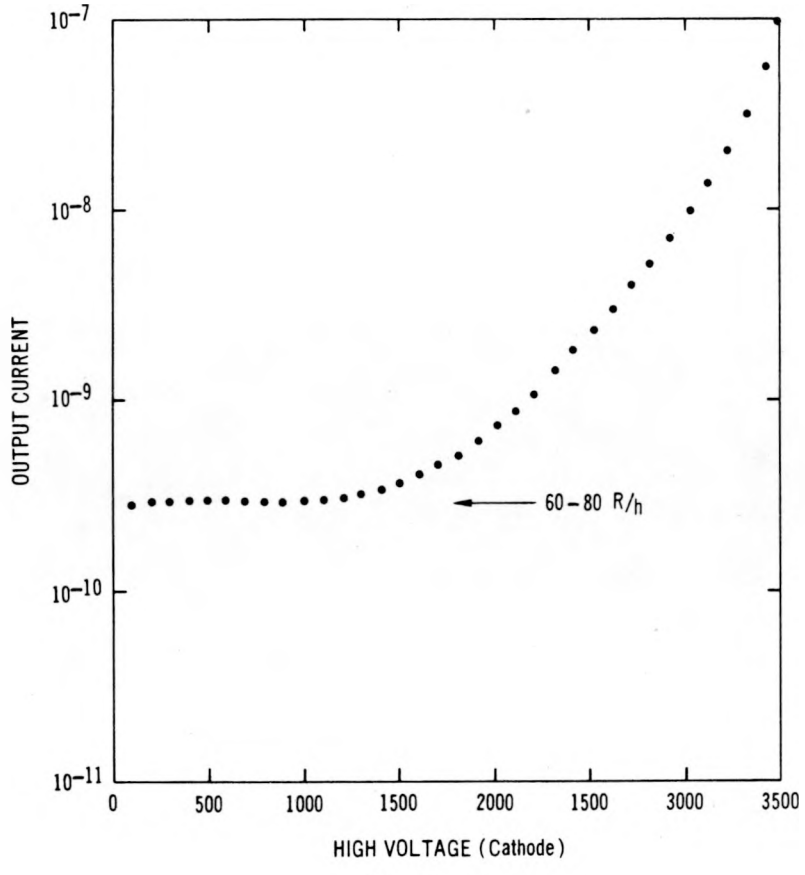

Fig. 6.

Operating characteristic of the BWR gas chamber. An intense ^{88}Y source was the source of radiation.

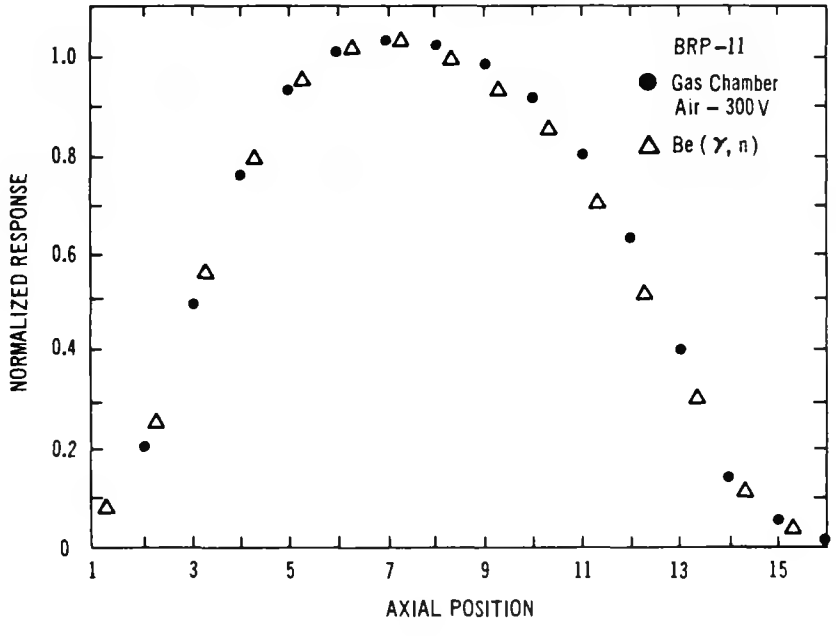

Fig. 7.

Axial profiles for a BWR irradiated fuel assembly. Axial position step size is 16.5 cm.

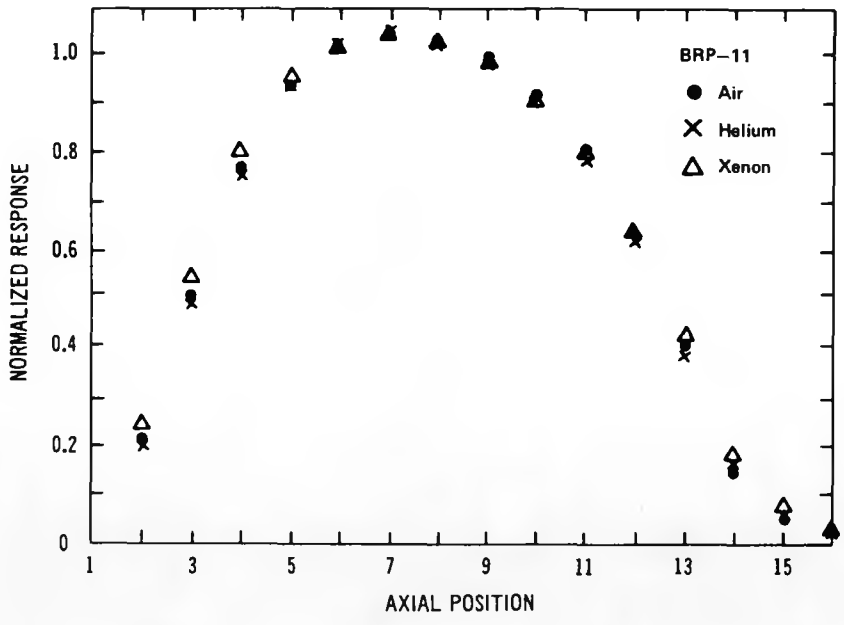

Fig. 8.
Axial profiles for a BWR irradiated fuel assembly for different gas chamber fillings. Axial position step size is 16.5 cm.

of the simplicity of an air-filled chamber, all later tests were done with an air filling.

We investigated the use of a gas chamber to obtain a unique two-dimensional map of the fuel assemblies in the storage racks and, specifically, we measured the strength of the signal contributed by adjacent fuel elements to a stationary fuel element. The results are shown in Fig. 9. The effect is dramatic and demonstrates that the burnup cannot be determined by measuring the top of a spent fuel assembly without unfolding the response of adjacent assemblies. However, because of the large amount of crosstalk among adjacent assemblies, any change in one assembly affects many others, and the phenomenon can be used as a measure of the integrity of the fuel assembly location. This "blueprint" of the racks, although not a measure of burnup, might be used to verify any change in fuel storage because it would be extremely hard to reproduce artificially. The precision of the measurements is <0.5%.

The PWR spent fuel examinations were similar to those for the BWR. A different gas chamber (Fig. 10) was used because the PWR assemblies had a higher burnup and greater radiation fields. The chamber's active volume was 10 cm^3 and all electrodes were flat plates. The chamber operated only in the ionization mode. A typical profile is shown in Fig. 11, where the gas chamber is compared with the ^{137}Cs profile as measured by the germanium detector. The precision of the ^{137}Cs profile is ~5% and that of the gas counter profile is ~0.5%. The good agreement between the two systems of profile measurement suggests that the gas chamber could replace the germanium detector when only axial profile information is required.

Axial profiles were measured at various distances from the fuel assembly to determine the effect of increased distance on the profile (see Fig. 12). Signals are obviously smaller at larger distances, but no significant changes in the profile occur up to 53 cm. (This observation is supported by theoretical arguments by P. Rinard.)

A full-scale prototype multiwire gas chamber is being constructed with which to obtain profiles of irradiated fuel assemblies without moving the assembly. A fixed fuel assembly and the ability to obtain a profile in <1 min will reduce significantly the time required to examine irradiated fuel. A system sensitive to neutrons alone also is contemplated.

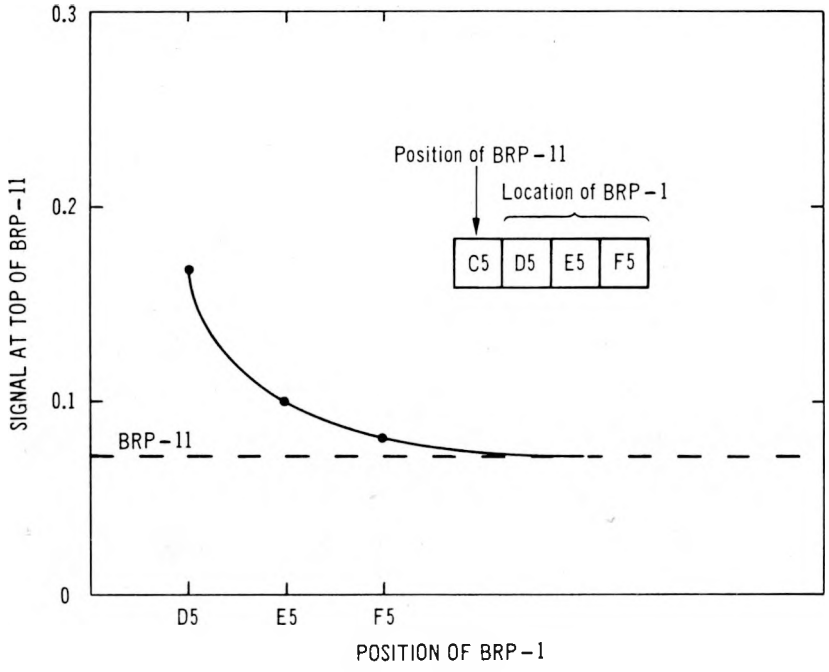

Fig. 9.
Effect of an adjacent fuel assembly on a stationary fuel assembly in a storage rack. Step size is 35.5 cm. Dashed line denotes the signal contribution from BRP-11.

F. Calculated Gamma-Ray Doses from Irradiated Fuel in a Storage Pool (P. Rinard)

A computational model has been created to provide interpretations and extensions of information from the passive gamma-ray examination (with an air-filled gas chamber) of an irradiated fuel assembly stored under water. The LWR (light water reactor) assembly is replaced by a line source capped by disk sources. The line source is positioned according to a standard radiation shielding technique[4] so that it is parallel to the assembly's longitudinal axis but displaced slightly toward the detector. The disk sources are centered on the axis of the assembly. The cylindrical space between the disks is assumed to be filled with UO_2 that is not emitting gamma rays but does cause attenuation.

The line source is further considered to be a collection of point sources so that for a given detector position an integration along the line yields the total dose from the line. The integration takes into account the attenuation in the UO_2 between the line and the cylinder's edge, the attenuation by the water between the cylinder's edge and the gas chamber, and the dose buildup from the scattering of the gamma rays in the water. The dose buildup factors for point sources were taken from earlier calculations,[5] which seem adequate here.

From examinations made with a germanium detector at the sides of assemblies, nine gamma-ray energies from 0.6 to 2.2 MeV were selected as having the most important intensities. The relative intensities were taken to be constant along the length of the line (which is only approximately correct), but the total intensity varied according to the measured germanium profile data.

Thus, the measurements used were taken from the sides of assemblies with no attenuation or buildup by water. The dose then was computed for a small air-filled chamber some distance away from the assembly, with water filling the remaining space. When only the line source is used, the dose field for a BWR assembly is that shown in Fig. 13. This 81-pin assembly is 178 cm long. The number of fissions (burnup), as well as the dose, had been largest near the assembly's center. The dose decreases almost exponentially with distance from the assembly. In fact, such a measurement shows the dose to be approximately halved every 9.47 cm, compared to 9.04 cm calculated for the gas chamber

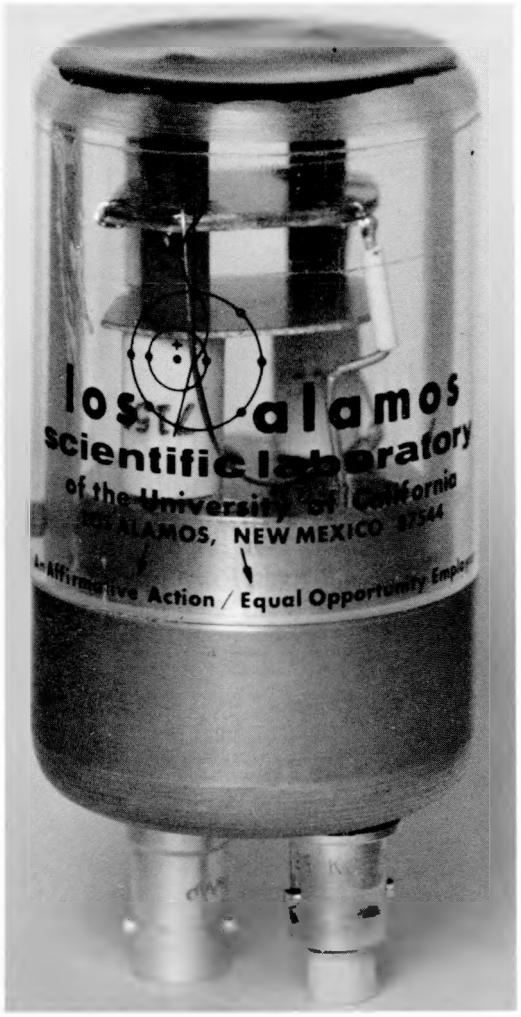

Fig. 10.
The PWR gas chamber.

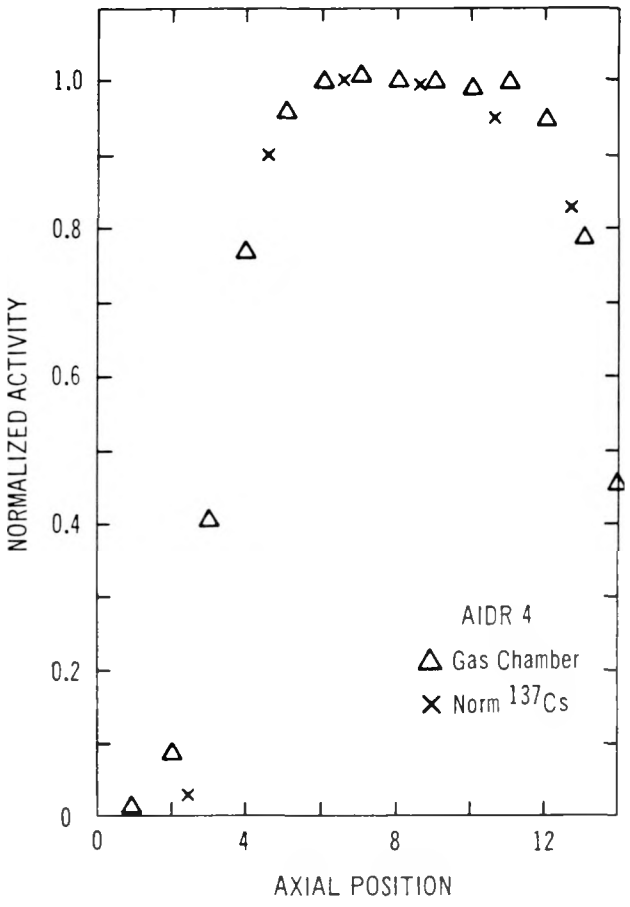

Fig. 11.
Axial profiles for a PWR irradiated fuel assembly. Step size is 30 cm.

at 25 cm beyond the assembly. The model reproduces the measured dose field rather well within the ends of the assembly.

The PWR assemblies had more uniform burnup along their lengths and the line source was adequate to reproduce the measured doses (Fig. 12,) which had lengths of 366 cm with 204 pins. The line source alone gave doses in agreement with measured doses.

To account fully for the BWR assemblies' doses, the disk sources on the ends of the line were necessary. The same nine gamma-ray energies were used again, but with relative intensities taken from germanium-detector data near the assemblies' ends. The disks were given a uniform total intensity over their areas. The flux at an off-axis point was calculated from previous work,[6] then a buildup factor by water was applied. To approximate the buildup effects of scattering by water with a disk source, (1) a point source was placed at the center of the disk and point-source buildup factors applied, (2) no radiation was allowed to penetrate downward through the UO_2 cylinder, (3) buildup slightly above the plane of the disk was reduced because radiation could not be scattered from below, and (4) radiation from above the plane was allowed to scatter below the plane by a Gaussian function of the distance below the plane. The dose field above such a disk is shown in Fig. 14.

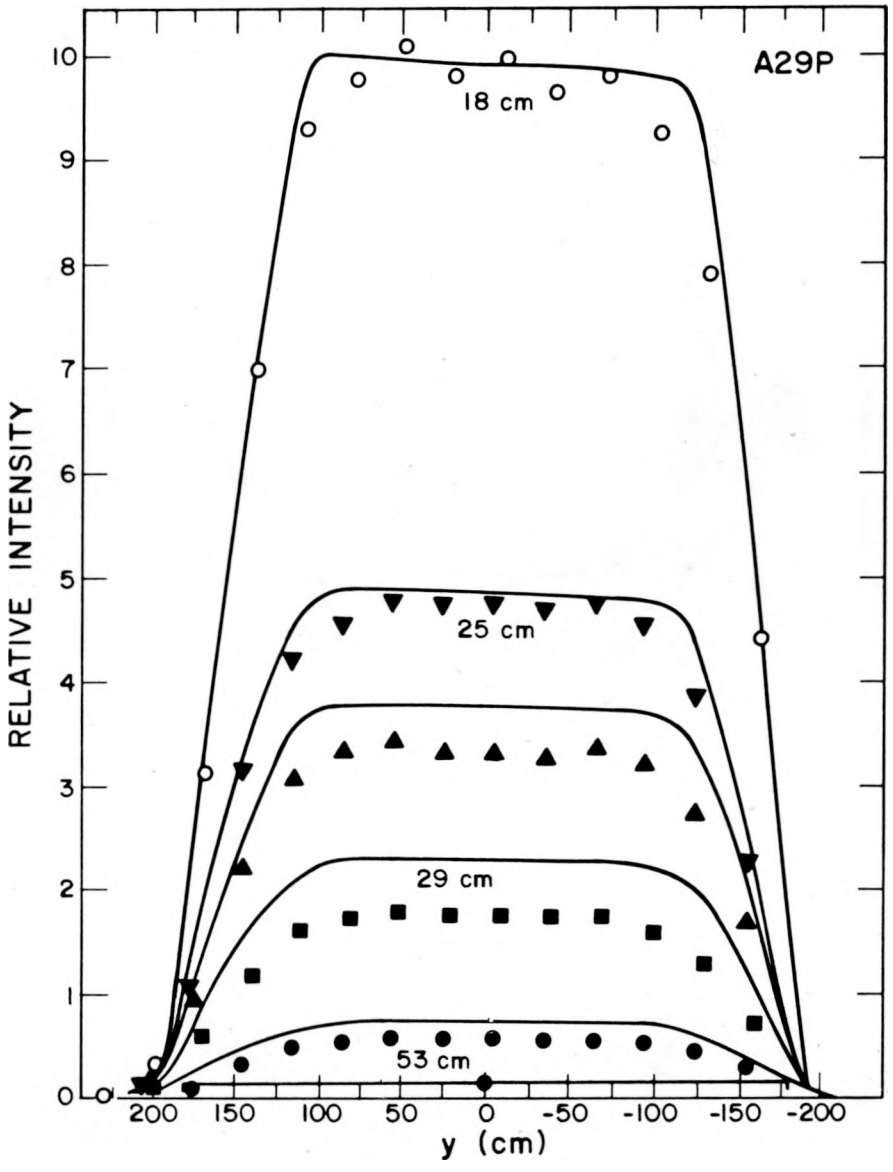

Fig. 12.
Measurements made along a PWR assembly at five distances from the side of the assembly. Position of the assembly is indicated by the line just above the abscissa. The five distances were known only approximately, therefore the calculated curves at the stated distances only approximate the data. The data sets and curves are relative doses; the 18-cm data and curve were arbitrarily chosen to coincide, thereby fixing the scale for the rest of the figure. Slight errors in the assumed distances could account for the noncoincidence of data and curves at greater distances from the assembly.

The combined effects of the line and a disk source in the case of the BWR assembly are shown in Fig. 15. Only the upper half of the assembly is illustrated because more data were obtained there. The line source by itself suffices within the assembly's ends until the detector is about 25 cm from an end, at which time only the disk source is important.

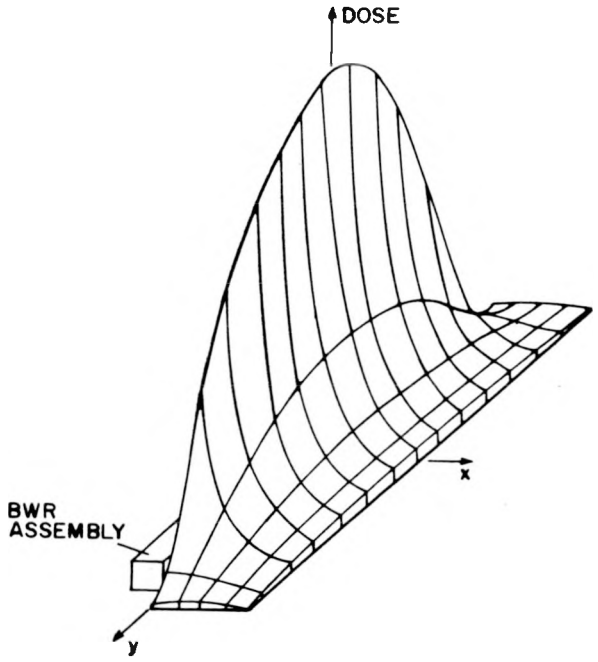

Fig. 13.
Dose field from a line source simulating a BWR assembly. A small portion of the assembly shows in the lower left corner. Intersections of the line have x from 12.7 to 63.5 cm (12.7-cm steps) and y from −116 to 116 cm (17-cm steps).

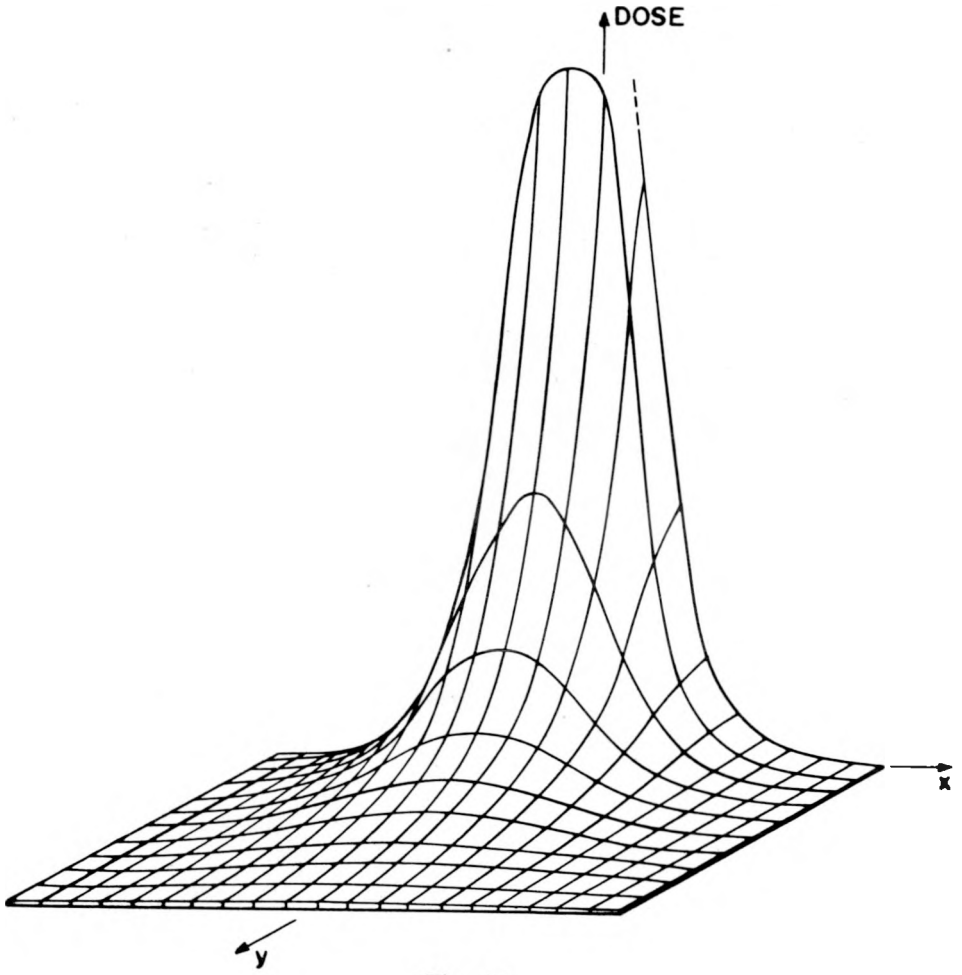

Fig. 14.
Dose field above a disk source. The disk is centered at the origin of the coordinates; its axis lies along the y axis. Intersections of the lines have x from −50 to 50 cm (5-cm steps) and y from 0 to 50 cm (5-cm steps).

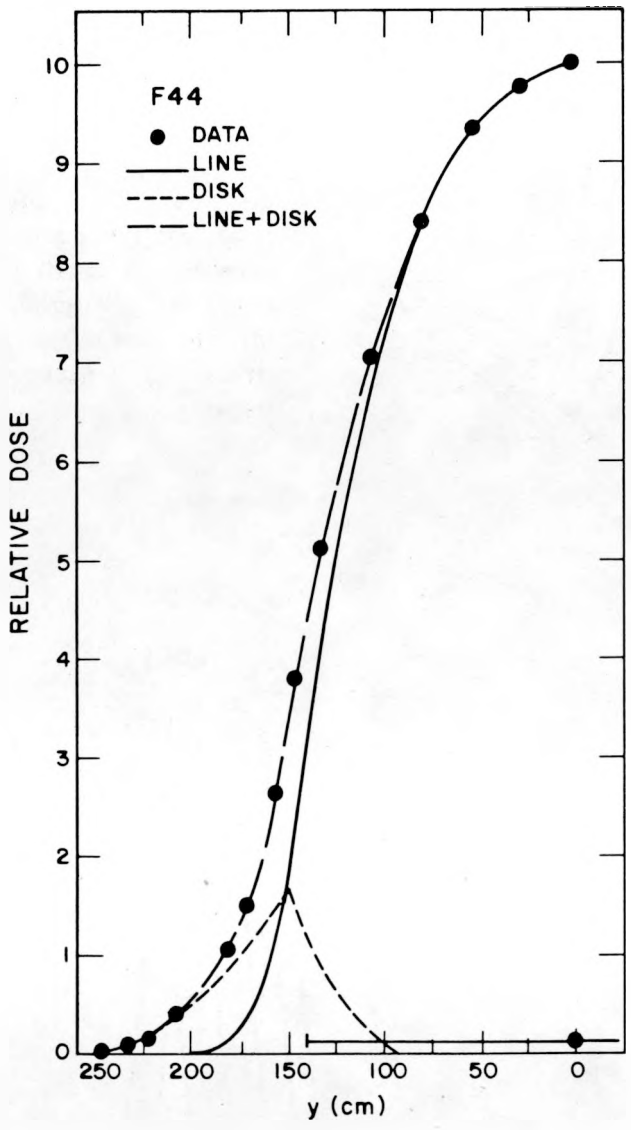

Fig. 15.
Doses at positions 33 cm from the side of a BWR assembly. To account for the data points, the dose curves from the line source (solid line) and the disk source (short dashes) must be added (long dashes). The line above the abscissa shows the assembly's position.

II. NEUTRON ASSAY TECHNIQUE DEVELOPMENT

A. Automated Data-Handling for the Laboratory Prototype Shuffler (T. W. Crane and G. W. Eccleston)

The laboratory prototype ^{252}Cf Shuffler[7] has been integrated with an LSI-11 microcomputer system.* In the initial version of the Shuffler the neutron-counting data were collected and displayed on visual scalers. Upon completion of an assay the measured counts were logged by the operator and data reduction was usually accomplished with a calculator. In the integrated system, not only is the manual mode of operation still available but data also can be transmitted directly to the computer via a six-channel scaler board (Ref. 1, pp. 51-53) mounted in the LSI-11 chassis. High-level languages such as FORTRAN IV permit automated data reduction. Results of the processing as well as the input Shuffler scaler data can be sent to output units such as the line printer or floppy disk.

A demonstration program was written to step the operator through the calibration procedure and then permit the assay of unknown samples. The response from each of the standards and the calibration parameters obtained (by a least squares best fit based on the Gauss method) are printed after completion of the calibration. For each of the unknown samples the Shuffler's response and the calculated mass and its uncertainty are printed for the operator's inspection.

B. Microprocessor-Based High-Level Neutron Coincidence Counters (C. A. Spirio, H. Menlove, C. R. Hatcher, M. Krick, J. Swansen, and P. Collinsworth**)

Seven HLNCCs (high-level neutron coincidence counters) were fabricated between May – August 1978. The shift register electronics package designed by LASL and packaged by EG&G incorporates state-of-the-art, microprocessor-based conditioning and display electronics in a desk-top packaged system. Nine complete systems, including well counters for the IAEA and LASL, were requested. Their purchase marks the transfer of HLNCC technology to commercial instrumentation suppliers.

*Digital Equipment Corp.
**Group E-2.

C. Evaluation of Methane Proportional Counters for Fast-Neutron Detection (M. P. Baker and H. O. Menlove)

Methane (CH_4) proportional counters are being evaluated for use as fast-neutron detectors in certain safeguards measurements systems. Helium-4 recoil proportional counters are in common use to detect fast neutrons from fissions in systems where samples containing fissile material are interrogated by a subthreshold neutron source. Examples of such systems are the photoneutron fuel-rod assay system (Ref. 8, p. 10), which uses the 24-keV neutrons from a ^{124}Sb-Be source for interrogation, and the portable neutron assay system for LWR fuel assemblies (Ref. 9, p. 27), which uses moderated Am-Li source neutrons.

The evaluation of CH_4 counters as a potential replacement for ^{4}He counters is motivated by several considerations. Perhaps the most important is that CH_4 has four hydrogen atoms per molecule, whereas ^{4}He has only one helium atom per molecule. Thus, if all other factors were equivalent, a CH_4 detector would have four times the counting efficiency of a ^{4}He detector. A second consideration applies to systems in which there is appreciable moderation of the fission-neutron spectrum before reaching the fast-neutron detector. There the relative energy dependence of the hydrogen and helium scattering cross sections would seem to favor CH_4 detectors (see Fig. 16).

For subthreshold interrogation systems, a pulse-height bias must be placed on the fast-neutron detector electronics to ensure that the fission-neutron signature can be discriminated from interrogation source neutrons and gamma-ray backgrounds. If the magnitude of the pulse-height bias is determined by the gamma-ray background,

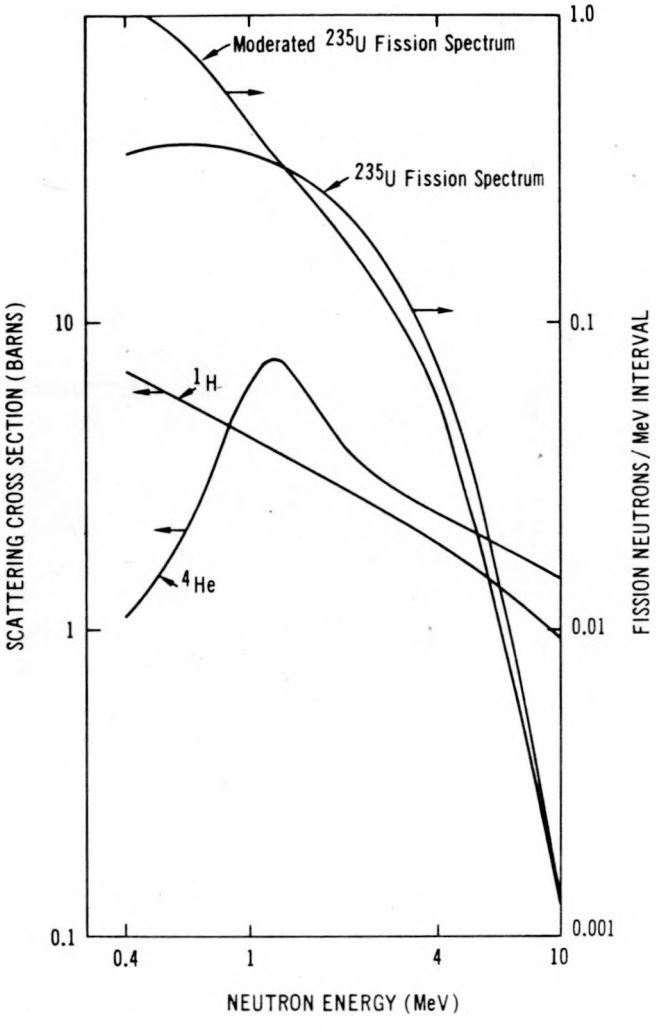

Fig. 16.
Cross sections for fast-neutron detection with counters containing ^{4}He and ^{1}H. Shown for comparison are moderated and unmoderated fission-neutron energy distributions.

CH_4 will again be favored over ^{4}He in that, on the average, a larger fraction of the incident neutron energy will be transferred to a recoiling proton than to a recoiling alpha particle. The potential disadvantages anticipated for CH_4 relative to ^{4}He are the increased gamma sensitivity and the increased high-voltage required.

The initial stage of the evaluation was performed in the configuration shown schematically in Fig. 17. The 5-cm-diam, 30-cm-long detector was irradiated with ^{252}Cf spontaneous-fission neutrons from one side and a mockup of a photoneutron source from the other side. The mockup consisted of an ~100-

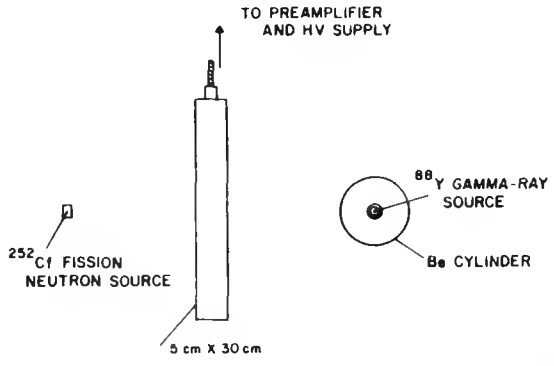

Fig. 17.
Geometry for evaluation of 5-cm-diam, 30-cm-long recoil proportional counter with ^{252}Cf spontaneous fission-neutron source and photoneutron source mockup.

mCi ^{88}Y gamma-ray source (E_γ = 0.90, 1.84 MeV) inserted into a hole along the axis of a 7.5-cm-diam, 10-cm-long beryllium cylinder. This combination produced a gamma dose of 1 to 2 R/h at the detector.

The anode of the proportional counter was operated at positive high voltage; the cathode was at ground potential. Signals from the counter were processed by a charge-sensitive preamplifier and an Ortec 450 amplifier before passing to a multichannel analyzer for pulse-height analysis.

The pulse-height spectrum obtained with an 18-atm ^{4}He counter is shown in Fig. 18. The spectrum has two distinct regions: at low pulse heights, a rapidly falling exponential distribution from gamma-ray interactions is observed; at larger pulse heights the events caused by neutron interactions show clearly. The dotted line shows the spectrum obtained when only the gamma-ray source is present. Thus, events above the discrimination level shown in the figure are caused only by fission-neutron interactions.

For a fixed source-detector geometry, the neutron counting rate above the discrimination level might be expected to depend on variables such as high voltage, amplifier time constant, and gas pressure. The effect of two of these variables for the 18-atm ^{4}He detector is shown in Fig. 19, where the neutron counting rate is plotted as a function of high voltage, with the amplifier time constant as a parameter. For a given time constant, the neutron counting rate has

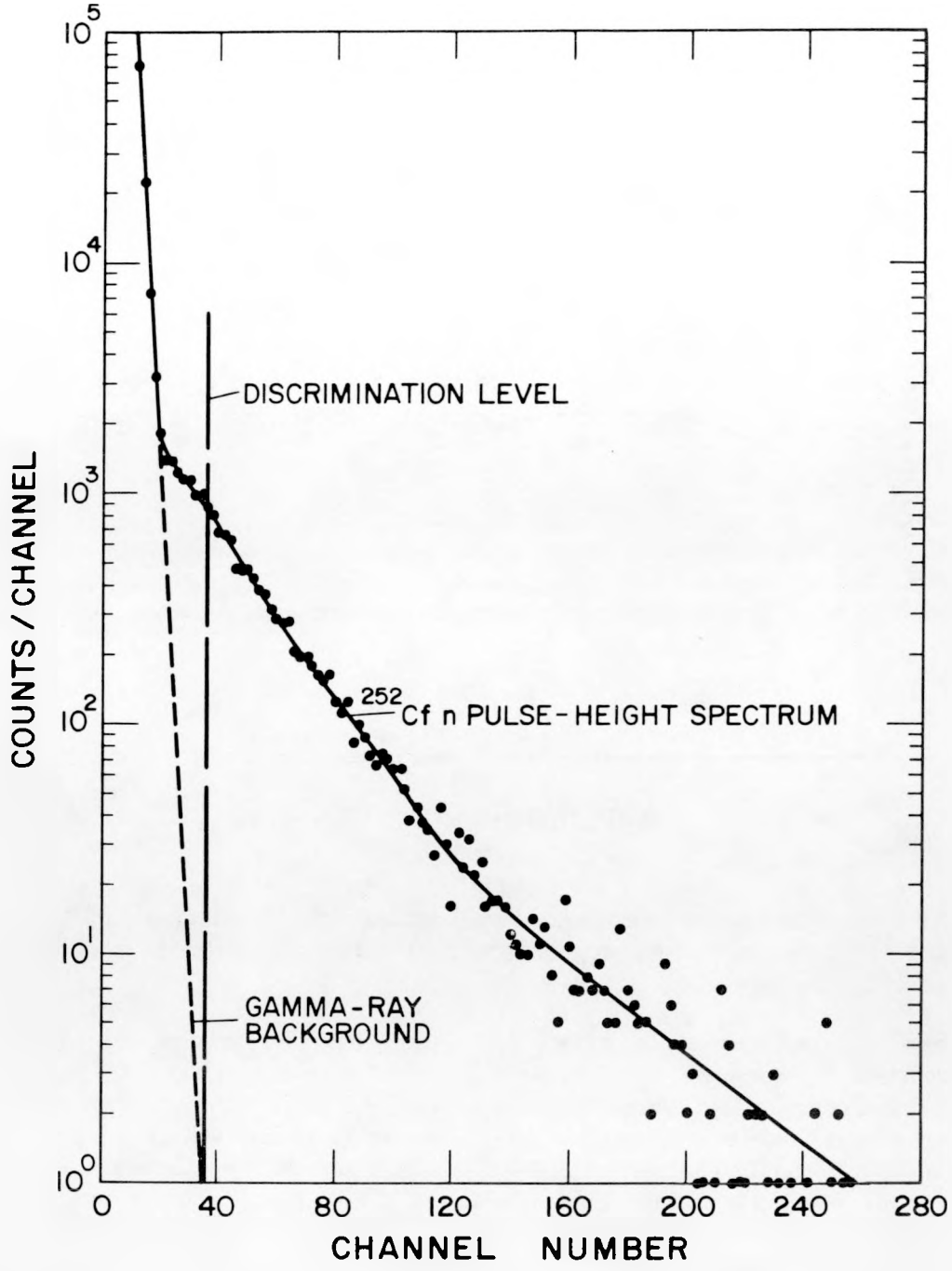

Fig. 18.
Pulse-height spectrum obtained from an 18-atm ^{4}He detector with incident neutron and gamma-ray fluxes described in Fig. 16.

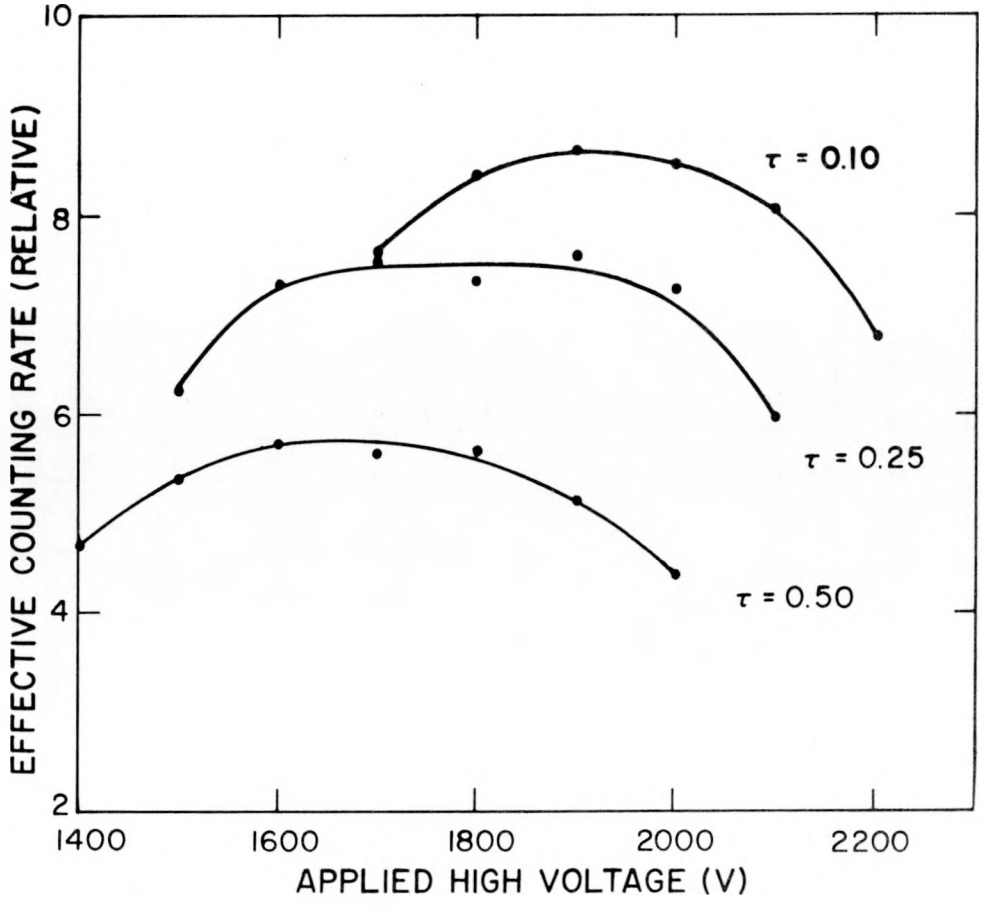

Fig. 19.
Effective neutron counting rate as a function of applied high voltage and amplifier time constant (τ) for 5-cm-diam, 30-cm-long, 18-atm ^{4}He recoil proportional counter.

a roughly parabolic dependence on high voltage. As the time constant is shortened, the maximum achievable neutron counting rate increases because of the increased pulse risetime for a gamma-ray interaction compared to a neutron interaction. A short clipping time, then, effectively diminishes the pulse height of gamma-ray events relative to neutron events. Disadvantages of the shorter amplifier time constants are that a larger amplifier gain is required for a given output signal size and somewhat higher voltage is required on the detector.

To evaluate the performance of CH_4 detectors on the basis of the above criteria, we obtained a series of 5-cm-diam, 30-cm-long detectors from Reuter-Stokes. The detectors had 0.8-mm-thick stainless steel walls and had fill pressures that varied from 3 to 18 atm (Table III). A series of measurements similar to those shown in Fig. 19 was carried out for the 3-atm CH_4 detector and, again, an amplifier time constant of 0.1 s gave the highest net counting rate. Of major interest, however, were the fill-pressure and high-voltage behaviors of CH_4 detectors. Figure 20 shows the results of changes in these parameters on net neutron counting rates.

The 3-atm and 5-atm CH_4 detectors behave as expected—the maximum neutron counting rate per unit pressure is roughly four times that obtained for the 18-atm ^{4}He detector. However, for CH_4 detector fill pressures >5 atm, the response per unit pressure begins to fall rapidly. For example, the 7-atm detector gives only ~6% more response than the 5-atm detector, whereas a ~40% increase would have been expected.

The saturation of and eventual reduction in the fast-neutron response of the CH_4 detectors with increasing fill pressure can be only partially explained

TABLE III

FILL PRESSURES, APPROXIMATE OPERATING POTENTIALS, AND RELATIVE NEUTRON COUNTING RATES FOR 5-CM-DIAM, 30-CM-LONG CH_4 RECOIL PROPORTIONAL COUNTERS

Pressure (atm)	Approximate Operating Voltage (V)	Relative Counting Rate
3	2500	6.6
5	3200	9.9
7	4000	10.5
10	5000	10.4
18	6400	6.8
(18-atm ^{4}He)	1900	8.6

by the increase in gamma sensitivity. Measurements conducted with monoenergetic neutrons produced by Q-1's Van de Graaff accelerator indicate that even with relatively weak background gamma radiation the fast-neutron response per unit pressure decreases as the detector pressure is increased. This effect is accompanied by a resolution that broadens with increasing pressure. The reason for that behavior is not understood, but may involve increased recombination of ions and electrons in the detectors as the pressure is increased.

Increased gamma sensitivity with increasing detector pressure is at least generally understood. The response of a gas proportional counter to gamma radiation is due to interactions both in the gas and in the container walls. In the latter case, only interactions in which an electron escapes from the wall into the gas will cause a pulse in the detector. As the pressure of the gas in the detector is

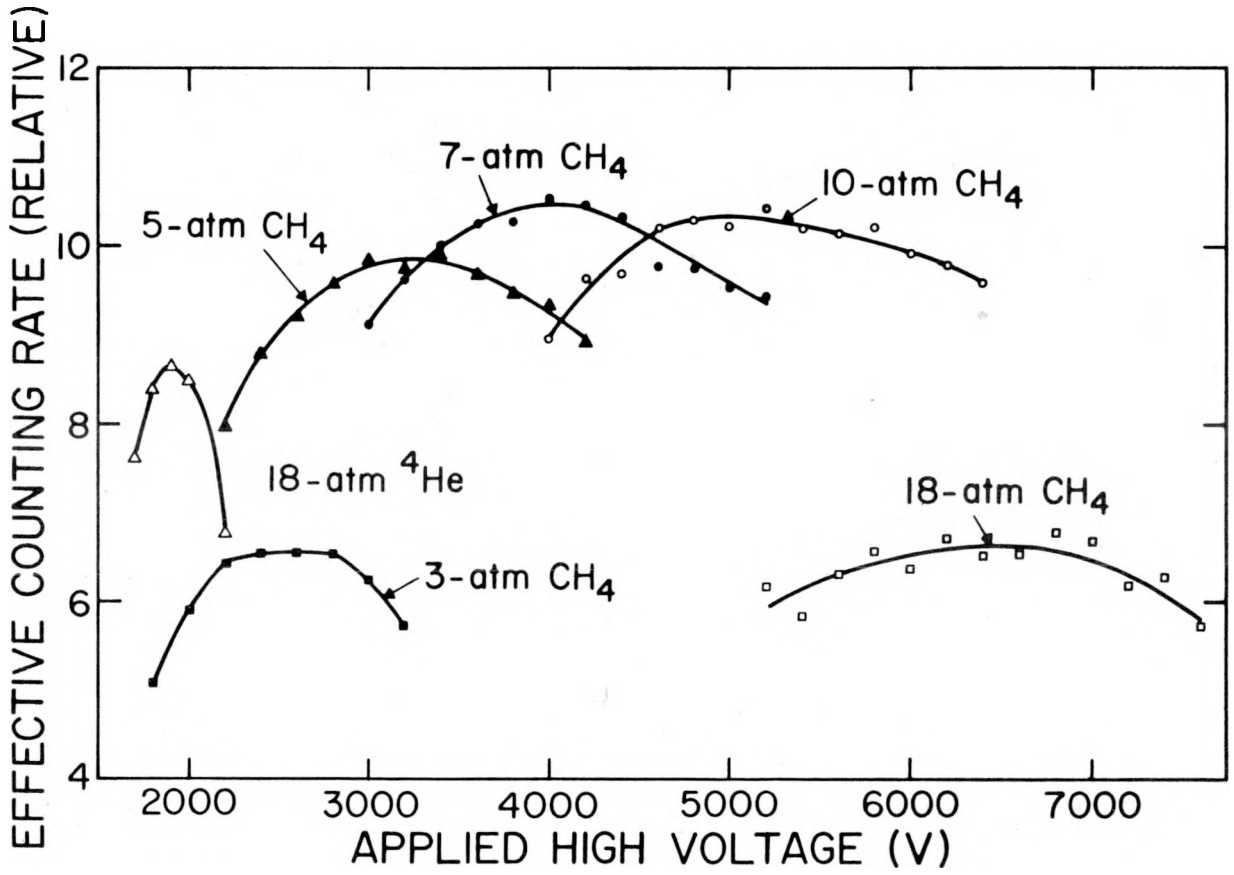

Fig. 20.
Effective neutron counting rate as a function of applied high voltage and detector gas and fill pressure for 5-cm-diam, 30-cm-long recoil proportional counters.

raised, the probability of direct interaction in the gas increases essentially linearly. In addition, the energy deposited in the gas by any recoil electron increases with pressure. The combined result of these effects is that the gamma-ray background, as shown in Fig. 18, extends to larger pulse heights as the gas pressure is raised. Thus the discrimination level must be raised to maintain the separation between neutrons and gamma rays. The increasing gamma sensitivity causes the effective neutron sensitivity to increase at something less than the expected linear rate with increasing fill pressure.

Observed effects of the gamma sensitivity on fast-neutron measurements depend critically on the gamma-to-neutron ratio, the gamma-ray and neutron energy spectra, and the type of gas used. For CH_4 the results with ~1 R/h of high-energy gamma radiation and 300 fission-spectrum neutrons/cm^2-s are shown in Fig. 20. For these conditions the 7-atm CH_4 counter is ~20-25% more sensitive than the 18-atm ^{4}He detector; however, the ^{4}He detector requires only one-half the high-voltage level of the CH_4 tube.

For a safeguards measurements system the situation is likely to be quite different in that both the neutron and gamma-ray spectra may be softened compared to the case just discussed. The measurements reported here serve as a high gamma-ray background fiducial from which guidance can be obtained for solving a particular fast-neutron detection problem. A series of similar low gamma-ray background, fast-neutron efficiency measurements is in progress.

D. Calculation of (α,n) Neutron Production from Light Elements in the Presence of SNM (Special Nuclear Material) (J. D. Brandenberger)

The interactive code ANN2 developed by the author for general (α,n) neutron production calculations[10] has been used extensively for wet PuO_2 precipitates, nitrate solutions, and oxalate precipitates in support of Q-1 programmatic needs. In addition to the numerical results, calculations indicate that the data base for O(α,n)C yields[11] may be insufficiently accurate. Compared to measurements of (α,n) neutron production of $^{238}PuO_2$ by LASL and ORNL[12] the O(α,n)C data base of Liskien and Paulsen[11] appears low by 30-50%—within their stated uncertainty,[11] but not entirely satisfactory. To generate an alternate data base for O(α,n)C neutron production, the author reduced a set of unpublished data obtained by bombarding a thick SnO_2 target with alpha particles as a function of alpha-particle energy.[13] If this O(α,n)C data base is used to calculate the (α,n) neutron production from pure $^{238}PuO_2$, the results are within the range of measured values shown in Table IV. Measured values are inherently high because of small contamination (a few ppm) by certain light elements, so our new values of O(α,n)C may well have errors of 20%.

Results from calculation of (α,n) neutron production indicate that for PuO_2 and wet PuO_2 assayed by Q-1, 30-50% of the (α,n) neutrons come from light-element contamination.[14] The chief suspected contaminant is fluorine. Because the fluorine contamination varies, it must be measured before accurate (α,n) neutron production calculations are possible. Calculations made for PuO_2 precipitate with varying amounts of H_2O content are being used for neutron multiplication calculations. Such multiplications would affect the accuracy of a coincident well counter assay unless corrections were made.[14]

TABLE IV

MEASURED AND CALCULATED VALUES OF (α,n) NEUTRON YIELD OF $^{238}PuO_2$

	Source Strength ($g\ ^{238}Pu\text{-}s)^{-1}$
Bair and Butler[12]	$1.50 \times 10^4 \pm <1.0\%$
Anderson and Neff[12]	$1.40 \times 10^4 - 1.52 \times 10^4 \pm 4\%$
Matlach[a]	1.176×10^4
Calculated using Ref. 11	$0.9 \times 10^4 \pm 30\%$
Calculated using data in Ref. 12	1.2×10^4

[a]In LA-4940 (Ref. 4).

III. GAMMA-RAY AND X-RAY ASSAY TECHNIQUE DEVELOPMENT

A. Uranium Solution Assay by Transmission-Corrected X-Ray Fluorescence (R. Strittmatter, M. Baker, and P. Russo)

The technique of TC-XRF (transmission-corrected, energy-dispersive x-ray fluorescence) is being developed for the NDA (nondestructive assay) of low-concentration (<20 g/ℓ) plutonium or uranium solutions. Assay precisions of 1% or better for low-concentration uranium solutions have been attained by a system reported previously.[15] The earlier XRF system suffered from low counting rates and long counting times. Recent development has been concerned primarily with minimizing the measuring time required to attain the desired assay precision and preliminary calculations necessary for design optimization.

The present TC-XRF system (Fig. 21) uses a Si(Li) detector with an active area of 80 mm^2 to measure the intensity of uranium L x rays fluoresced with 22-keV x rays from a 20-mCi ^{109}Cd annular source. Aqueous uranium solutions were contained in 5-cm-diam, disk-shaped plastic holders, which provided 3.85-mm sample thickness. Correction for attenuation of source and uranium x rays in the sample solution was achieved by measuring the transmission through the sample of characteristic x rays from a thorium foil. During the measurements, the distance from the sample to the detector was varied between 4.0 and 10.5 cm. Stored event rates >6000 s^{-1} were achieved for uranium concentrations of 0.2 to 20 g/ℓ. To retain the desired x-ray resolution of ~300 eV at 13.6 keV, pulse pile-up rejection was employed. Corrections for source decay and deadtime resulting from pulse pile-up rejection, resetting of the pulsed optical feedback preamplifier, and analog-to-digital conversion were accomplished by monitoring the intensity of K x rays fluoresced in a 24-gauge copper wire stretched across the source holder (see Fig. 21).

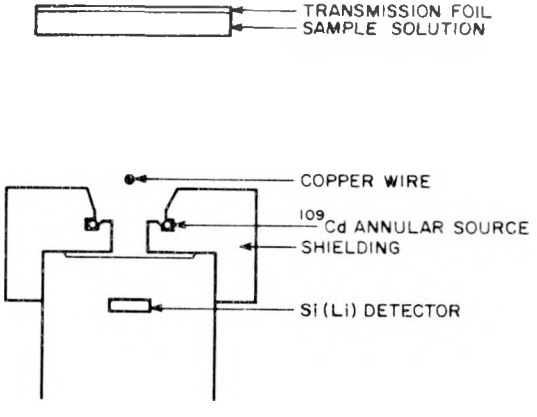

Fig. 21.
Arrangement of Si(Li) detector, ^{109}Cd source, copper wire, uranium solution sample, and thorium transmission foil for TC-XRF areas.

With an optimum count rate the ratio of fluoresced uranium L x rays from a foil to the K_α copper x rays from the wire was constant to ±0.15% for measurements extending over a 12-h period. Precisions of <1% were achieved for uranium concentrations of 1 to 20 g/ℓ with counting times of 5 x 10^2 s. The relative statistical error as a function of uranium concentration obtained with counting times of 500 s is given in Fig. 22.

The x-ray attenuation correction factor for a plane geometry is given by ℓnT/ (T − 1), where T is the product of the transmissions at the source and fluoresced x-ray energies. T was calculated for a set of samples of known composition under the assumption of a far-field geometry (sample to detector distance is large compared with the dimensions of the source and detector) and compared with measured values.

A value for the linear attenuation coefficient was obtained with photoelectric and incoherent scattering cross sections. Because the effect of incoherent scattering on the measured transmission in the present sample-transmission foil geometry is not well known, an upper bound on the expected transmission was calculated by using only the photoelectric cross section. For example, incoherent scattering of the source x rays in the sample does not preclude the fluorescing of thorium x rays unless the angle of scatter is sufficiently large that the scattered source x ray misses the thorium foil. The coherent scattering was not included because it is predominantly forward-peaked and does not remove a significant number of x rays from the full-energy peak.

Calculated transmissions and the transmissions measured at a detector-to-sample distance of 10.5 cm for 13.0- and 15.6-keV thorium x rays are plotted

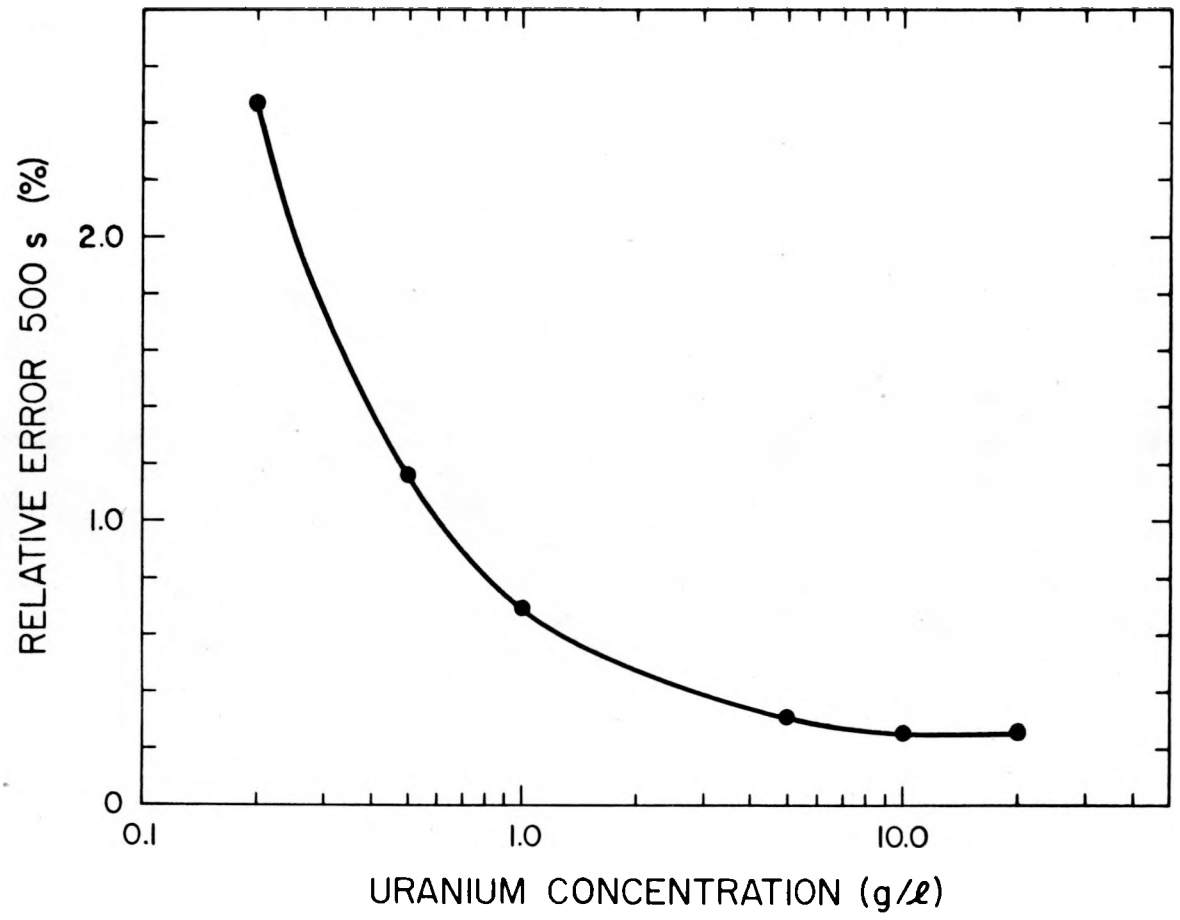

Fig. 22.
Relative statistical error as a function of uranium concentration obtained with present TC-XRF system for counting times of 500 s. (Solid line drawn to guide the eye through data points.)

in Fig. 23 as a function of uranium concentration. The measured transmission values generally lie between the values calculated with incoherent scattering and the values calculated without incoherent scattering. The agreement between calculated and measured transmission values indicates the validity of the far-field approximation for the present geometry. Further investigation is necessary to determine the range of geometries over which the attenuation correction factor $\ell nT/(T - 1)$ is valid.

B. High-Resolution Gamma-Ray Spectrum Analysis (J. K. Sprinkle, Jr.)

Raygun,* a hands-off computer code designed for the rapid analysis of relatively simple, high-resolution gamma-ray spectra, was implemented on the PDP 11/60. Its accuracy and reliability were

*Developed by R. A. Gunnick (Lawrence Livermore Laboratory) and B. R. Erdal and T. A. Kelly (LASL).

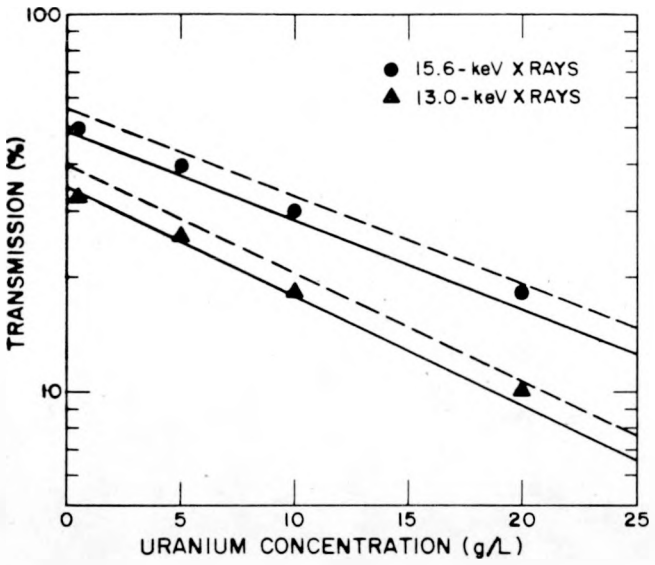

Fig. 23.
Calculated and measured transmission through various concentrations of uranium solutions, where 13.0- and 15.6-keV thorium x rays fluoresced with 22-keV source x rays. Solid and dashed lines, respectively, were calculated with and without contribution from incoherent scattering.

carefully evaluated with a reference spectrum from a spent fuel measurement (see Part 1, Sec. I-A).

During initial evaluation, the graphics capability of the 11/60 was useful for displaying the program's background estimation and its choice of peak regions. The program was setting 2 channels out of every 64 equal to zero during the background estimation procedure because of a logic error in the routine to find the lowest channel containing nonzero data. That error caused an array to be overwritten such that an important parameter was changed to zero.

Another problem arose when two resolved peaks were separated by a few channels. The peaks were treated as a multiplet unless they were separated by four or more channels in which differences in the number of counts per channel were not statistically significant. This treatment led to peak areas ~5% higher than those obtained by a careful hand integration of the two peaks. The solution to this difficulty was to change from four to three the number of consecutive points required to end a peak region.

Another stage in the analysis involved comparison of the peak areas computed by Raygun with the areas obtained by hand integration. Results of this comparison are given in Fig. 24, where the difference between Raygun's area and that determined by the hand integration (normalized by the standard deviation of the hand integration) is plotted as a function of the peak area. The units for the vertical scale—standard deviations of the hand integration—were considered more meaningful than percentages because the statistical errors associated with the peak areas vary by more than an order of magnitude. The accuracy of Raygun's area determinations is not expected to be better than ~1%;[16] consequently, 1% was used for the unit standard deviation when the statistics implied a more precise determination. Raygun's results are shown as triangles. They are consistently low, except for the three largest areas. The average of Raygun's calculations is -0.26 ± 1.08 standard deviations. If we neglect the three points with the largest areas, the average is -0.49 ± 0.68 standard deviations. The solid points in Fig. 24 are the results of a similar analysis in which the Nuclear Data 660 programs* were used on the same input spectrum. Clearly, Raygun does the better job of determining the peak areas.

These data were also plotted as a function of gamma-ray energy and peak-to-background ratio in an attempt to find a systematic variation related to Raygun's underestimation of the areas. No trends were apparent. However, the widths of the Raygun peak regions showed considerable scatter. Figure 25 plots the integration widths, crudely corrected for the known energy dependence, vs the peak areas. Here the integration widths increase with increasing peak area at a rate faster than expected, leading to overestimation of the largest peak areas. It is probably due to the unsophisticated peak-finding routine and is not easily correctable. As far as the peak regions corresponding to smaller areas are concerned, it is not yet clear if it is easy or necessary to make them more self-consistent for the planned applications of this code.

We also examined Raygun's capabilities with doublets. A simple spectrum was integrated by the program, then modified and integrated again. The

*Nuclear Data Inc., Schaumburg, Illinois.

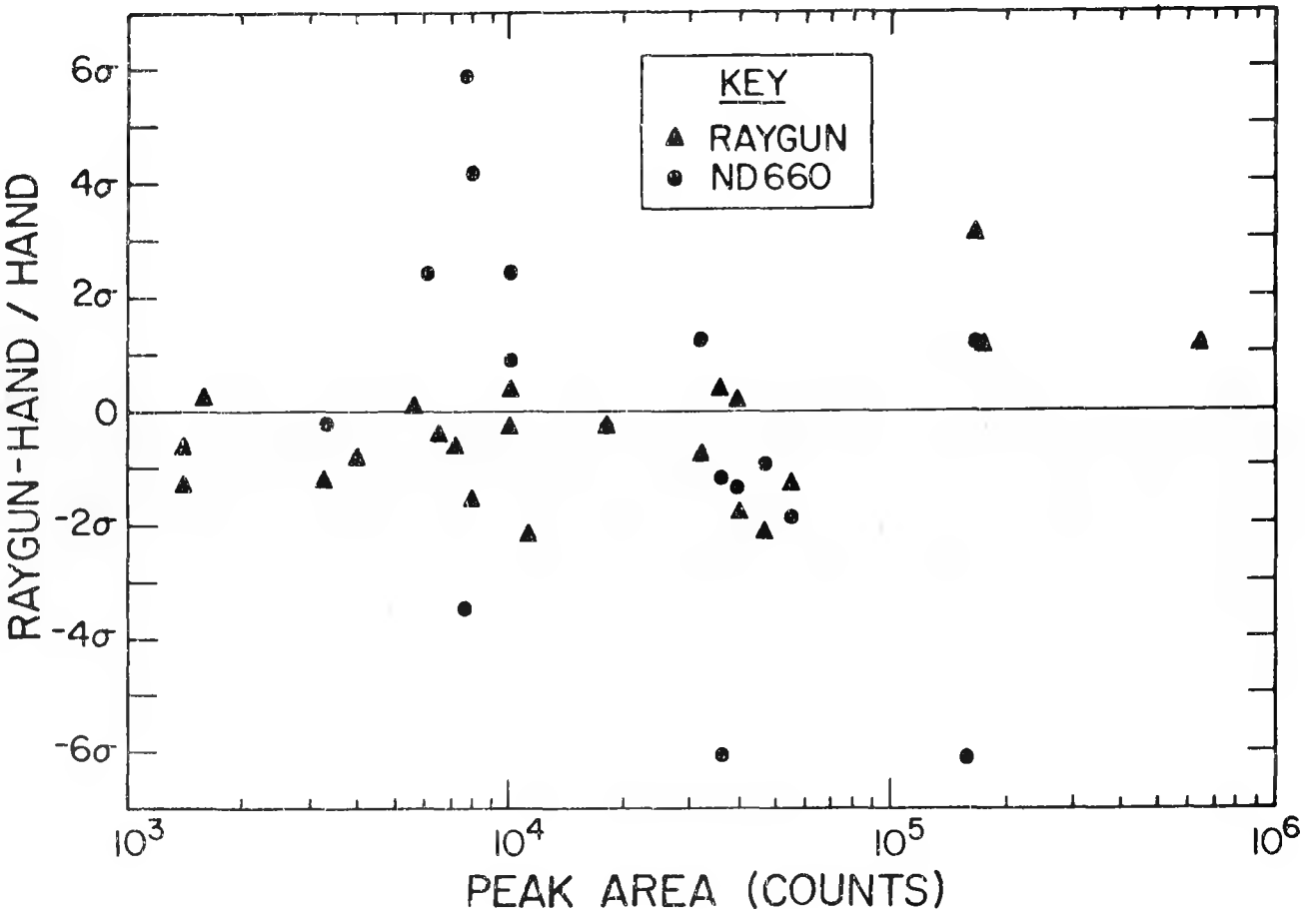

Fig. 24.
The difference, as a function of peak area, between the peak area determined by Raygun and that determined by a hand integration. Nuclear Data 660 results are shown for comparison. One σ corresponds to one standard deviation in the corresponding hand integral.

modification consisted of shifting and multiplying the data by constants and adding the results to the original spectrum. If N(i) is the number of counts in channel i, then

$$\text{Modified Data (i)} = N(i) + a\,[N(b + i)],$$

where a and b are user-chosen constants.

Table V has some preliminary results for a = 2 and b = 6. Column A has four peak areas corresponding to four isolated peaks in the original spectrum; columns B and C are Raygun's integrals for the modified spectrum corresponding to the same and the shifted peak locations, respectively; and columns D and E are the percentage differences between the original and the modified data area determinations. The factor of 2 used in creating the modified spectrum was removed before the column E comparison. Raygun found 31(58) peaks in the original (modified) spectrum. Of the four missed in the modified spectrum, all were either shifted beneath another peak or had very small areas (<2000 counts). These results indicate that Raygun probably will perform nearly as well with multiplets as with singlets if the multiplets are not too complicated and if the members of the multiplet are not too close in energy.

The feasibility of using Raygun to analyze spent fuel data will be tested and, to facilitate the simultaneous handling of 100 to 200 spectra, programs have been written to automate the analysis procedure. The user enters the file names

for the input spectra; then the two conversion programs and Raygun are run automatically. As many as 14 files (one floppy disk) can be processed at once. Test runs with some Zion and BRP data are planned.

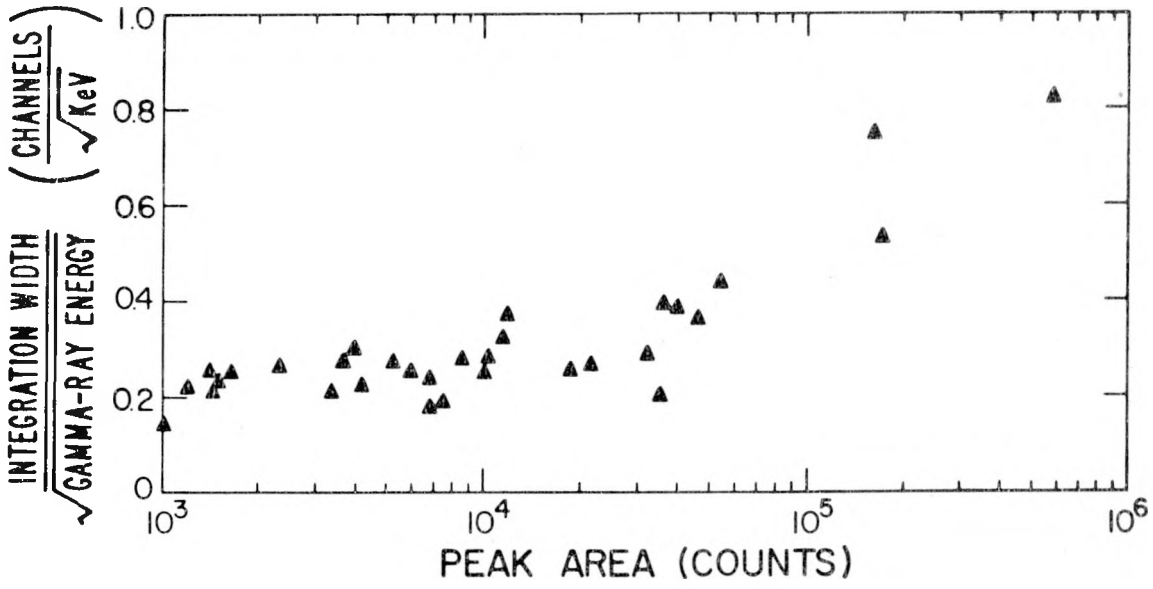

Fig. 25.
Number of channels chosen by Raygun for the peak integration regions, corrected for the known energy dependence, and as a function of peak area.

TABLE V

RAYGUN'S ANALYSIS OF ISOLATED PEAKS vs THE SAME PEAK IN A MULTIPLET

Modified Data (i) = Data(i) + 2.0[Data(i+6)]

A	B	C	D	E
	Modified Area		% Difference	% Difference
Original	Same	Shifted	(a-b)/a	[a−(c/2)]/a
7439 ± 164	7392 ± 163	14915 ± 316	0.6%	−0.2%
9216 ± 175	9282 ± 186	18391 ± 338	−0.7	0.2
22415 ± 267	22576 ± 271	45327 ± 513	−0.7	−1.1
166679 ± 667	167219 ± 669	334411 ± 1418	−0.3	−0.3

IV. FIELD TESTS AND EVALUATIONS

A. ^{252}Cf Shuffler for the Savannah River Plant (T. W. Crane, S. E. Beach, S. C. Bourret, P. Collinsworth,* L. R. Cowder, H. R. Dye, G. W. Eccleson, E. A. Gallegos, D. C. Garcia, D. L. Garcia, K. E. Kroncke, G. G. Ortiz, and L. G. Speir)

A ^{252}Cf Shuffler has been built for the test and evaluation program at the SRP (Savannah River Plant) (see Ref. 1, pp. 39-44). The Shuffler, an NDA instrument, is designed to measure the ^{235}U content of recycled scrap and waste materials at the SRP reactor fuel fabrication facility. The fissile uranium isotope ^{235}U is measured by active assay in which a ^{252}Cf source is used for neutron interrogation of the sample, followed by detection of delayed neutrons from ^{235}U fissions produced during sample interrogation. The spontaneous fission neutrons from the ^{252}Cf source are reduced in energy to enhance ^{235}U fissions while decreasing fissions in the nonfissile uranium isotopes ^{234}U, ^{236}U, and ^{238}U present in the SRP materials.

The complete Shuffler system, which includes the assay unit, electronics rack, and communications terminals, is shown in Fig. 26. During the test and evaluation program at the SRP reactor fuel fabrication facility, the assay unit will be placed in the scrap storage vault while the electronics rack and terminals will remain outside the vault (to reduce the chance of contamination). The system status will be displayed on a CRT terminal screen visible to the operator through a vault window. The operator communicates with the control electronics through a keyboard located in the vault and adjacent to the assay unit.

The Shuffler assay system is undergoing a thorough check-out, which will be followed by an initial calibration with materials supplied by SRP and verified by LASL using gamma-ray spectroscopy, neutron activation with the Q-1 Van de Graaff, and chemical sampling and analyses by Group CMB-1. SRP representatives are to attend a training session at LASL and will be given further instruction in the operation of the Shuffler when it is assembled at their facility.

*Group E-2.

B. Seismic Calculations on the ^{252}Cf Shuffler for the Idaho Chemical Processing Plant (G. W. Eccleston, L. S. Speir, H. O. Menlove, and E. G. Endebrock*)

The delayed neutron Shuffler (Ref. 15, p. 30) being designed for FAST, the Allied Chemical Fluorinel and Storage Facility, is being investigated to determine its resistance to seismic loads. The DBE (design basis earthquake)** postulates a 0.5-g loading in the room containing the Shuffler. The system is to remain operational during an operating basis earthquake (OBE = DBE/2). Conditions of the DBE require that there be no penetration or loss of integrity of the system, consequently no leakage and ensuing environmental contamination.

A schematic of the Shuffler is shown in Fig. 27. The two through-pipes constitute a containment barrier separating the Shuffler system from the contaminated Fluorinel dissolution cell. Spent fuel elements and waste canisters to be assayed are lowered into the tubes in the dissolution cell and then withdrawn. High dose rates from the sample require that the outside of the tubes be surrounded with ~10 cm of lead. The seismic resistances of the tubes and surrounding lead were evaluated on the basis of the postulated DBE.

This system was too complex for accurate appraisal of its seismic resistance; however, a conservative evaluation was made on the basis of the following assumptions.

- The lead shielding provides no load resistance.
- The waste canister and fuel package tubes provide the total lateral load resistance.
- Constraints induced by the CH_2 block are disregarded.
- The building is designed to withstand the DBE.

Calculations indicate a fundamental frequency of 191 Hz for the tube and shielding system. Because amplification of structural responses occurs only for frequencies up to 33 Hz, seismic loads can be considered as statically applied loads. Stresses produced by the 0.5 g's postulated DBE are <1000

*Group WX-8.
**Private transmittal from Ralph M. Parsons Co., Job 5586.

Fig. 26.
Complete Shuffler system for SRP.

psi, hence the tube and shielding system can survive the DBE.

The lead shielding system surrounding the interrogator tubes must be designed so that all lead is securely attached to the tubes. A lead section that became detached during an earthquake could damage the system considerably. The neutron interrogator will withstand the DBE if the lead is securely fastened to the tubes.

C. Calibration of High-Level Neutron Coincidence Counters by the IAEA (J. E. Foley, D. Reilly, M. S. Krick C. R. Hatcher, H. O. Menlove, A. Ramalho,* and J. Womack*)

Between July 23 and August 4, 1978, personnel from the Department of Safeguards, Division of Operations A, of the IAEA calibrated two HLNCCs at LASL on a wide variety of nuclear samples. The new electronics packages for the HLNCC that are directly interfaced to the HP-97 calculator were used on both HLNCCs during the calibration exercise.

Calibrations of the two HLNCCs were made on the following types of plutonium samples:

- Mixed-oxide fuel rods and fuel assemblies,
- PuO_2 powder,
- ZPPR plates.

In addition, the IAEA evaluated the use of the HLNCC in the active mode for assay of uranium-aluminum alloy disks and high-enriched uranium metal buttons.

An example of the work done during the calibration exercise is illustrated by the calibration information obtained for mixed-oxide fuel assemblies. An earlier calibration curve had been obtained[17] by using a mock-up fuel assembly that could contain as many as 28 BWR mixed-oxide fuel rods. Mixed-oxide fuel rods were added to or removed from this

*IAEA staff member.

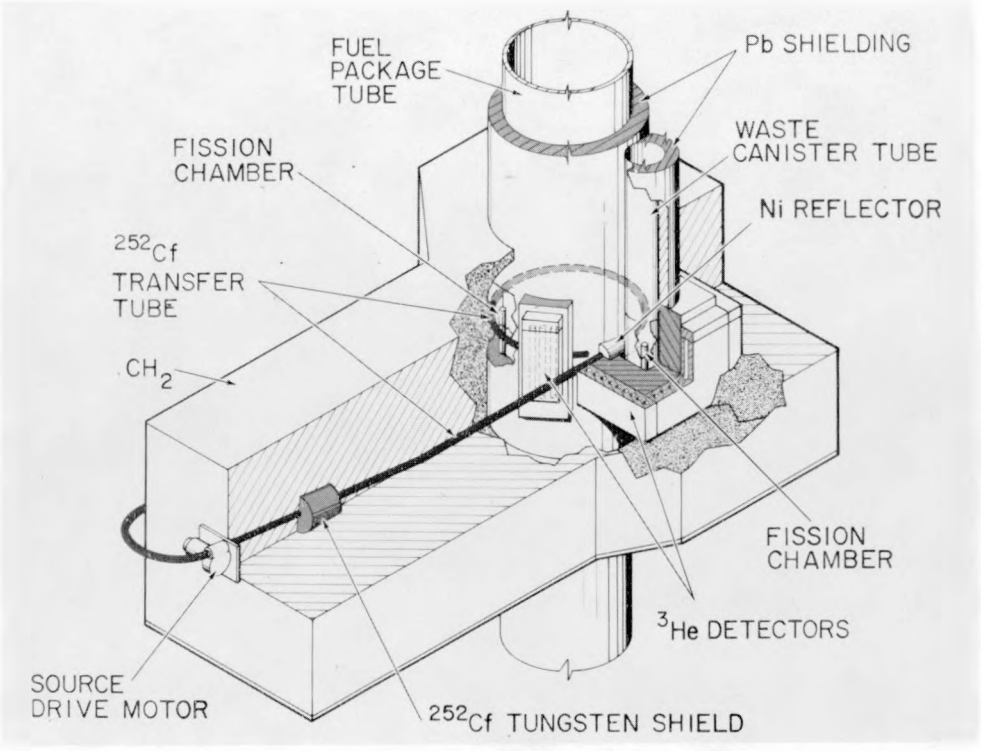

Fig. 27.
Schematic of the Shuffler for FAST.

assembly and a calibration curve was generated that gives the coincidence response of the HLNCC as a function of the number of rods (or the amount of plutonium) in the assembly.

The IAEA[18] pointed out that a calibration curve generated in the above manner could lead to incorrect assay values if the amount of uranium, or heavy metal, in the sample being assayed differs from that in the standards used for calibration. The IAEA argued (1) that a mixed-oxide fuel assembly should be viewed as a uranium assembly containing a small amount of plutonium, not as a plutonium assembly, and (2) that the calibration curve should be linear with plutonium content (at least for low plutonium content). The nonlinearity observed in the earlier calibration curve[17] (generated in the manner discussed above) was postulated to be due to the varying amount of uranium in the assembly. The variations changed both the value of the fast-neutron multiplication of the assembly and the efficiency of neutron detection of the HLNCC by decreasing the neutron leakage from the open ends of the HLNCC. The IAEA postulated that the response should be linear with the plutonium content if the heavy metal content of the assembly (primarily uranium) remains constant.

IAEA made measurements during the calibration exercise to study the importance of the heavy metal content of the assembly and to establish adequate calibration curves.

Mock-up fuel assemblies were loaded with a mixture of low-enriched uranium rods and mixed-oxide rods to give both uranium and plutonium loadings nearly identical with the loadings of actual assemblies. Both a 28-rod mock-up assembly (giving a loading of ~34 g heavy metal/mm) and a 37-rod assembly (~45 g heavy metal/mm) were used in the measurements. The two assemblies had the same outside diameter (~113 mm); only the fuel rod densities differed. Calibration curves were generated by exchanging mixed-oxide fuel rods for uranium rods and vice versa. This calibration method produced a variation in the plutonium content of the assembly, but kept the heavy metal (mainly uranium) loading nearly constant. Figure 28 shows the calibration curves, along with a curve obtained from the earlier described calibration method.

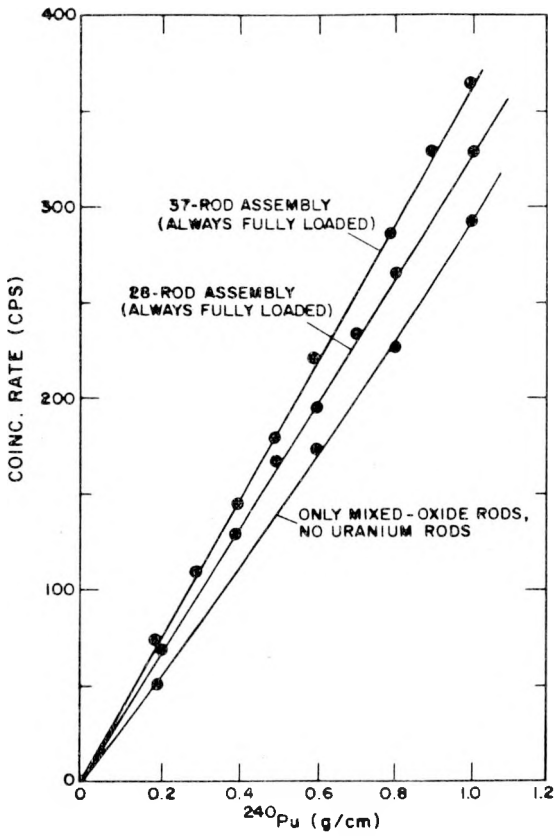

Fig. 28.
Coincidence response of the HLNCC for various mixed-oxide fuel assemblies. The 28-rod and 37-rod assemblies always are completely loaded and the plutonium content is varied by exchanging low-enriched uranium rods for mixed-oxide rods and vice versa. The lower curve is the response for an assembly that is partially loaded with only mixed-oxide rods.

The results in Fig. 28 verify the hypothesis that the HLNCC's response to mixed-oxide fuel assemblies depends not only on the amount of plutonium in the assembly but also on the amount of heavy metal there. With a fixed amount of heavy metal in the assembly, the response per gram of plutonium is constant and is independent of plutonium content. When the amount of heavy metal in the assembly increases (37-rod assembly vs 28-rod assembly), the response increases. For example, the response of the 28-rod assembly is ~330 coincidence counts/s per gram ^{240}Pu/cm in the assembly, and the response of the 37-rod assembly is ~365 coincidence counts/s per gram ^{240}Pu/cm.

D. Evaluation of Fuel Pin Scanners for the Hanford Engineering Development Laboratory (M. S. Krick and H. O. Menlove)

HEDL (Hanford Engineering Development Laboratory) contracted for the design and manufacture of an intermediate fuel pin scanner (Ref. 15, p. 34) that can assay FFTF-type (Fast Flux Test Facility) mixed-oxide fuel pins. The advanced scanner, whose specifications are outlined in Ref. 15 and which was scheduled for delivery in 1981, is no longer a requirement for HPFL (High Performance Fuel Laboratory).

LASL is supplying documentation on the LASL-designed mixed-oxide scanner[19] and performing detector stability studies to assist HEDL with the intermediate scanner. LASL will also perform moderator calculations to evaluate the new ^{252}Cf irradiation assembly.

The vendor for the intermediate scanner is considering NaI and proportional counter systems for the assay of the total fissile content of the fuel pins. The stability of these gamma-ray detectors is the primary consideration, because the standard deviation of the precision must be <0.2% to meet the accuracy specification of <0.65% (2σ) for the total fissile content.

LASL measurements indicate that under laboratory conditions a stability <0.1% (1σ) can be achieved with either a proportional counter or a stabilized NaI system, although the detection efficiency of a proportional counter is an order of magnitude lower than that of an NaI detector.

E. NDA Methods for Process Control Study at TA-55 (C. A. Spirio, N. Ensslin, J. Parker, L. Speir, G. Walton, R. B. Walton, and D. Bowersox*)

Planned in-line measurements of plutonium-containing solids and mixed oxides in a glovebox

*Group CMB-11.

will involve use of neutron and gamma-ray techniques. The measurements will be made at TA-55 and will be supported by SRL (Savannah River Laboratory) Contract 820.3. This joint CMB-11/Q-1 effort will evaluate the effects of boat geometry, mass, moisture, treatment, and chemical and isotopic compositions of the measured samples.

The system will consist of the following items: (1) microprocessor-based HLNCC system (well counter) for neutron measurements, (2) germanium detector-gamma ray detector system, (3) integral computer system with mass storage, (4) mechanism for the well counter to handle the plutonium samples, (5) instrumentation, interfaces, and display for weight balances and furnace, and (6) glovebox with appropriate plumbing penetrations, view ports, and instrumentation penetrations for sample-handling.

The layout of the facilities and a detailed design of the mechanism are almost complete. The electronics for the well counter are checked out and the germanium detector is ready for installation. The gamma station is undergoing final engineering and physics reviews, with a purchase contract to be let in late August. Detailed design (hardware and software) for the interfaces and system integration will begin soon.

F. Standards for CMB-8 Random Driver (J. D. Brandenberger and E. L. Adams)

Large SNM standards of the order of several kilograms and containing 3-90 g of ^{235}U are being fabricated for use with the CMB-8 random driver. CMB-8 will use these standards to assay cans of leached solids containing widely varying amounts of uranium enriched to 93% in ^{235}U in a leached solid matrix similar to that of the standards. These standards will be used not only for NDA of SNM at DP Site but also the set of six will be available to Q-1 for other programs requiring the use of large standards.

The fabrication of each large standard requires that the standard be split into a set of much smaller samples that can fit into 200- to 400-cm^3 containers. Assays of the smaller samples then are made on the Van de Graaff SSAS (small sample assay station) (Ref. 9, p. 44). The merit of this process is that samples can be assayed in a reasonable time. Because the 200- to 400-cm^3 samples are much larger than the samples ordinarily used for SSAS high-accuracy measurements, a set of data has been taken to evaluate biases introduced by geometric and matrix effects. After the assay data are evaluated, the large samples will be reconstituted from the set of 40-60 small samples. In June and July, assays of six large samples showed a ^{235}U content between 3 and 90 g. Accuracy of the present set of six standards is expected to be 2-4%. As the method is used and further refined, the accuracy should improve to ~1%.

V. DETECTOR AND ELECTRONICS DEVELOPMENT

Enrichment Plant Safeguards: Neutron-Based Enrichment Measurements of Uranium-Fluorine Compounds (J. W. Tape and M. P. Baker)

International safeguards inspectors may have only limited access to enrichment facilities that they must inspect. In a previous report[1] a number of possible instruments and methods are discussed for use in an international safeguards system for a GCEP (Gas Centrifuge Enrichment Plant). One technique involved a combination of neutron singles and coincidence measurements to verify the enrichment of uranium contained in alumina trap material. A simple preliminary experiment was performed in which a standard thermal-neutron coincidence counter with shift-register electronics[20] and a series of well-characterized UF_6 samples were used to verify that the method can be used to "flag" UF_6 samples (or any well-characterized uranium-fluorine compound) having more than a few percent of ^{235}U.

Eight 1S cylinders of UF_6 originally obtained from GAT (Goodyear Atomic Corp.)[21] were measured in a standard well-counter configuration with a singles

counting efficiency of ~15%. Table VI lists the sample mass, enrichment, singles counts, real plus accidental counts, and accidental counts for the indicated counting times.

In the simple picture described in Ref. 1 the singles rate was expected to be proportional to the ^{234}U mass and the ^{238}U mass in the sample, whereas the coincident neutrons arise mainly from ^{238}U spontaneous fission neutrons and are indicative of the ^{238}U mass alone. Therefore, a ratio of singles to coincidence rates should be an increasing function of the ^{235}U enrichment if the ^{234}U enrichment tracks the ^{235}U enrichment. The data of Table VI, corrected for background, are plotted in Fig. 29 as the ratio of singles counts to real coincidence counts vs the sample enrichment. The ratio R behaves as expected up to enrichments near 20% where the curve begins to flatten out and then may decrease.

The deviation of the ratio behavior above 20% enrichment is due primarily to (α,n) neutron-induced fission of the ^{235}U in the sample. In the simple picture, coincidence neutrons arise only from ^{238}U spontaneous fission, and one expects the coincidence neutron rate per gram of uranium to decrease as the ^{235}U enrichment increases. The addition of coincidence neutrons from induced fission actually results in an increase in the coincidence counting rate as a function of increasing ^{235}U enrichment.

The points denoted by a triangle in Fig. 29 were determined by calculating a coincident neutron rate and dividing the calculated rate into the singles rates for samples taken from Sampson.[21] The coincidence rate was calculated from the product of the effective ^{238}U mass for each sample and the ^{238}U spontaneous fission rate. (The effective ^{238}U mass can be calculated from the total uranium mass, the known isotopic distribution for these samples, and the ratio of the spontaneous fission rates for each isotope to the ^{238}U spontaneous fission rate.) These "simple model" points were normalized to the experimental data point for the normal enrichment sample. Clearly, this model fails to explain the data for these samples when the enrichment exceeds 20%.

The points denoted by a square in Fig. 29 were determined by first calculating the coincident neutron rate with a semi-empirical formula that attempts to account for induced fission effects and then again dividing the results for each sample into Sampson's singles rates and normalizing to the data for the normal enrichment sample. The general form of the expression for the coincidence neutron rate is given by

$$N_c = A \cdot M_{eff}^{238} + B \cdot M_U^2 \cdot I_{234} \cdot I_{235} , \qquad (1)$$

where M_{eff}^{238} is the effective ^{238}U mass, M_U is the total uranium mass, I_i is the enrichment of the indicated

TABLE VI

COINCIDENCE COUNTER DATA FOR UF_6 SAMPLES

Sample UF_6 Mass (g)	Enrichment (%)	Time (s)	Singles	Real & Accidental	Accidental
385.0	0.1977	1000	6133	232	4
398.0	0.7108	1000	7841	278	2
364.0	3.001	1000	14079	246	21
398.4	18.15	1000	38206	375	102
364.0	31.71	1000	53114	465	180
357.0	57.38	100	9539	109	55
359.0	69.58	100	11988	176	101
362.5	97.65	100	34484	982	772
Empty 1S cylinder		1000	4143	91	1

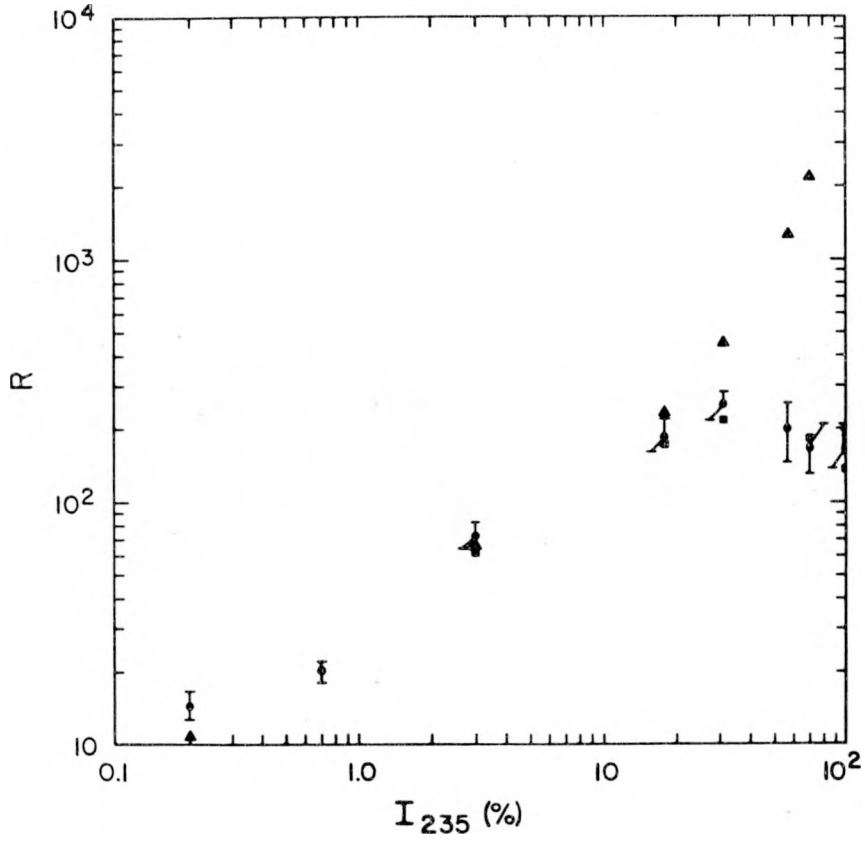

Fig. 29.

Coincidence counter data of Table V, corrected for background. The dots (with error bars) are the experimental ratios of neutron singles to real coincidence counts for UF_6 samples in 1S cylinders plotted against the ^{235}U enrichment of the samples. The triangles are calculated by using a simple model; the squares are based on a model that includes the effects of (α,n)-induced ^{235}U fission.

isotope, and A and B are constants to be determined. This model assumes that, in addition to spontaneous fission neutrons (first-term), ^{235}U fissions are induced by neutrons from ^{234}U associated (α,n) reactions. The constant A was determined by neglecting the second term and using the 0.2% enriched sample data for N_c. The experimental coincidence rate for the 97.7% enriched sample and the value of A were then used to solve for B. Agreement is excellent between this model and the experimental data.

The alumina trap material that this singles/coincidence method is designed to screen is not likely to exhibit the (α,n) multiplication effects shown by the compact 1S UF_6 cylinders measured here. However, even with these samples the technique is capable of alerting an inspector to the presence of high-enrichment uranium-fluorine compounds. Also of interest is the fact that the ^{235}U to ^{234}U ratio for these samples varied from 94.4 to 395.4, resulting in the lack of smoothness of the data and the calculated singles/coincidence ratios when plotted against the ^{235}U enrichment. In spite of the large variation of the 235/234 ratio the data indicate that a screening can still be accomplished.

The presence of recycle uranium with ^{232}U would interfere significantly with the relationship between the neutron singles rate and the ^{234}U content of the sample. In such a case, direct measurement of the ^{235}U content of the sample by gamma-ray methods or active neutron interrogation techniques should be considered.

VI. TRAINING AND TECHNOLOGY TRANSFER

Safeguards Technology Training Program (T. R. Canada and J. W. Tape)

Two courses of the DOE/LASL Safeguards Technology Training Program were offered during this reporting period.

During May 9-11, 34 representatives of the domestic and international safeguards community attended the course, "Measurement and Accounting Systems for Safeguarding Nuclear Materials." Table VII is a list of the lecture topics. A tour was given of the DYMAC (dynamic materials control) system in the new plutonium facility at TA-55, and the afternoon of the last day was reserved for small group conferences and consultation.

Twenty-four people attended the laboratory/lecture course, "Gamma-Ray Spectroscopy for Nuclear Material Accountability," July 10-14. A list of lecture topics and laboratory exercises is given in Table VIII. This year we included new laboratory exercises or demonstrations on x-ray fluorescence and on peak fitting for spectral analysis.

Two LASL instructors participated in the NDA segment of the 9th Introductory Course in Agency Safeguards, given by the IAEA in Vienna. The course was at a technical level suitable for new inspectors. Use of the Eberline SAM-2 was emphasized for identification of source material, as was its use as an enrichment meter. Transmission-corrected gamma-ray techniques were not covered and no gamma-ray plutonium measurements were made. Some neutron experiments with the SNAP detector were conducted and the HLNCC and Silena analyzer were demonstrated. Lack of available SNM in Vienna is a serious handicap to such a course, and the LASL instructors felt that the 15 new inspectors taught in Vienna would also benefit from the LASL "Fundamentals" course to be offered in October 1978.

TABLE VII

PROGRAM FOR "MEASUREMENT AND ACCOUNTING SYSTEMS FOR SAFEGUARDING NUCLEAR MATERIALS"

FUNDAMENTALS
Overview of the LASL Safeguards Program
Goals of Material Accounting
Structure of Safeguards Systems
Impact of Process Design
Safeguards Systems Modeling and Simulation
Decision Analysis
Decision Analysis Exercise
IMPLEMENTATION
Review of Available NDA Techniques and Instrumentation
Personnel Monitoring and Vaults
Computer Systems and Communications
Reliability and Security of Information Systems
DYMAC at TA-55 as an Example
COORDINATED SAFEGUARDS FOR MATERIALS MANAGEMENT IN A FUEL REPROCESSING PLANT
Introduction
Facility Description
NDA Instrumentation
Chemistry Techniques
Model—Simulation, Cost, and Manpower

TABLE VIII

LECTURE TOPICS AND LABORATORY EXERCISES FOR "GAMMA-RAY SPECTROSCOPY FOR NUCLEAR MATERIAL ACCOUNTABILITY"

Principles and Methods of Gamma-Ray Spectroscopy—Laboratory Exercises

Gamma-Ray Techniques for Nondestructive Assay of Special Nuclear Materials in Solution

Quantitative Passive Gamma-Ray Measurements of Plutonium and Uranium

Absorption Edge Densitometry—Laboratory Exercises

U-Pu Solution Assay by Transmission-Corrected X-Ray Fluorescence—Laboratory Exercises

Peak Fitting and Spectral Analysis

Spent Fuel Measurement

Nondestructive Analysis Techniques and Instrumentation Based on Neutron Measurements

A ^{252}Cf-Based Nondestructive Assay System for Fissile Materials

Enrichment Plant Safeguards

PART 2

DETECTION, SURVEILLANCE, VERIFICATION, AND RECOVERY

GROUP Q-2

Carl Henry, Group Leader

E. J. Dowdy, Alternate Group Leader

Activities of Group Q-2 are directed toward the development of compact and highly sensitive instruments for the detection and surveillance of SNM. The group actively participates in NEST (Nuclear Emergency Search Team), DOE's program to provide immediate response to nuclear emergencies involving accidents, lost or clandestine materials, and terrorist threats. Q-2 provides personnel, techniques, and procedures for NEST exercises as well as design data for new and/or improved portable and mobile nuclear search systems in support of the NEST program. Because much of the effort in this area is classified or sensitive, the work is reported separately in classified progress and topical reports.

During May-August the design of a fixed vehicle monitor was completed and construction starts soon. We continued to evaluate parameters related to hand-held SNM monitors. We have had interactions with SLA (Sandia Laboratories, Albuquerque) on the Fast Critical Assembly Safeguards and the Enrichment Plant Safeguards projects. Progress continued on the Real-Time Inventory project with the computer checkout of the 16-shelf system. We continued support of Safeguards Training and Technology Transfer.

I. PERIMETER SAFEGUARDS

A. Personnel and Vehicle Monitors

1. Vehicle SNM Monitor Study (P. E. Fehlau, R. Payne,* R. Hemphill,** R. Zirkle,** and J. Landt***)

Our study of the effectiveness of vehicle SNM monitoring began with the determination of the optimum configuration of gamma and neutron detectors for a gate monitor that would detect plutonium in a vehicle. A test-bed monitor using these detectors was designed and construction will start soon.

A primary concern in monitoring vehicles for SNM is the shielding afforded by the vehicle itself. The capability of a vehicle to carry a substantial amount of additional shielding material is also a concern. A detector for vehicle monitoring should be capable of detecting both lightly and heavily shielded SNM. Previous experience with personnel SNM monitors[22] showed that plutonium can be detected with a gamma-ray or neutron detector even though shielded by a moderate gamma-ray absorber. We chose plutonium as a target material for detector optimization and for monitor design. The monitor also can be used to determine a threshold detection level for more easily shielded materials. We can also use this test bed to establish those situations where the fixed gate monitor approach to vehicle monitoring may not be cost-effective.

We started optimization of the gamma detector on the basis of previous work[3] that developed a NaI(Tℓ) gamma detector array for detection of low-level radiation sources. The published work provided two parameters, the NaI(Tℓ) detector optimum thickness and the optimum energy window. A conclusion was that for unshielded plutonium, NaI(Tℓ) thicknesses of 1.3 to 7.6 cm are essentially

*Group E-2.
**Group ENG-4.
***Group E-4.

equivalent and a window from just above the amplifier noise to 450 keV was best. On the other hand, a NaI(Tℓ) thickness of 3.8 to 7.6 cm and a window from 330 to 450 keV was optimum for material shielded with 0.32- to 1.27-cm-thick lead. The results for iron or concrete shielding were similar to those for the unshielded case. It is desirable to detect both shielded and unshielded plutonium for our vehicle monitor application, so the referenced study was re-examined to determine the best window for the mixed case. The decrease in the detectability S^2/B, where S is the net signal and B is the background, was determined to be 70% for an unshielded source using the 330-450-keV window optimum for a shielded source, but was only 20% for a shielded source using the window between noise and 450 keV. Consequently, we plan to use the wide unshielded source window for this application.

Two considerations determined the particular NaI(Tℓ) detector geometry: the ratio detectability/cost of each detector used in the previous study[23] and the off-axis response of two detector shapes. The two shapes were 12.7-cm-diam, 5.08-cm-thick NaI(Tℓ) and 5.08-cm-diam, 15.2-cm-long NaI(Tℓ). The off-axis response of the two was essentially equivalent. An advantage of the latter detector is that for a given amount of money and a given detectability requirement, we can design a detection system that will provide a more uniform sensitivity over the monitor area.

The gamma detector enclosure is shown in Fig. 30. The NaI(Tℓ) is enclosed in 0.16-cm-thick cadmium that does not attenuate gamma radiation significantly but attenuates thermal neutrons appreciably. Neutrons are frequently present in large numbers from burst reactor operation and cause a transient increase in background through production of ^{128}I in the detectors. A 0.64-cm lead collimator limits the field of view and reduces background. Styrofoam and fiber glass provide weather protection.

The neutron detector design shown in Fig. 31 uses eight 5.1-cm-diam, 53.3-cm-long, 900-mm-pressure $^{10}BF_3$ gas proportional counters. The moderator is shaped to fit the proportional counter tube and covers only the back side of the tubes. This detector has high sensitivity for thermal neutrons. A series of experiments with bare and moderated fission spectrum neutrons showed that a thin polyethylene

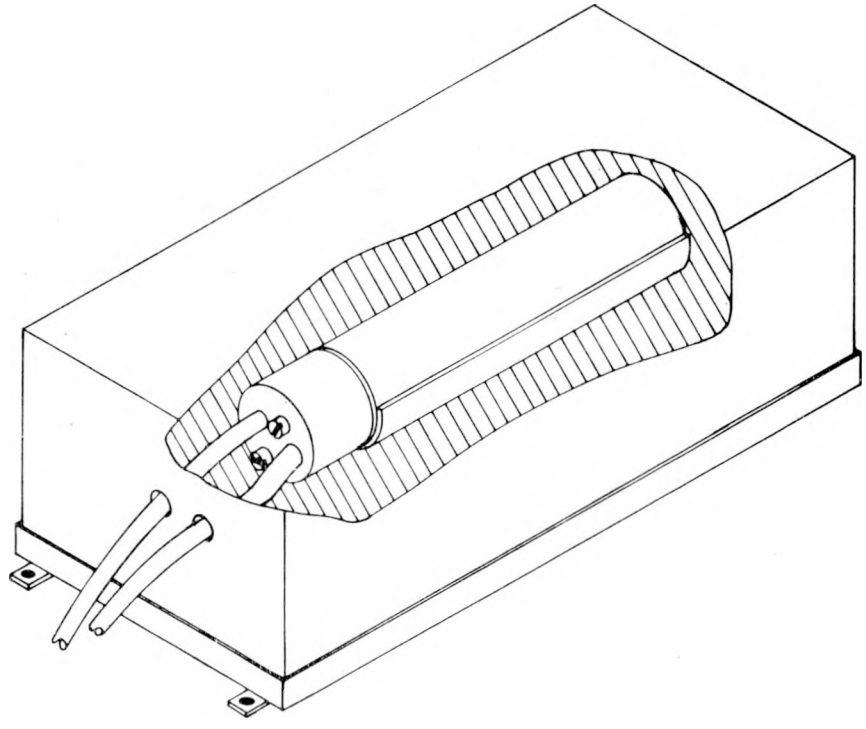

Fig. 30.
Vehicle monitor gamma-ray detector.

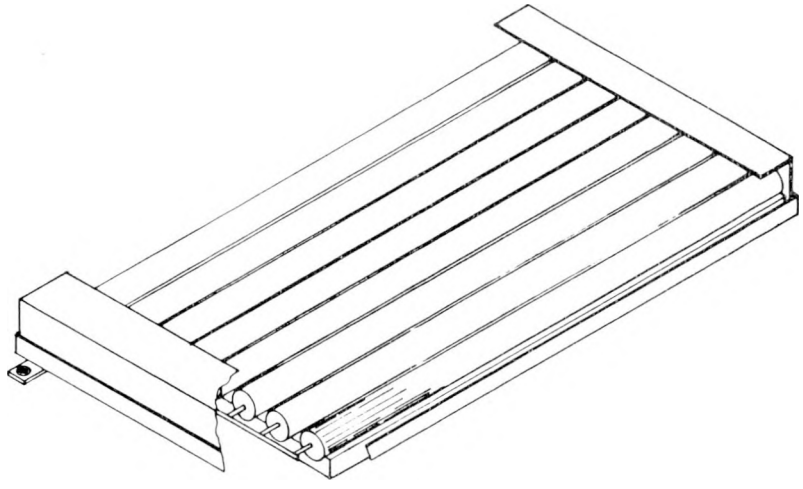

Fig. 31.
Vehicle monitor neutron detector.

sheet up to 1 cm thick placed on the neutron detector assembly between the bare tubes and the source enhanced the detectability of a bare fission-source spectrum and reduced the detectability of a moderated fission-source spectrum. Detailed calculations[24] of detector efficiency variation as a function of neutron energy were made. Some of the material normally present in the vehicle, such as plastic, rubber, and fuel, serves as moderator; but iron is a thermal-neutron absorber. Therefore, the resultant neutron spectrum may have a small thermal component. The question will be addressed further when the vehicle monitor is fully assembled. The response of the detector (Fig. 31) will be determined for selected fission-source positions in a variety of vehicles. Then the response can be determined with varied layers of polyethylene and cadmium on top of the bare tubes for the same variety of source-containing vehicles. From these data and theoretical calculations, we can determine the configuration that offers the best detectability and add the necessary materials to the basic detector package.

The detector assemblies are to be placed in the roadbed at pass-inspection locations. The detector array will then be near the vehicle; will permit the entire vehicle to be monitored during the time it is stationary, which can include time for repeated or extended counts to verify alarms; and will not obstruct normal traffic flow. The array includes eight NaI(Tℓ) detectors and six neutron packages. The placement of detectors provides uniform sensitivity over a rectangular area that will accommodate most of the vehicles being monitored. Long vehicles will be monitored in two stages. Detectors are positioned so they do not lie directly under areas of strong gamma or neutron absorption. Aluminum grating and plate are used as roadbed material to minimize absorption. The detector array placement relative to the protective force station is shown in Fig. 32.

The vehicle shields the detector array from much of the background radiation normally striking the detector. The usual monitoring scheme uses an accurately determined background count rate to calculate an alarm level. Then, when the monitor area is occupied, the count rate, which includes background and possibly source counts, is compared to the alarm level. However, the background reduction by the vehicle reduces the monitor sensitivity. To minimize the sensitivity loss, we plan to predetermine the background reduction for various vehicle types so that a correction can be included in the alarm level calculation. To identify each vehicle in a reasonable time and in a manner easily communicated to the microprocessor control unit, an electronic identification scheme[25] developed at LASL for livestock monitoring will be adapted. A microwave interrogator/receiver in the roadbed is activated when a vehicle enters the monitor. A transponder mounted on the vehicle returns a unique identification signal that will be communicated

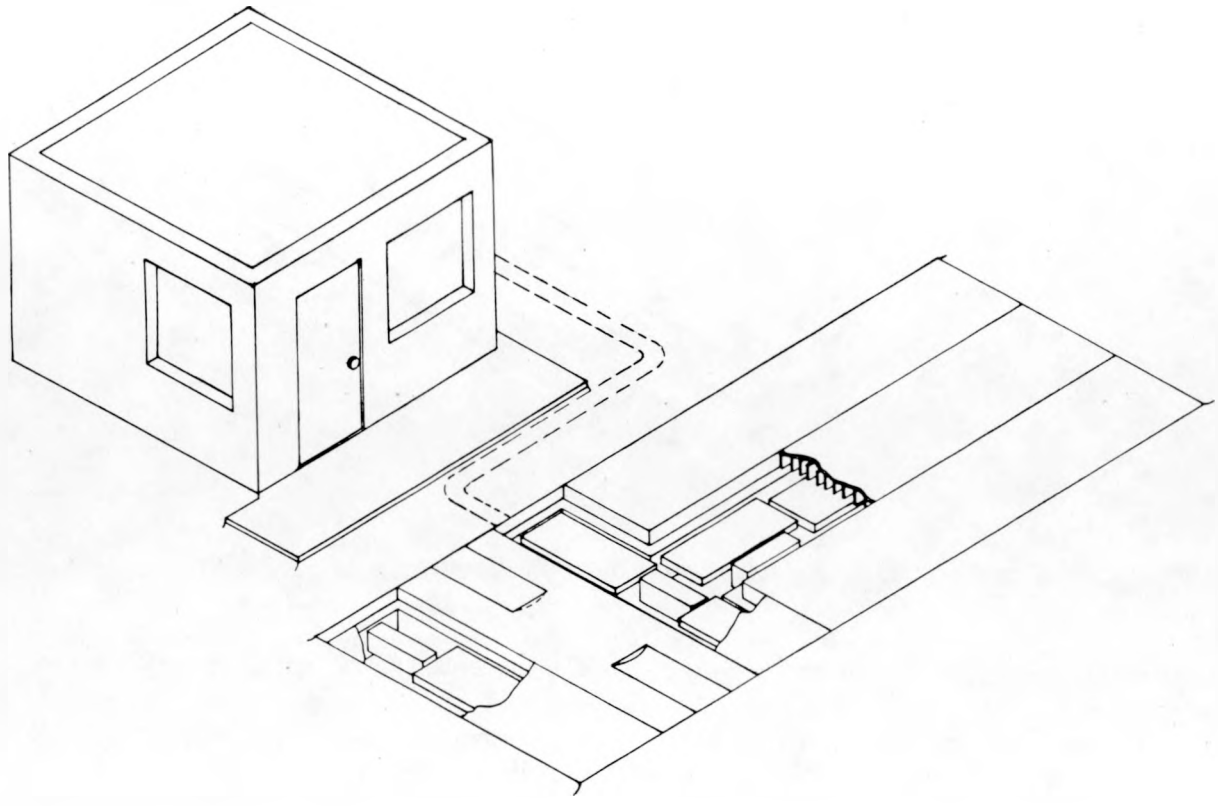

Fig. 32.
Radiation detector placement in the roadbed.

to the microprocessor and used to determine the necessary correction factor in memory.

A final component of the monitor system is a remote detector package that keeps track of the gamma and neutron backgrounds, which can vary because of the monitor's proximity to critical assemblies. These data can be used to compensate for small background variations. If the background increase is excessive, an indication can be given to use alternate means of searching. This component will be located well away from the vehicle monitor so that it is not influenced by sources that may be present in the monitored vehicles. These detector packages are similar to but smaller than the vehicle monitor components. Single neutron and gamma units are in place and being operated to evaluate detector packaging and to gain experience in background variation.

2. Hand-Held SNM Monitor Sensitivity vs Detector Size (W. E. Kunz)

a. Monitor Description. Hand-held SNM monitors are available from National Nuclear Corp. The current model, the HM-3, is a somewhat smaller and lighter version of the earlier model, the HM-1, and the LASL HSS-1050, Mod III. The HM-3, unlike the other models which used only 38-mm-diam, 38-mm-thick NaI(Tℓ) crystals as the gamma-ray detectors, can be obtained with detector crystals of either 38- or 19-mm thickness. The objective of this study was the determination of the effects of varying detector thickness on detection sensitivity.

All monitor models use the same gamma-ray pulse counting system and digital logic.[26,27] Scintillations produced by gamma rays in the NaI(Tℓ) crystal are viewed by a photomultiplier, changed to

electric pulses, and amplified. Pulses that exceed the lower-level-discriminator setting produce logic pulses that are routed to the alarming circuits. A background count rate is determined and a trip level is established that is some preselected multiple of the background count rate and the selected counting interval. If the trip level is equaled by the accumulated counts during the counting interval, an audible alarm is produced. The alarm continues until the end of the counting interval. A new counting interval is initiated, and if the trip level is reached again, the alarm sequence is repeated.

During normal operations the logic pulses are stored in accordance with the settings of the trip-level update, the counting interval, and the preselected multiple of the background rate which is called the alarm level. The counting interval is normally 0.3 s. Alarm levels can be set for multiples of the background: 1.0 to 1.9 (in 0.1 increments) times the background.

Depression of the trip-level update button causes background counts to be accumulated during an interval that is 10 times the product of the counting interval and the alarm level (10 x 0.3 s x 1.4) = 4.2 s, where the alarm level here is assumed to be 1.4. If the background count rate is 100 counts/s, then 420 counts are collected and scaled by 10 (divided by 10 and truncated to an integer) to produce the integer 42, which is added to the 1 (which always remains in the trip-level-storage register) to become a trip level of 43.

The monitor then counts continuously for 0.3-s intervals. If the accumulated count during any interval equals 43, the tone is activated and continues until the end of the interval. This process is repeated during every 0.3-s interval.

b. Performance Testing. The standard test of SNM monitor detection sensitivity simulates the procedure used during actual personnel searches. The standard test is designed so that test results are more reproducible than those from actual searches. For the test the monitor remains stationary and a standard test source (a sphere of uranium containing 10 g of ^{235}U with enrichment of 93% or greater) is moved past the monitor at 0.5 m/s, with the distance of closest approach equal to 0.25 m.

Detection sensitivity was determined for each of the two detector options available for the HM-3 by the test method described above.[28] Standard laboratory electronics were used for gamma-ray pulse processing. A laboratory version of the digital logic system allowed the setting of any desired trip level for the test. The standard test source was rotated past the detector by a 0.796-m radius arm attached to a 0.1-rps motor. With a nominal 0.3-s counting interval, detection probability at a particular trip level and the average count rate were determined from data obtained from an automated system that used timer-scalers to record the elapsed time, the number of times the source passed the detector, the number of counts, and the number of detections. Only the first detection per pass was counted, even though several intervals during the pass might produce alarms. Detection probability determination at each trip level involved at least 4000 passes of the source past the detector.

The count rate produced by the test source as a function of position as it moved past the detector was determined by multiscaling the resulting counts into 0.020-s bins. The multiscale sweep was gated on for the same portion of each pass and continued until each 0.020-s bin contained counts accumulated for 30 000 or more passes. The data are shown in Figs. 33 and 34. The total count rate for every second or fifth bin is displayed. The distance of closest approach of the test source to the crystal was measured from the source center to the nearest point on the detector enclosure. Data were obtained for three detector orientations: with the angle between the source and the longitudinal axis of the detector equal to 0° at the point of closest approach, and similarly for angles of 45° and 90°. Only the 0° and 90° data are displayed. The 90° data show a difference between the two detectors: for the 38-mm-thick crystal, the count rate at the peak is higher for 90° than for 0° because this crystal has a larger cross-sectional area when viewed from the side than from end-on (0°). For the 19-mm-thick crystal, the viewed area at 90° is smaller than at 0°, thus the lower count rate.

Detection probability as a function of trip level was determined for the 19-mm-thick crystal at the 0°, 45°, and 90° angles and for the 38-mm-thick crystal at the 0° angle only. For the thicker crystal, the 0° angle produces the lowest source count rate.

The criterion for comparing monitor sensitivity between these two crystal thickness options was the false-alarm rate. The 38-mm-diam, 38-mm-thick detector's mean background count rate (we assume

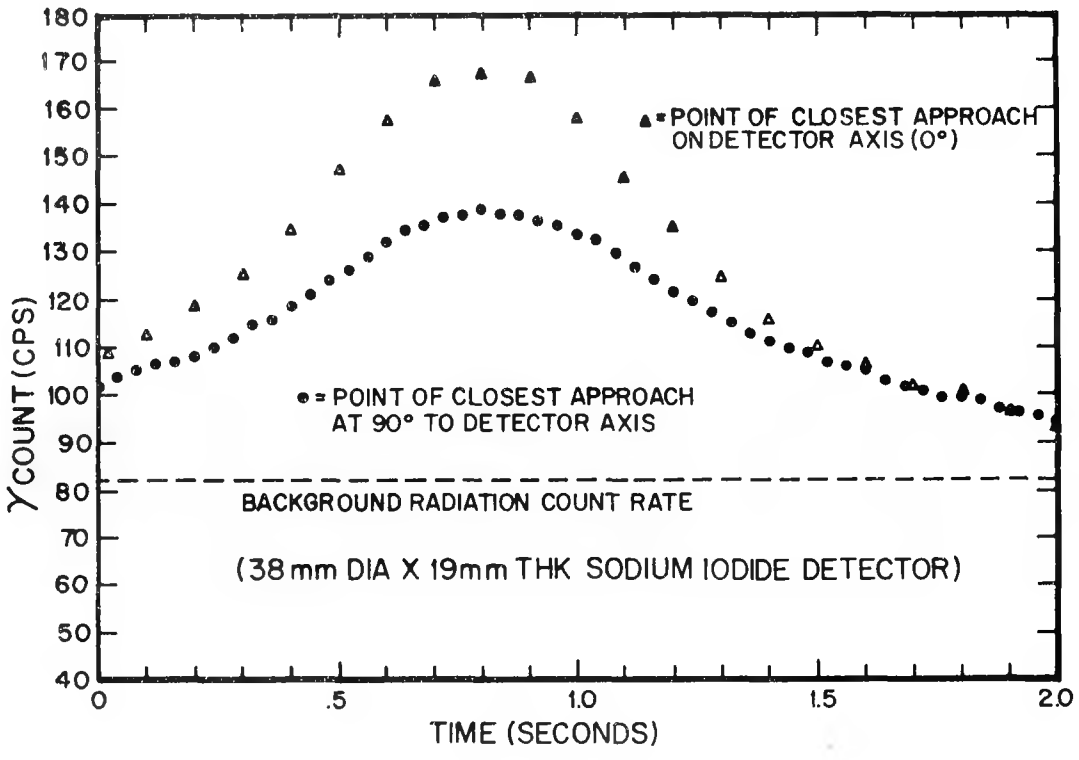

Fig. 33.
Repeat multiscales of the total gamma-ray count rate. Multiscale sweep was started each time the test source passed through the start position, hence the time axis is equivalent to source positions as it was rotated past the detector. Every other 0.02-s bin for 90° points and every fifth for the 0° points are plotted.

that the rate determined during a many-hour counting period is indistinguishable from the mean) was 36 counts/interval; that of the thinner crystal was 22.5. Calculations of the probability of storing each particular trip level were made using the normal distribution and alarm levels of 1.4 for the thick crystal and 1.5 for the thin crystal. Thus, with the thick crystal, the mean stored background count for a trip-level-reset operation is 36 counts/interval x 1.4 x 10 = 504 counts. For example, the probability of storing a trip level of 50 is the probability of obtaining a count that lies between 490 and 500. This count, scaled by 10, is equal to 49, which, when added to the permanently stored 1, produces a trip level of 50.

The results of these calculations are shown in Figs. 35 and 36. False-alarm rates, also shown, were obtained from the Poisson distribution. The probability of storing a trip level that produces a false-alarm rate >3.2% for the thicker crystal is 6.5%; for the thinner crystal, the probability of a false-alarm rate >3.5% is 6.6%. Thus, the 1.4 and 1.5 alarm levels for the two crystal options produce about the same percentage of trip levels with >3% false-alarm rates.

Also shown are the experimentally determined detection probabilities for each trip level and source-detector angle. For the thicker crystal, detection probabilities were measured for the source on the detector axis at the point of closest approach (0°). Any other angle will produce a higher source count rate at the point of closest approach, hence a higher detection probability than that shown. The 0° data for the thinner crystal show essentially equal sensitivity to that of the thicker one. The 90° data show ~4% probability of storing a trip level high enough to reduce detection probability to 75% or less. Thus, depending on the type and method of the

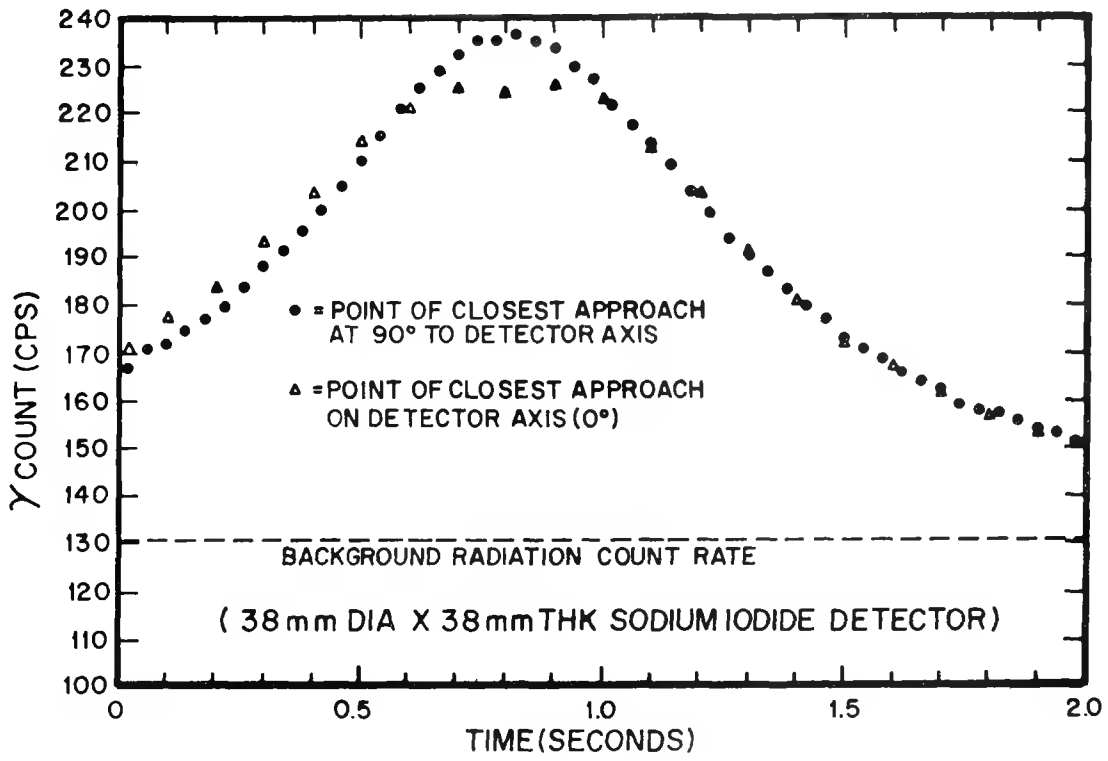

Fig. 34.
Repeat multiscales of the total gamma-ray count rate. Multiscale sweep was started each time the test source passed through the start position, hence the time axis is equivalent to source positions as it was rotated past the detector. Every other 0.02-s bin for 90° points and every fifth for the 0° points are plotted.

searches envisioned for the monitor, the drop in sensitivity for the source passing at 90° may be significant enough to warrant the use of the thicker crystal.

B. Fast Critical Assembly Safeguards (J. T. Caldwell, P. E. Fehlau, A. A. Robba, H. F. Atwater, and S. W. France)

1. Perimeter Safeguards Subsystems—Cooperative Efforts with SLA

Much of Q-2's effort has been devoted to assisting SLA personnel involved in the FCA (Fast Critical Assembly) safeguards effort. Specific tasks are described below.

a. ^{3}He Proportional Counter Purchase. Q-2 specified and ordered a large number of ^{3}He proportional counters for use by SLA. Consolidation of the SLA order with a Q-2 ^{3}He proportional-counter order resulted in a significant price break. The SLA portion of the order is for 74 counters in a variety of sizes and fill pressures. We provided SLA with information to help determine the actual set of ^{3}He counters suitable for those SLA subtasks involving neutron counting.

b. Sandia Comprehensive Personnel Portal Monitor. This personnel portal monitor contains both gamma and neutron detection systems, metal detection, and may include positive personnel identification.

We designed the passive neutron detection system to take advantage of the "neutron tunnel" effect (see Ref. 1, p. 70) by providing polyethylene moderator/reflector on all sides, top, and bottom of the enclosure. Specific thicknesses required were determined in mockup measurements done at LASL

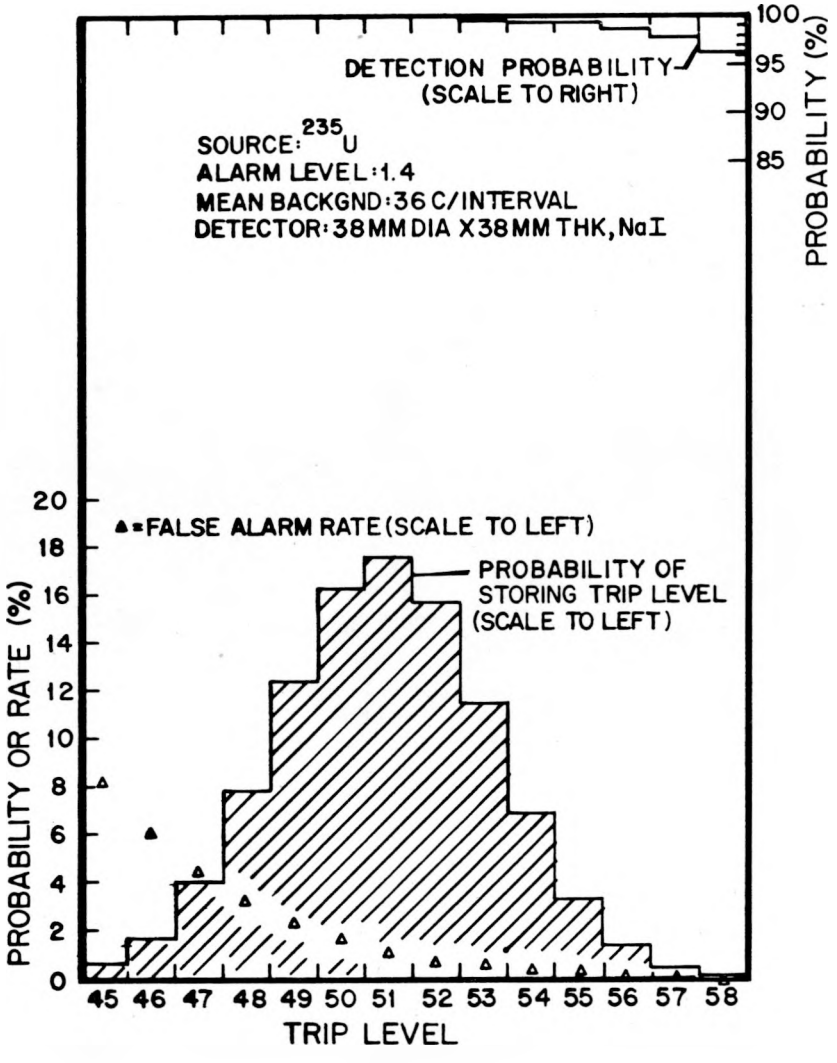

Fig. 35.
Measured detection probability at each trip level is plotted for a source-detector angle of 0° at the point of closest approach. Probability of storing each trip level was calculated from the mean background count, as was the false-alarm rate for each trip level.

by Q-2 and SLA personnel. Helium-3 counter placement was changed from the original "imbedded-in-polyethylene" configuration to the neutron tunnel bare tube on the surface of the polyethylene configuration.

Measured plutonium sensitivity was improved by a factor of ~4 for the same number of ^{3}He detectors in the system. We also studied this system by Monte Carlo neutron transport computer code calculations. These studies are intended to determine general sensitivity changes with alterations in moderating/shielding materials present in the portal.

c. Perimeter Material Pass-Through Monitor. This system is intended to deter or detect passage out of the FCA of high-enriched uranium or plutonium materials that might be hidden in lunch boxes, tool boxes, etc. An SLA D + T neutron generator and a LASL/Q-2 ^{3}He neutron detection system were used to demonstrate delayed neutron detection of contained fissionable materials. These joint measurements were made at LASL. Differential sensitivity for ^{235}U and ^{238}U with a variety of counting geometries and shielding materials was explored.

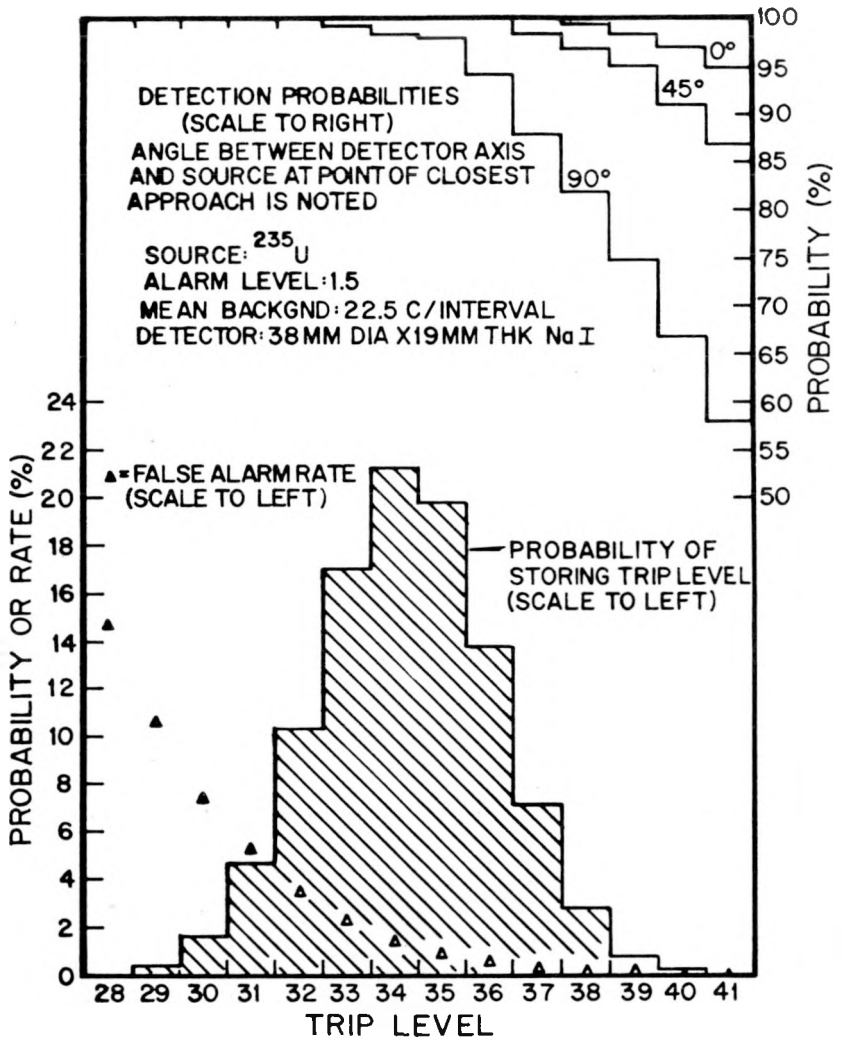

Fig. 36.

Measured detection probabilities at three angles for each trip level are plotted. The probability of storing each trip level was calculated from the mean background count for the trip level update operation. False-alarm rates for each trip level were calculated from the mean background rate per interval.

We suggested another approach for this system that was essentially a version of the ^{252}Cf-based Shuffler system. A movable ^{252}Cf source induces fissions in the sample and subsequent delayed neutrons are detected in a 4π ^{3}He counting system. Basic sensitivities as a function of shielding materials and source strength were determined by measurements done at Q-1 with one of their Shuffler systems. Results were given to SLA.

A third system could be based on the random driver. We and Q-1 have cooperated in several basic sensitivity measurements made with one of the Q-1 random driver systems. Evaluation of commercially available units also has been performed by Q-2, and the information made available to SLA. Joint SLA/LASL measurements with a large commercial random driver unit are to be made soon.

A large collection of the most relevant publications in the fields of passive and active neutron counting and photofission was given to SLA. In exchange, they made available to us their considerable expertise in the neutron generator field. SLA has ordered two neutron generator systems for us. Both

systems will be stabilized pulsed units capable of indefinite 100-pps operation. One unit will be a D + T system and the other will be a D + D unit.

C. Enrichment Plant Safeguards

1. Large-Vehicle Portal Monitor (H. F. Atwater, J. M. Bieri, J. T. Caldwell, P. E. Fehlau, and C. E. Moss)

The tunnel neutron detector has been proposed (Ref. 1, p. 70) for use as a large-vehicle portal monitor at the CTF (Centrifuge Test Facility). The purpose of the tunnel is to detect SNM located in cars, trucks, boxcars, or other carriers which exit through the CTF vehicle portal. Such vehicles would be required to stop in the tunnel long enough for neutron detectors to indicate the presence of any SNM. The portal monitor is designed to detect passive neutrons emitted from UF_6 in the form of feed, tails, or product.

The proposed tunnel has concrete floor, walls, and ceiling with the following nominal inside dimensions: 6.1 m high, 6.1 m wide, and 18.3 m long. The inside walls and ceiling are lined with polyethylene, while the end doors are entirely of polyethylene. The polyethylene serves as a neutron moderator and reflector. The concrete floor has no lining. Neutrons emitted in the tunnel are detected by wickets of ^3He detector tubes. Each wicket is an inverted U-shaped length of detector tube extending vertically along one wall from floor to ceiling, across the ceiling to the other wall, and down that wall to the floor. The detector tubes are positioned against the polyethylene liner rather than being embedded in the liner. A conceptual view of the tunnel neutron detector is shown in Fig. 37.

In effect, the tunnel detector is a large 4π neutron detector in which source neutrons are quickly moderated by the polyethylene liner. The polyethylene albedo for thermal neutrons is $\epsilon = 0.82$, so thermal neutrons can be repeatedly scattered by the liner until they are captured by the ^3He detectors, the polyethylene, or the concrete. The ^3He proportional counters placed within the enclosure see a much greater effective neutron flux than would be the case for isolated slab geometry counters.

Scale-model versions of the design have been tested experimentally and detailed Monte Carlo neutron calculations have been performed on the full-scale version.

a. Experimental Measurements. The tunnel concept was tested experimentally in scale-model polyethylene-lined (rectangular parallelepiped geometry) enclosures ranging in size from 0.48 m x 0.58 m x 0.55 m to 2.44 m x 2.44 m x 3.66 m. These data are shown in Fig. 38, in which the quantity K is plotted as a function of enclosure surface area. Here:

$$K = \frac{\text{Detector Count Rate} \div \text{Neutron Source Strength}}{\text{Projected Detector Surface Area} \div \text{Enclosure Surface Area}}$$

The quantity K is essentially constant over a wide range of enclosure surface area and thus is a convenient parameter to use for detector/enclosure scaling purposes.

The Monte Carlo-calculated K value for the proposed 2.44 m x 2.44 m x 3.66 m full-size enclosure is also shown in Fig. 38. The experimental results are in excellent agreement for smaller size enclosures and the calculated full-size enclosure. Both the calculated K and the measured K values were obtained for a bare, unshielded F(α,n) neutron source at or near the enclosure center. Figure 39 is a photograph of the 2.44 m x 2.44 m x 3.66 m scale-model mockup enclosure.

A number of results can be obtained from Fig. 38. For instance, in the full-size version, if we consider a ^3He proportional counter array of 4.74 m^2 projected area (51 counters, 5-cm o.d., 1.83 m long, 2-atm ^3He fill pressure) and the observed K = 1.7 value, we obtain for the overall detection efficiency a value of 1.7%. One kilogram of UF_6 feed provides a neutron source of ~40 n/s (see Ref. 21); thus, in the absence of shielding, the detection system net count rate would be ~0.68 cps.

If the detection enclosure has been shielded from cosmic radiation with ~5 m of dirt overburden, the 51 ^3He counter system will have a background count rate of ~1.5 cps.* In a 200-s counting time a net of ~136 counts would be recorded. The corresponding background count is 300 ± 17.3. With a 200-s count time, 1 kg of bare UF_6 feed would be detected at 7 or 8 standard deviations above the background level.

*Calculated cosmic-ray shielding effect is based on data in **Handbook of Physics** (McGraw-Hill, New York, 1967), pp. 9-272; measurement of ^3He backgrounds made by J. T. Caldwell (private communication).

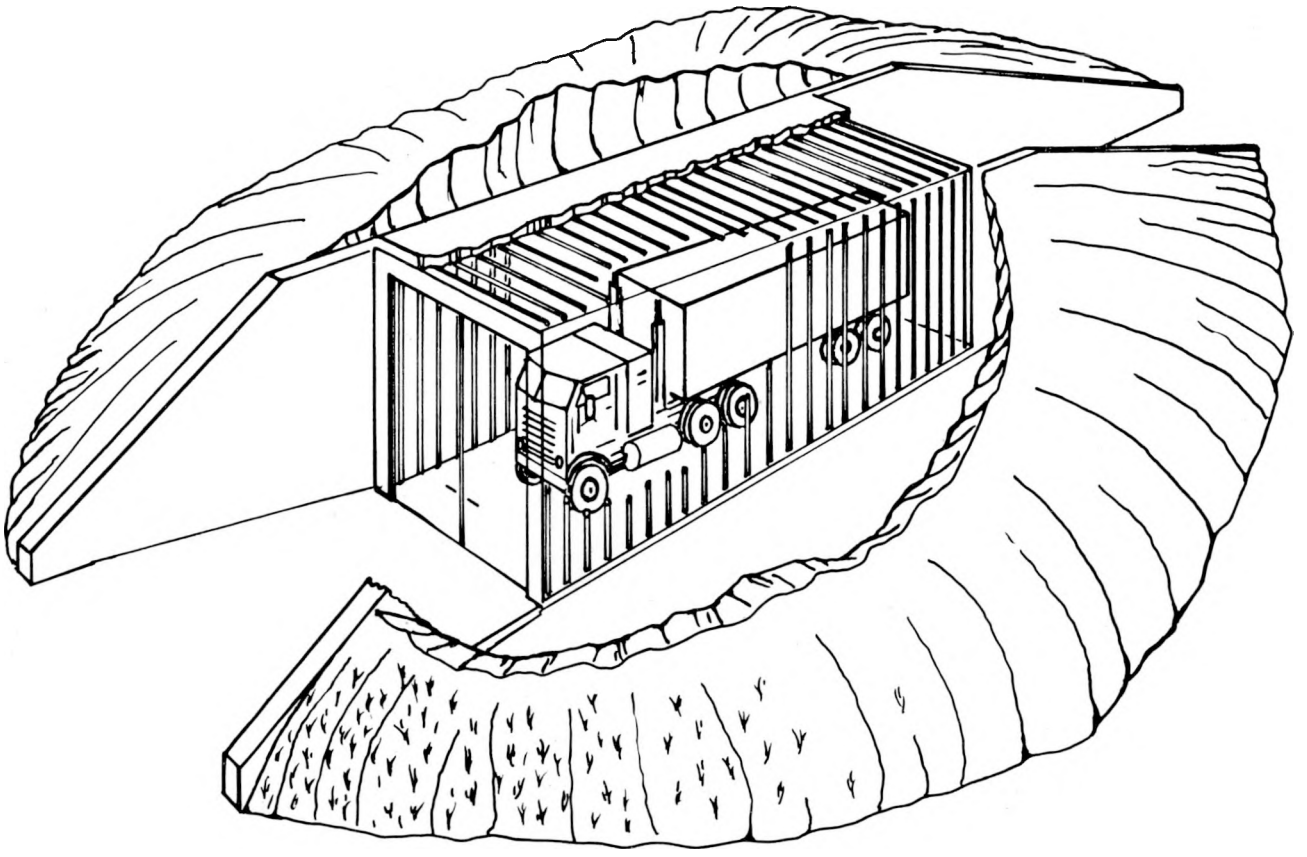

Fig. 37.
Tunnel neutron detector.

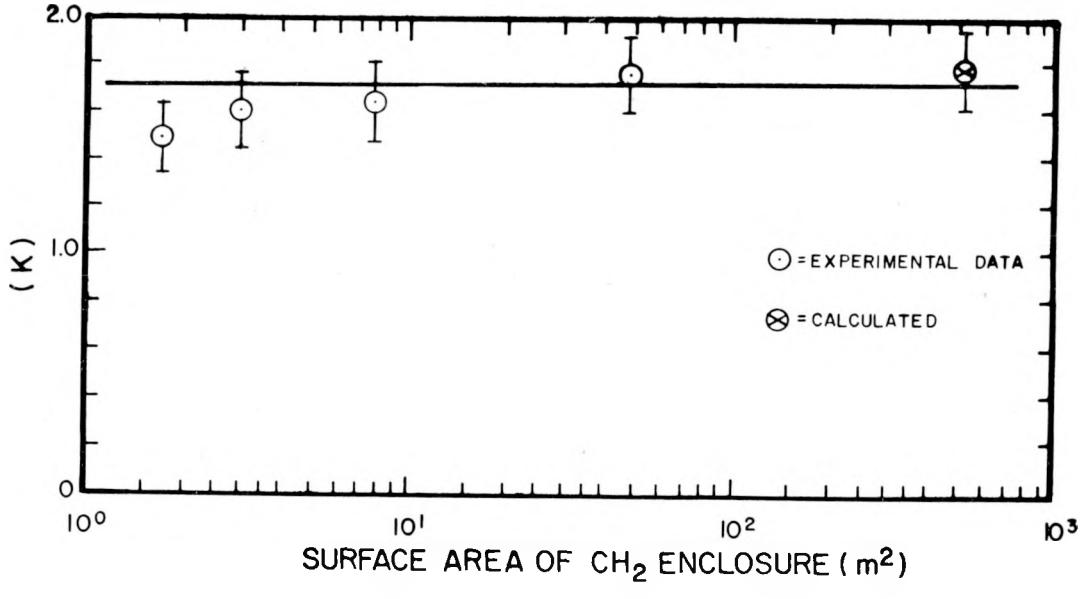

Fig. 38.
Plot of experimental and calculated K values for tunnels of different surface areas. K is a dimensionless neutron detection sensitivity scaling factor (see text).

If a vehicle contained 5 kg of UF_6 feed surrounded by sufficient shielding materials to reduce neutron output by a factor of 10, the same 200-s counting time would result in a net count of ~68. Thus, a heavily shielded 5-kg UF_6 feed package could still be detected with this system at an ~4 standard deviation level.

Because the system sensitivity depends strongly on detector background levels, the cosmic-ray component must be considered carefully. The current design calls for a 5-m-thick dirt overburden on top and on all sides of the neutron tunnel. Measurements of the neutron cosmic-ray background have been made in highway culverts in the Los Alamos area using 1.82-m-long ^3He counters of the type to be used in the ultimate neutron tunnel system. In a culvert roughly 2.4 m wide and 2.3 m high with an average rock and dirt overburden thickness of 1.5 m, we observed a cosmic-ray neutron flux reduction factor of 6.0 ± 0.6. In another culvert having a circular 3.0-m-diam cross section and an average overburden thickness of 3.7 m, we observed a cosmic-ray neutron flux reduction factor of 38 ± 2. On the basis of these measurements, the 5-m-thick dirt overburden specified for the neutron tunnel system is reasonable.

Another source of cosmic-ray-induced background is cosmic-ray spallation reactions in massive materials. We measured this effect by using scrap iron (40 kg total) inside a sensitive, calibrated 4π neutron detector. At a 2000-m elevation (Pajarito Site, LASL) ~0.026 n/kg/s are produced by cosmic-ray interactions in iron. To put those results in perspective, 10^4 kg of iron (a reasonable figure for a tractor-trailer rig or railroad freight car) would result in a 260 n/s source, or the equivalent of ~5 kg of UF_6 feed in neutron output. With 5 m of dirt overburden, this production rate should be reduced by a factor of more than 20—a level that should be a small contribution to the expected total background. Higher Z materials are a considerably greater neutron source. Our results for lead, for instance, indicated 0.20 n/s/kg at 2000-m elevation, or 7.5 times the production rate from iron.

In the 2.44 m x 2.44 m x 3.66 m scale-model system (Fig. 39) measurements were made to investigate relative sensitivities along the tunnel length. Some of these results are shown in Fig. 40. The bottom set of data in Fig. 40 shows how, for a fixed detector location, count rate varies as a neutron source is moved along the tunnel. The count rate is virtually constant for all source positions along the tunnel. (All these measurements were taken with a bare AmF neutron source.) Additional data taken with the neutron source at different heights along the tunnel, at corners of the tunnel, etc., indicate a virtually constant sensitivity for a source at any location within the tunnel—a remarkable result that indicates essentially uniform sensitivity for the system regardless of where an actual UF_6 source might be located in a vehicle being inspected.

Fig. 39.
Scale mockup (2.44 m x 2.44 m x 3.66 m) of polyethylene-lined tunnel neutron detector.

The top part of Fig. 40 shows relative sensitivity for detectors located at different positions in the tunnel for a fixed source location at the tunnel center. Here one observes a slight fall-off of tube sensitivity as a function of position. Detectors located at tunnel ends are ~15% less effective than detectors located at the tunnel center. For all measurements shown in Fig. 40, detectors were located 10 cm from the polyethylene wall and at roughly the mid-height position.

In one of the smaller scale-model tunnels a detector placed a few centimeters from a polyethylene

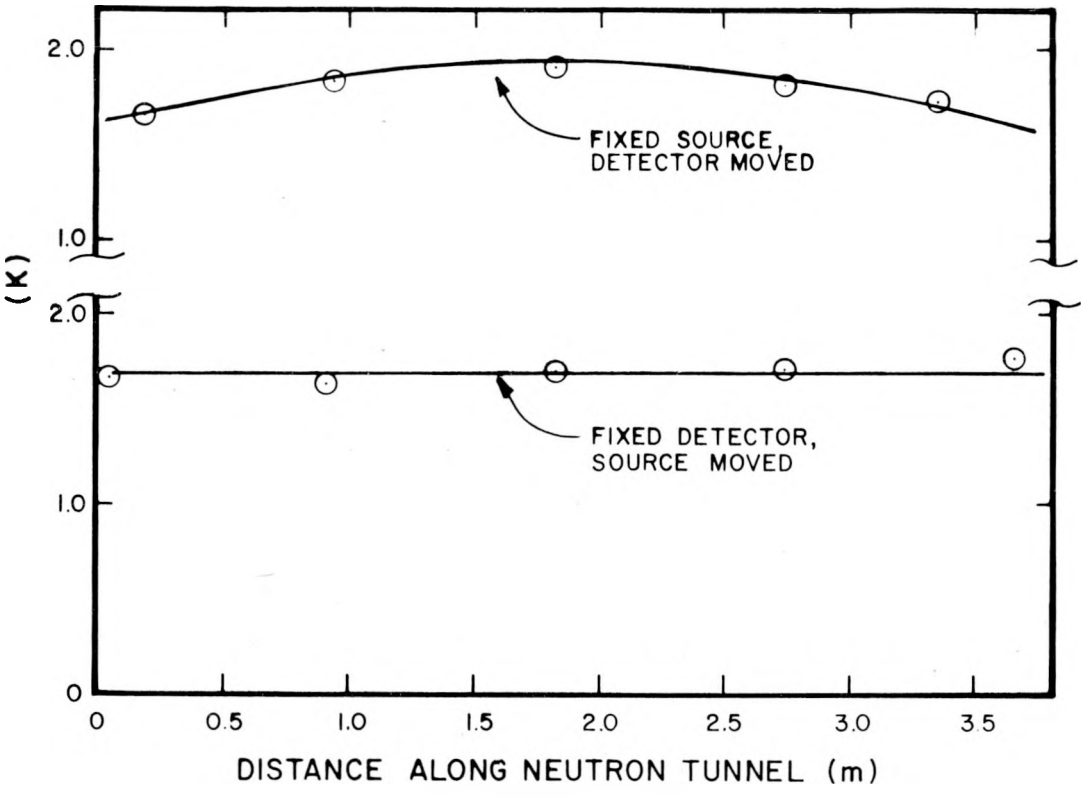

Fig. 40.
Top: measured K variation for a fixed source position and variable detector position. Bottom: measured K for fixed detector and variable source location. All measurements done in 2.44 m x 2.44 m x 3.66 m scale-model system.

wall was more sensitive than when it was placed directly against the wall. In an approximately 10-m² scale model this effect was 15% or more. Detailed measurements in the 48-m² model indicate a 9.5% increase in count rate for a ^{3}He counter placed 8 cm from a polyethylene wall, compared to the count rate from the same counter when it was placed against the wall. Increasing the separation from the wall more than 8 cm did not result in additional increase in count rate.

The observed value of K is a fairly strong function of source neutron energy. Data taken with a variety of calibrated neutron sources are shown in Table IX. Generally, the lower the average source energy, the greater the corresponding K value.

Table X shows the effect on K of various amounts of polyethylene moderator placed around a ^{252}Cf fission spectrum neutron source. K increases with moderator thickness up to an ~5-cm thickness. For this case, K is ~70% greater than for a bare fission source. Small amounts of moderating materials in vehicles evidently tend to increase detection sensitivity.

It was not possible in the 48-m² scale model to enclose a large vehicle completely. However, some measurements were made with a typical large (~1800 kg) American sedan, about 95% of which was within the enclosure. One wall had to be left open for these measurements to be taken. For purposes of comparison, bare source measurements were also made with the enclosure empty and the one wall down. (The vehicle was a 1966 Pontiac sedan and not the sports car shown in Fig. 39.)

Some of the results are given in Table XI. The car degraded sensitivity at all source locations, probably because of competing Fe(n,γ) reactions. However, the degradation was not large, with an average value of 30% loss of signal. The fractional loss probably is proportional to iron mass divided by tunnel volume. If that is true, the presence of large freight cars or

TABLE IX

MEASURED K VALUES FOR BARE SOURCES

Source	E_n(MeV)	K
^{238}PuLi	0.5	2.51 ± 0.02
^{241}AmF	1.2	1.99 ± 0.02
^{252}Cf	2.2	1.76 ± 0.02
^{241}AmBe	4.2	1.51 ± 0.02

TABLE X

MEASURED K VALUES FOR POLYETHYLENE-MODERATED ^{252}Cf SOURCE

Moderator Thickness (cm)	K
0	1.76 ± 0.01
1.3	2.13 ± 0.02
3.2	2.76 ± 0.02
3.8	2.85 ± 0.02
4.4	2.96 ± 0.02
6.4	2.68 ± 0.02

tractor-trailer rigs in the full-scale tunnel should not result in significant signal loss.

Some measurements were made with shielded sources. A reduction in sensitivity of a factor of 9 ± 1 was observed with an AmF source surrounded by a 20-cm-thick (on the average) shield of borated polyethylene (5% B).

Although no measurements have yet been made, a technique has been proposed to determine the presence of large amounts of neutron shielding materials. The technique consists of a measurement of the tunnel neutron die-away time, τ. A diffusion theory calculation for a full-size empty tunnel (with 51 1.83-m ^{3}He counters) yields a τ value of 18 ms. With 10 metric tons of iron (freight car) inside the tunnel, τ becomes 6.3 ms. If 10^2 kg of 5% B-loaded polyethylene is added to the system, the calculated τ value is 4.4 ms. That is, only 100 kg of 5% B polyethylene apparently causes an ~50% change in the detector die-away one would expect from a typical freight car inside the tunnel.

We propose that a detector die-away measurement be included in the tunnel system. The measurement could be performed easily with a pulsed neutron generator and the tunnel ^{3}He detectors. A 1% statistical accuracy measurement could be obtained in ~10 s of pulsed operation so the measurement would not add significantly to the total inspection time.

TABLE XI

EFFECT OF 1800-kg AUTOMOBILE ON K (AmF SOURCE)

Source Location	K (Empty)	K (Auto In)	K(Auto In) / K(Empty)
Top of engine block	1.65	1.51	0.91
Front-seat floorboard	1.55	1.09	0.70
Front dash	1.53	1.34	0.88
Under car (center)	1.59	0.99	0.62
Top of right hood	1.46	1.26	0.86
In front seat	1.40	1.15	0.82
In back seat	0.98	0.67	0.68

b. Calculated Efficiencies. Neutron detection efficiencies are calculated with the LASL MCNP Monte Carlo transport code. A three-dimensional model is used to describe the tunnel, detector, and source geometry. The concrete walls, ceiling, and floor are 15.24 cm thick. Polyethylene liner thicknesses of 1.27, 2.54, or 5.08 cm are used. The cylindrical ^{3}He detectors have a 5.08-cm diameter and a fill pressure of 1, 2, 3, or 4 atm. To simplify the calculations, each 6.2-m section of detector wicket is considered to be a single cylindrical tube. In the actual tunnel, several detector tubes will be placed end-to-end to make a 6.1-m section. Twenty-five detector wickets are evenly spaced at 76.2-cm intervals along the length of the tunnel. That number of detectors corresponds to ~5% detector coverage of the inside tunnel area (projected detector area = detector length x diameter). Neutrons are emitted isotropically from a point source at the geometric center of the tunnel. The density of polyethylene is 0.95 g/cm^3. The composition of concrete is given in Table XII. Figure 41 shows the tunnel geometry used in the calculations.

Neutron detection efficiency is computed as ϵ = number of neutrons captured in ^{3}He tubes per

TABLE XII

COMPOSITION OF CONCRETE[a]

Element	Grams of Element/cm^3
H	0.020
O in water	0.159
O in dry mix	0.957
C	0.118
Mg	0.057
Al	0.085
Si	0.342
S	0.007
K	0.004
Ca	0.582
Fe	0.026
Na	0.011
P	0.007
Mn	0.002

[a]E. P. Blizard, Ed., *Shielding, Reactor Handbook*, Vol. III, Part B, 2nd Ed. (Interscience Publishers, New York, 1962), p. 92.

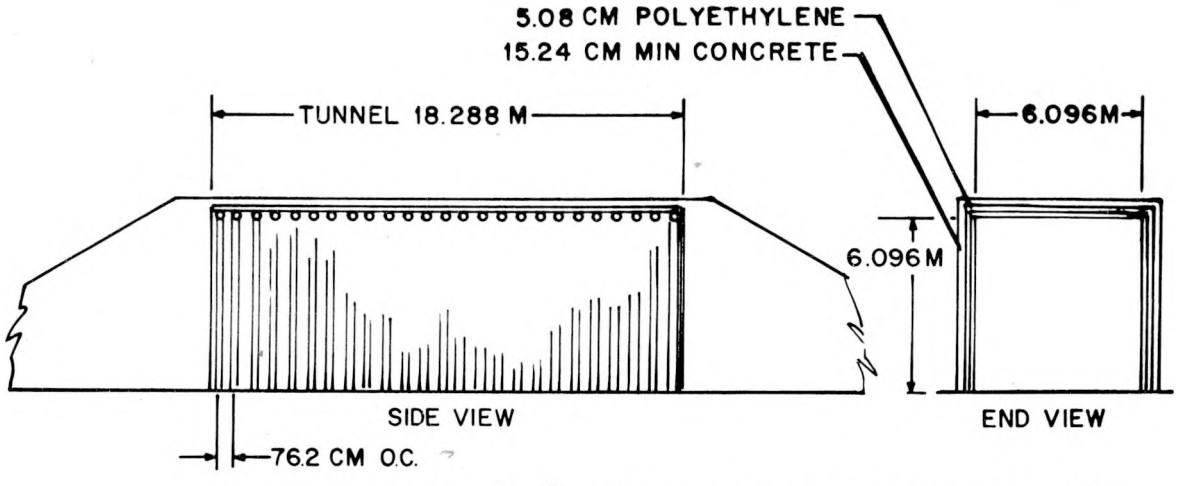

Fig. 41.
Tunnel neutron detector.

neutron started from the source. A reference case was defined as P = 2 atm ^{3}He fill pressure and a polyethylene liner thickness = 5.08 cm. Figure 41 gives the reference case efficiencies with a bare, monoenergetic point source for neutron energies from thermal to 10 MeV. The efficiency varies smoothly from ϵ = 0.22 for thermal neutrons to ϵ = 0.033 at 10 MeV. For 3-atm ^{3}He detectors with a 5.08-cm liner, calculated efficiencies are 14% higher than 2-atm efficiencies over the energy range from thermal to 10 MeV. Statistical uncertainties are <10% for the Fig. 42 calculations.

Table XIII gives calculated efficiencies for the three neutron spectra: ^{235}U(n,f), ^{18}O(α,n), and ^{19}F(α,n). The ^{3}He fill pressure is 2 atm. Each bare point source emits isotropically. The polyethylene thickness is 5.08 cm.

Figure 43 shows the relative efficiency of the 2-atm detector wickets as a function of wicket location along the length of the tunnel. Neutrons are emitted from a bare, isotropic ^{235}U(n,f) point source. The liner thickness is 5.08 cm. Efficiencies are calculated at discrete 76.2-cm intervals, but a continuous efficiency curve is shown because the variation is fairly smooth over the length of the tunnel. Relative efficiencies are normalized to a value of 1.0 at the center wicket. Detection efficiencies are shown for only one-half the tunnel length because neutron detection is symmetric about the center of the tunnel. Detector wickets at the end of the tunnel (9.1 m from the source) have an efficiency that is 40% of the center wicket efficiency.

Figure 44 gives tunnel detection efficiency for 5.08-cm-diam ^{3}He tubes (fill pressures from 1 to 4 atm) with a bare, isotropic ^{235}U(n,f) point source. The liner thickness is 5.08 cm. Detection efficiency

TABLE XIII

TUNNEL DETECTION EFFICIENCIES FOR SEVERAL BARE NEUTRON SOURCES

Source	Mean Source Energy (MeV)	Efficiency
^{235}U(n,f)	2.00	0.078
^{18}O(α,n)	2.05	0.073
^{19}F(α,n)	1.39	0.079

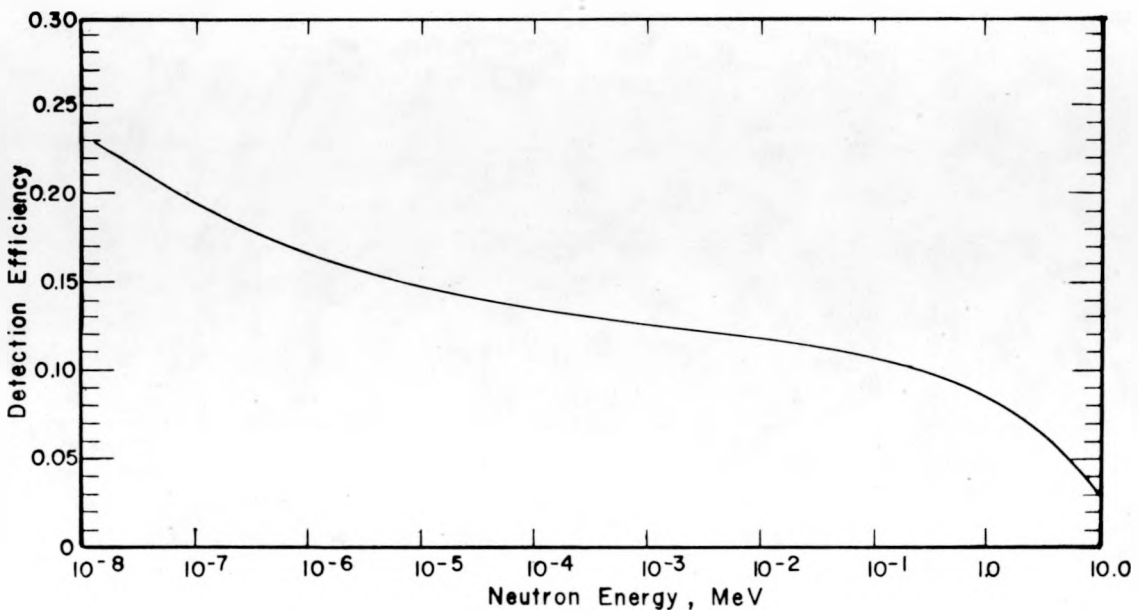

Fig. 42.
Tunnel neutron detection efficiency as a function of neutron energy. Twenty-five detector wickets, 5.08-cm-diam, 2-atm pressure. A 5.08-cm polyethylene liner. Isotropic point source of monoenergetic neutrons at center of tunnel.

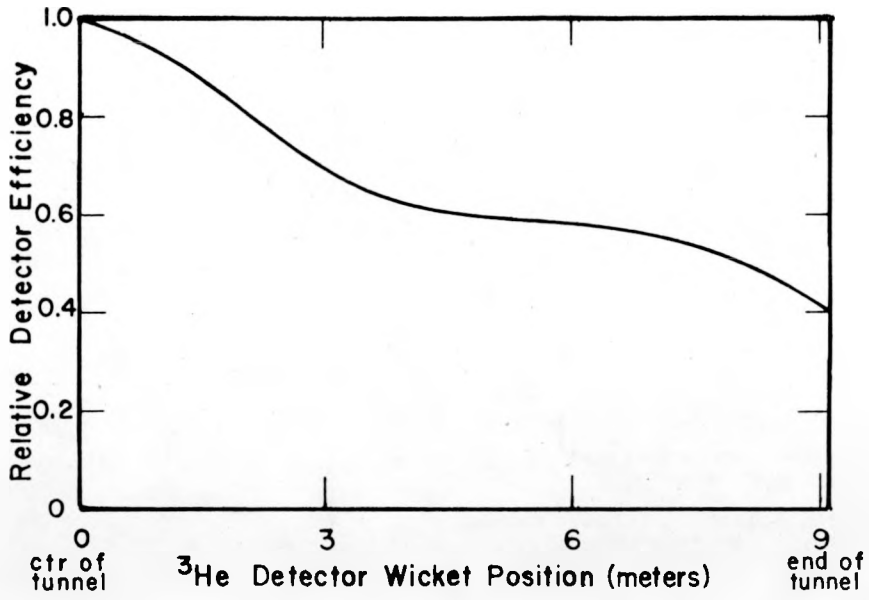

Fig. 43.
Relative detection efficiency as a function of detector wicket position. Twenty-five detector wickets, 5.08-cm-diam, 2-atm pressure. A 5.08-cm polyethylene liner. Isotropic point source of $^{235}U(n,f)$ neutrons at center of tunnel.

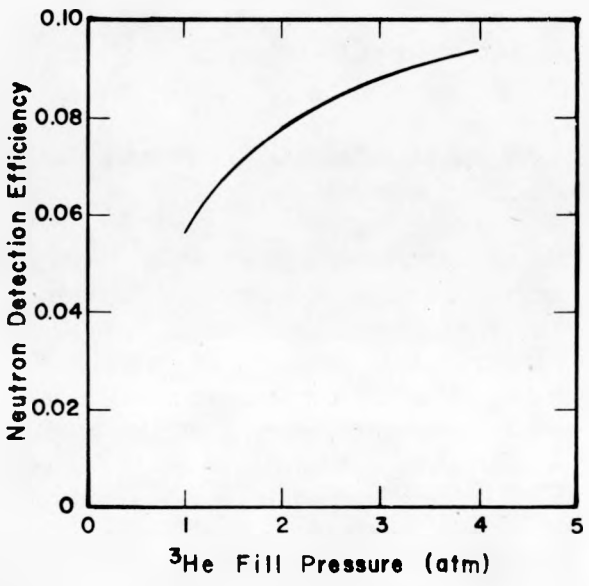

Fig. 44.
Tunnel detection efficiency as a function of ^{3}He fill pressure. Twenty-five detector wickets, 5.08-cm-diam. A 5.08-cm polyethylene liner. Isotropic point source of $^{235}U(n,f)$ neutrons at center of tunnel.

with 2-atm tubes is 39% greater than with 1-atm tubes. Increasing the fill pressure above 2 atm does not increase the efficiency proportionately because the 2-atm tubes are nearly black to thermal neutrons.

Figure 45 shows the effect of polyethylene liner thickness on detection efficiency. With a bare, isotropic $^{235}U(n,f)$ point source and 2-atm ^{3}He tubes, the efficiency with no polyethylene (concrete walls, ceiling, and doors) is $\epsilon = 0.049$. A liner thickness of 1.27 cm gives an efficiency of $\epsilon = 0.063$, an increase of almost 30% over the unlined tunnel efficiency. A 2.54-cm-thick liner gives $\epsilon = 0.072$, an increase of ~50% over the unlined case. Increasing the liner thickness from 2.54 to 5.08 cm results in only a moderate additional increase of 10% (from 50% to 60%, relative to the unlined case). To convert the 2-atm Fig. 42 efficiency curve to equivalent values for a 2.54-cm polyethylene liner, all efficiencies should be multiplied by the factor 0.92.

Because detection efficiencies are sensitive to the source energy, the effect of moderating a fission source was examined by enclosing an isotropic $^{235}U(n,f)$ point source in spherical polyethylene

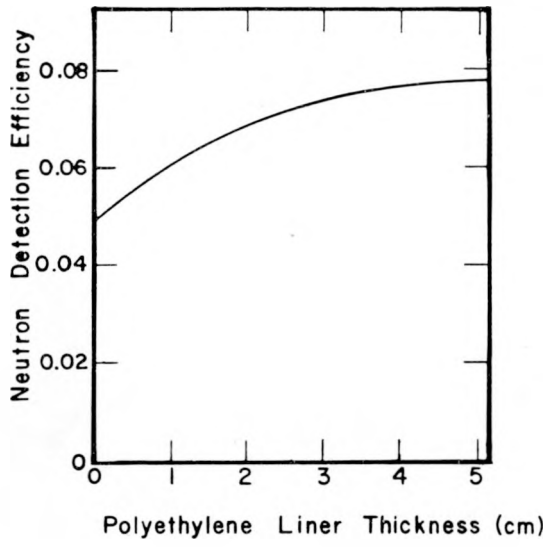

Fig. 45.
Tunnel detection efficiency as a function of polyethylene liner thickness. Twenty-five detector wickets, 5.08-cm-diam, 2-atm pressure. Bare isotropic point source of $^{235}U(n,f)$ neutrons at center of tunnel.

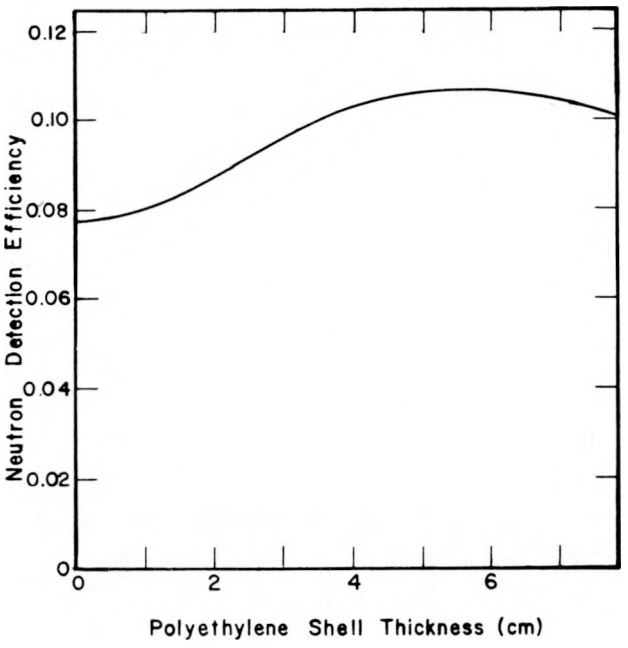

Fig. 46.
Tunnel detection efficiency as a function of source moderator thickness. Twenty-five detector wickets, 5.08-cm-diam, 2-atm pressure. Isotropic point source of $^{235}U(n,f)$ neutrons surrounded by spherical polyethylene shell at center of tunnel.

shells. The shell i.d. is 1.0 cm and the thickness varies from 3.0 to 7.0 cm. Figure 46 shows detection efficiency as a function of shell thickness, with 2-atm detectors and a 5.08-cm liner. A shell thickness of ~5.08 cm gives the highest efficiency. Shells thicker than 5.08 cm overmoderate the source because hydrogen capture effectively competes with scattering in the thicker polyethylene shells.

The tunnel efficiency is expected to vary linearly with the number of detector wickets. For the tunnel with 2-atm tubes, a 5.08-cm-thick liner, and the bare $^{235}U(n,f)$ source, the efficiency was calculated with 13 of the 25 wickets present (alternate tubes were removed). The ratio of efficiencies is (13 wickets efficiency)/(25 wickets efficiency) = 0.56, which is nearly equal to the ratio of wickets, 13/25 = 0.52. Thus, the efficiency can be scaled by the number of detector wickets.

In summary, detailed experimental measurements made on neutron tunnel scale-model systems indicate that excellent sensitivity for the detection of UF_6 in large transport vehicles will be obtained. Concurrent Monte Carlo calculations of the proposed full-size neutron tunnel system are in excellent agreement with the scale-model measurements.

2. Uranium Hexafluoride Enrichment Measurements (E. J. Dowdy)

The GCEP safeguards program plan includes the determination of the enrichment of the audit samples routinely drawn from product cylinders. The samples consist of ~1700 g of UF_6 in stainless steel cylinders. We applied the neutron correlation method, using the moments of the count distribution.[29] UF_6 standard cylinders, described in Table XIV, were interrogated inside a well counter by two different random neutron sources, $^{241}AmLiF(4 \times 10^4\ s^{-1})$ and $^{241}AmB(3 \times 10^6\ s^{-1})$. The correlation parameter, $Q = \overline{C^2} - \overline{C}^2 - \overline{C}$, was measured in each case. The value of Q is a measure of fission-correlated neutron counts, unaffected by singles from (α,n) reactions in the fluorine. The value of Q is expected to be a function of the mass of ^{235}U contained in the sample and, for samples of constant total mass, a function of the enrichment. Results of the preliminary measurements are given in Fig. 47. The correspondence between enrichment

TABLE XIV

ISOTOPIC COMPOSITION OF UF_6 SAMPLES

UF_6 Mass (kg)	Isotopic Composition (wt%)			
	^{234}U	^{235}U	^{236}U	^{238}U
0.3850	0.0005	0.1977	0.0036	99.80
0.3980	0.0049	0.7108	---	99.28
0.3640	0.0244	3.001	0.0184	96.96
0.3984	0.0865	18.15	0.2313	81.53
0.3640	0.1404	31.71	0.3506	67.80
0.3570	0.2632	57.38	0.5010	41.86
0.3590	0.3338	69.58	9.5358	29.55
0.3625	1.032	97.65	0.2523	1.07

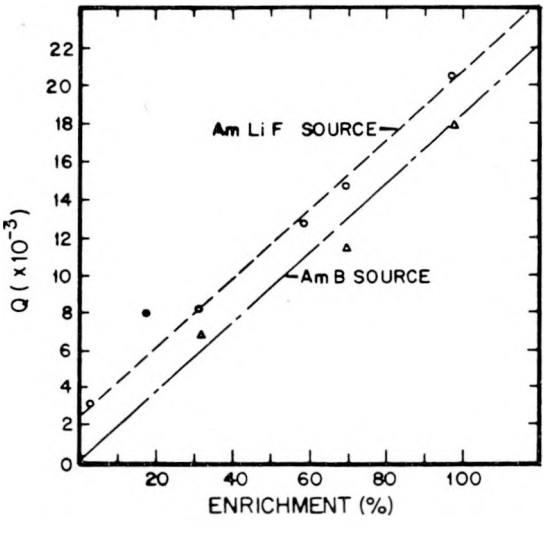

Fig. 47.
Percentage enrichment vs neutron correlation parameter Q for UF_6 sample cylinders.

and Q is established even though the masses of the samples are only of the order of 20% of the mass of the audit samples to be measured. No attempt was made to optimize the characteristics of the well counter or the interrogating neutron source strengths.

D. Real-Time Inventory

1. Shelf System (N. Nicholson, T. R. Capelli, C. D. Ethridge,* and T. H. Kuckertz*)

The electronics boards for the 16-detector array are assembled except for the GM tubes and their lead shields. The boards were checked by placing them in the shelf array and attaching the array to the Nova 3 computer. A small capacitor was inserted in place of the parallel plate capacitance of the scale, allowing the oscillator to operate and permitting that portion of the circuit to be checked. The gamma section of the circuits cannot be exercised until the GM tubes are installed. Each detector was checked for its responsiveness to commands: recognition of its identification and transmission of information stored in its registers. The checking uncovered programming errors which are now corrected. Modifications were made to the printed circuit board to eliminate the capacitive effect of two adjoining parallel runs which affected the operation of the scale.

A new version of the printed circuit board has been designed. The original 20 cm x 20 cm board was reduced to 10 cm x 10 cm, an area reduction of 75%. This reduced circuit board, shown in Fig. 48, is now being used in the 16-detector array and will be used in the array planned for TA-55. The primary purpose of the smaller circuit board is to allow four shelf monitors to fit into a single, 1 ft^2 shelf location, such as those in the new plutonium storage facility at TA-55.

After the 16 electronic boards were completely checked and debugged, they were tested continuously for 10 days, during which each monitor was read twice each second. The data were then checked for consistency. The readings, obtained only from the scale portion of the monitor, were read by the computer, and the minimum and maximum values, together with a mean value, were recorded on disk. A report log was printed out to ascertain that the system was functioning properly. The results of these tests indicate that the scale portion of the monitors is stable, with a 0.5% variation between

*Group E-5.

the minimum and maximum values for any individual monitor. The testing enabled us to establish the reliability of the systems electronics, software, and hardware. The parallel plate weight sensor and the Geiger tube will be assembled into a complete detector configuration (Fig. 49), and the completed monitor will be checked in a similar manner. The 16 completed and checked monitors will be installed in the storage vault at Pajarito site and plutonium samples will be placed on each detector.

A time monitor, which supplies accurate time information to the Nova 3 computer, will occupy a location and an address in the shelf monitor array. One time monitor is required for every set of 127 shelf monitors and provides the precise time duration that the array of monitors has been instructed to count. The monitors are designed to eliminate any time jitter that occurs in the computer software and internal timer. The software for the timer has been written, debugged, and is operating satisfactorily.

A diagnostic monitor is being fabricated to test the shelf monitors as they are completed. This monitor was designed to test individual monitors or to be placed in the array, much like the time monitor, to provide information on the status and operation of the array in real time. It will save hours of effort spent in debugging the monitors and will be used extensively during the testing of the 250 detectors planned for the TA-55 vault.

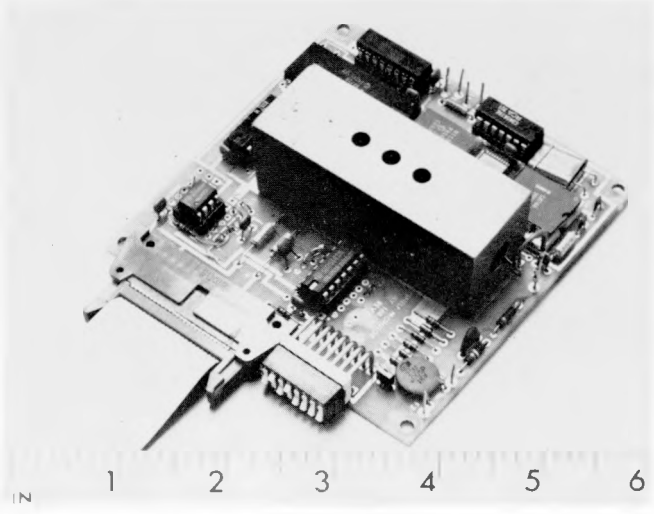

Fig. 48.
Shelf monitor; assembled printed circuit card.

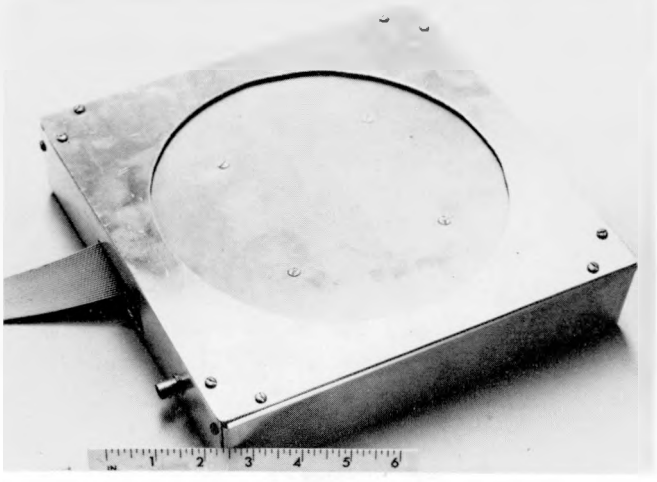

Fig. 49.
Assembled shelf monitor.

2. Proposed TA-55 Shelf System

A Nova 3 computer located at TA-18 will control and monitor the more than 200 shelf detectors planned for TA-55. The scheme is contingent upon obtaining two or three dedicated phone lines between the two sites so that the shelf array can report to the Nova 3 and the Nova 3 can communicate with the DYMAC computer at TA-55. With that arrangement our existing computer system can provide computer monitoring and control of the shelf array without being relocated to TA-55. If the demonstration period of the shelf system is greatly extended or if the number of shelf detectors is increased substantially, a dedicated computer will be required at TA-55.

3. Computer System/Software

Software has been written for a 16-shelf-monitor system plus the time monitor. This software now exercises each of the shelf monitors and keeps in a disk file the appropriate statistical data on their operation. This system has demonstrated the stability and reliability of the shelf monitors and software.

The new Versatek printer-plotter is operational. Its software has been written, assembled, and is performing satisfactorily. The printer-plotter has been useful for plotting high-quality curves and for fast counting of data. A logarithmic axis routine has been written for these and other data that require logarithmic plots.

The Nova 3 computer system has been configured for simultaneous operation of a portal security station and a shelf system. A possible physical layout for such a system is shown in Fig. 50. Figure 51 indicates how the various devices interface with the Nova 3 computer. The present peripherals of the computer system also show. Figure 52 shows the CAMAC subsystem, the specific CAMAC modules used, and their functions. All instrumentation used in the Real-Time Inventory system, except for the shelf monitors, is connected to the Nova 3 through the CAMAC crate. The Bi Ra, Model 1303 crate controller, has proven reliable with the Nova 3 computer.

E. SLA/Rockwell Plutonium Protection System (N. Nicholson and T. H. Kuckertz*)

The "hot" portion of the demonstration period was completed August 25 and is now in the debug and analysis phase, which should be complete by the end of October and will include a 4-wk period during which tours of the plutonium protection system will be given. The system will be dismantled and returned to SLA by the end of the year.

The basic verification station functioned well during the hot demonstration period and proved the importance of nuclear detection techniques in confirming plutonium within the sealed SLA overpacks. For example, recently we were told that the verification station was malfunctioning, and SLA suspected the logic system or detectors to be at fault. SLA personnel at Rockwell were given a diagnostic procedure by which to isolate the problem so that defective components could be shipped to LASL for repair or

*Group E-5.

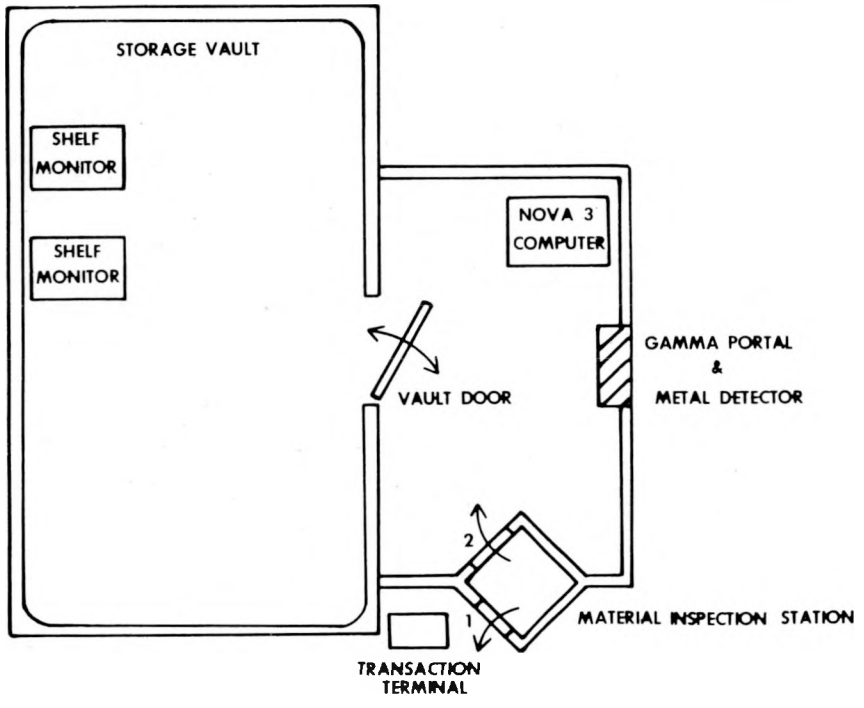

Fig. 50.
Layout of physical system.

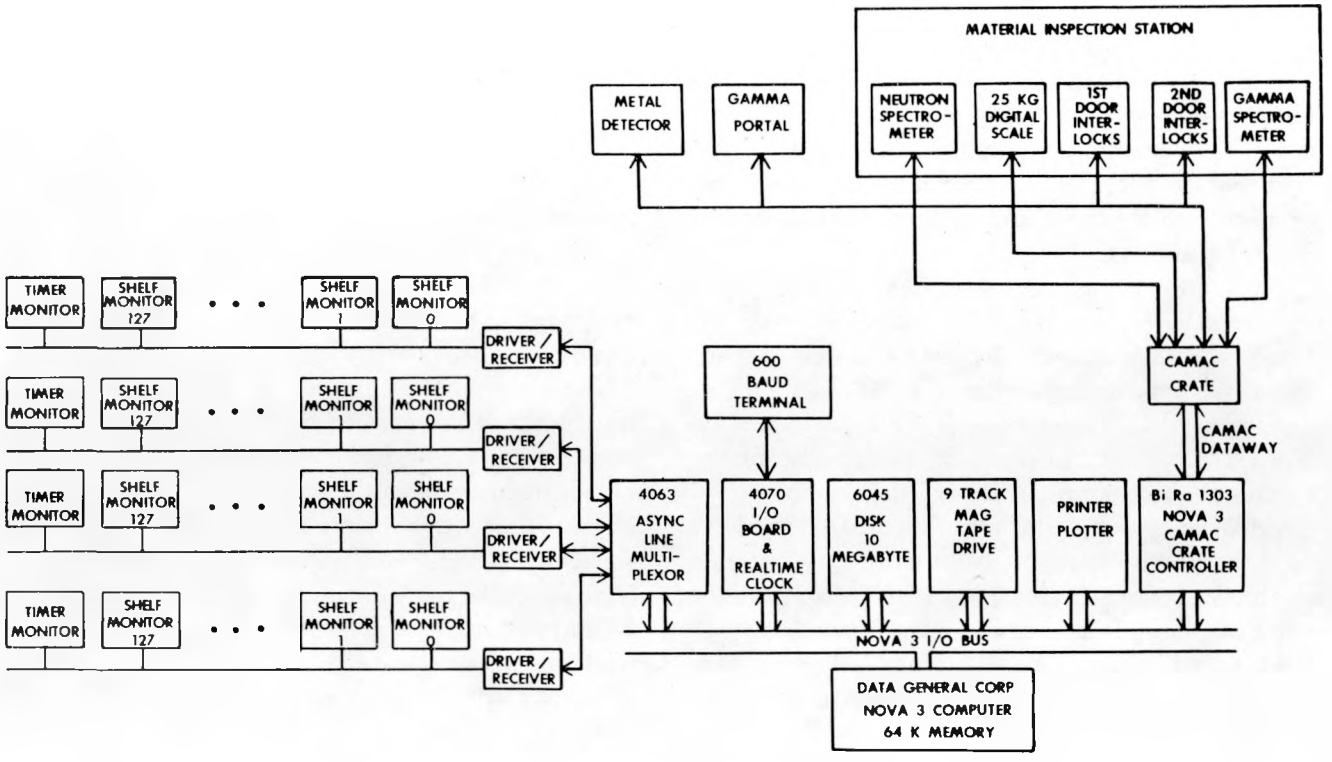

Fig. 51.
Schematic of system.

replacement. We were then notified that the verification station was operating normally. Apparently, the container of plutonium used to check the station did not contain sufficient material to satisfy the threshold conditions initially set into the logic system. The threshold settings were based on the minimum amount of material expected in any container designated to pass through the station. The system did what it was designed to do, but failure to verify the container was interpreted as a malfunction of the verification chamber or its electronics.

F. Reactor Power Monitor (ISPO TASK E-24) (E. J. Dowdy, A. A. Robba, and R. D. Hastings)

The prototype reactor power monitor was completed and tests were conducted at the Ft. St. Vrain nuclear power station (see Fig. 53). A presentation of the design and performance characteristics will be made at the fall Am. Nucl. Soc. meeting. A summary of the presentation follows.

An Operator-Independent Reactor Power Monitor

As part of a scenario for production of plutonium for use in nuclear weapons, illicit operation of a central station nuclear power plant might be expected. Such operation would be deviant from the normal electrical power producing mode of operation and could be discovered by an examination of the power traces from the normal power range monitors. Falsification of such records would be an obvious action of the plant operator, requiring an operator-independent power monitor for central station power plants under IAEA surveillance.

We have developed, in collaboration with the computer systems and electronic engineering group at LASL and under the U.S. program for technical assistance to IAEA Safeguards, a microprocessor-based reactor power monitor that

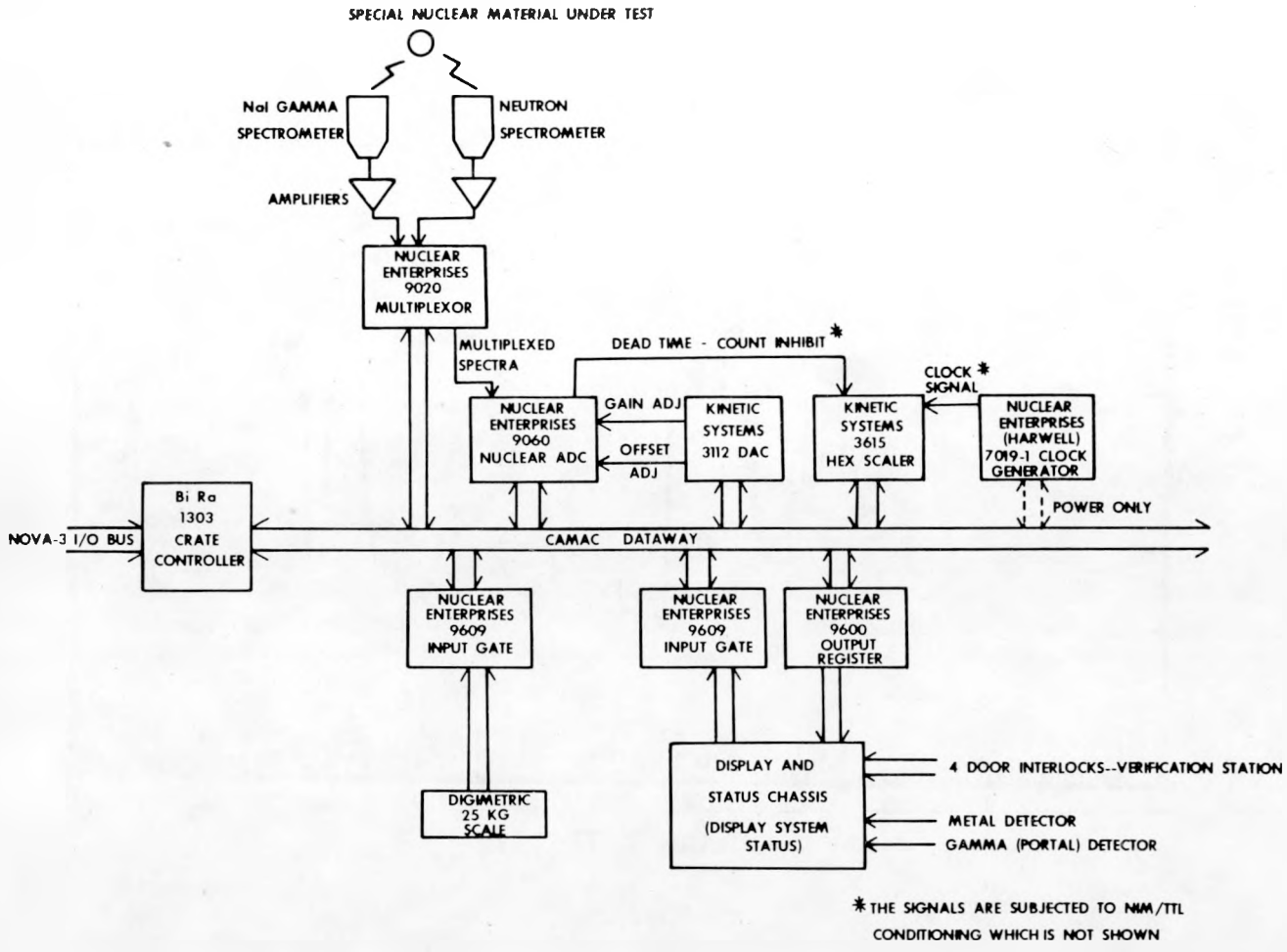

Fig. 52.
CAMAC subsystem.

provides the desired operator-independent history. The monitor is based on the principle of the correspondence between leakage neutron flux and reactor thermal power. The sensor in the monitor is a ^{3}He-filled proportional counter, which is used to detect thermal neutrons outside the biological shield. The monitor is intended to be placed in a tamper-resistant, tamper-indicating enclosure against the biological shield wall. The detector is bare on the side facing the shield wall, and shielded with polyethylene and cadmium on other surfaces. The high voltage for the detector, preamplifier and amplifier, and all logic circuits, including the RCA 1802 microprocessor, are contained on cards in a card cage. Electrical power is supplied by gel cells that are under constant charge from plant AC power but have a stand alone capability of approximately 4 days.

The reactor power monitor is calibrated and initialized by thumbwheel switch insertion of the declared operating power, in percent of rated capacity, and the Julian date and time of day via pushbuttons. Under software control, the count rate from the detector during the calibration period is related to the thumbwheel value of percent power to provide a normalization for all subsequent periods. The pulses from the detector are scaled

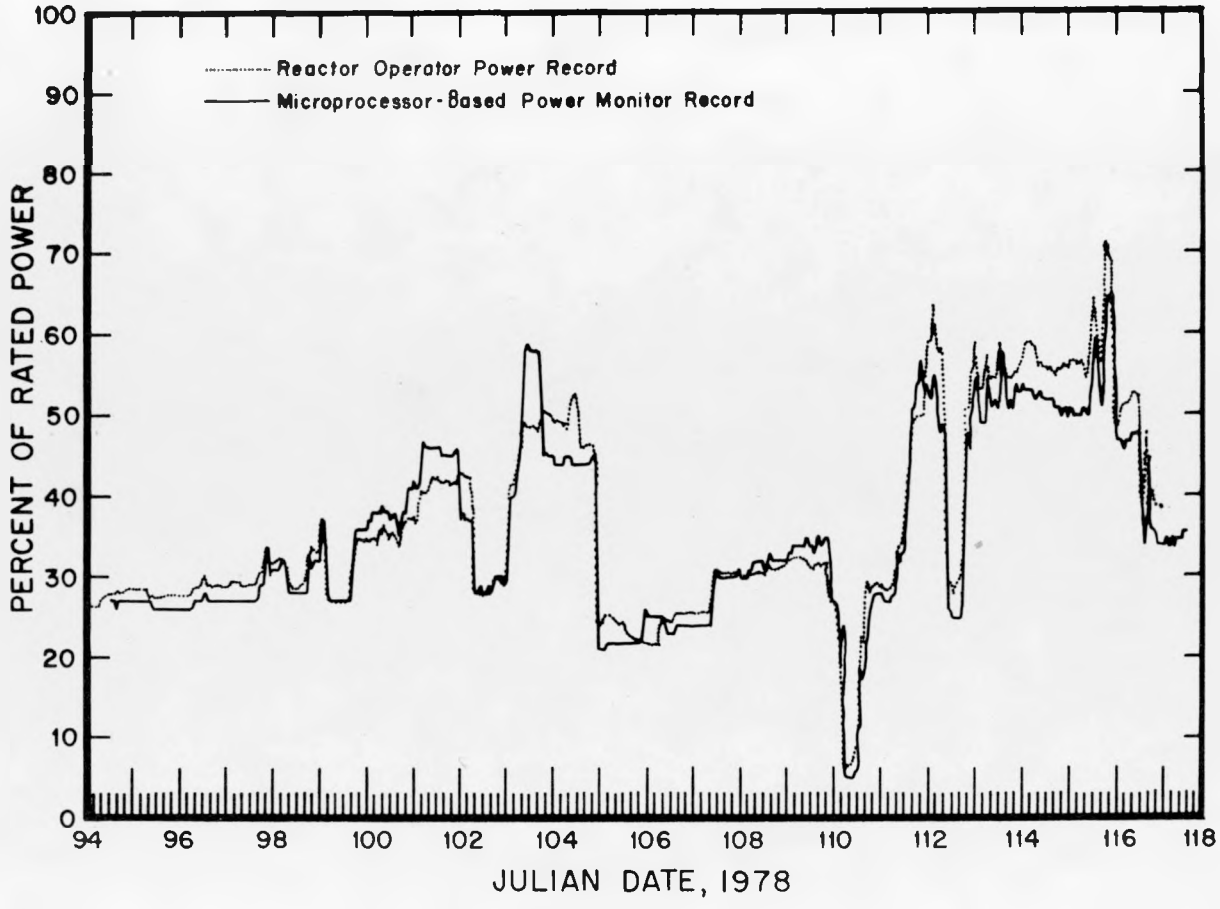

Fig. 53.
Results of the test of the prototype reactor power monitor at the Ft. St. Vrain Nuclear Power Station.

for an hour, the scaled counts compared with the normalization constant, and the hourly average reactor power, in percent of rated capacity, is recorded in digital fashion on redundant cassettes and stored in CMOS memory. More than three months of hourly records can be stored in memory. The Julian date is provided as part of the record once each 24-h period. The data are retrieved by removal of the cassettes for subsequent analysis, or a memory dump command can provide a TI-terminal record or a strip chart record through a digital-to-analog converter.

The monitor has been tested at the Ft. St. Vrain Nuclear Power Plant for approximately one month during the power ascension phase of operation. The records from this test are shown in Fig. 53 which confirm that the external flux variations follow the reactor thermal power within approximately 20% and that the microprocessor-based power monitor can provide an operator-independent record of that power history.

II. SUPPORTING RESEARCH

Plutonium Sample Assay (E. J. Dowdy, C. Henry, A. A. Robba, and J. C. Pratt)

Our correlation measurement technique for assay of plutonium-containing samples is described in a paper to be included in the Int. Symp. Nuclear Materials Safeguards, Vienna, October 1978. The abstract and conclusions of the paper follow.

ABSTRACT

Assay of plutonium samples using the moments of the neutron count distribution from a well counter has been demonstrated. Samples of various composition and ranging in mass from a few tens of grams to several kilograms have been used in this demonstration. Several advantages over conventional coincidence counting methods have been realized. Among these are the ability to account for sample multiplication and the ability to detect and correct for detection system malfunction without the loss of even a single analysis cycle.

DISCUSSIONS AND CONCLUSIONS

This initial study has confirmed the utility of the moments method for SNM assay applications. We have assayed samples ranging from a few tens of grams to those as large as criticality safety limits allow. The measurement precision has been demonstrated to be as good as the measurement precision of the coincidence counting technique. The advantages provided by the moments method include: the simplicity of the associated circuitry (we have built hard-wired versions in four-wide NIM modules); the fixed counting period, which is determined only by the counter characteristics and not by random neutron source strength contamination; and, perhaps most importantly, the moments method provides a diagnostic capability unavailable with the other techniques. Equipment malfunction can be immediately signaled by an inordinately skewed count probability distribution output *for each sample*. In our newest software versions, inordinately large single interval counts are automatically eliminated so that even a single measurement cycle is not lost. This is considered an extremely important characteristic of counting stations in DYMAC-type assay applications so that processes can be operated without interruptions except for discovery of real material differences.

We are in the process of extending the moments method to the assay of ^{235}U using an active well counter. Additional algorithms and detection schemes are being examined to attempt extraction of additional information from the moments of the neutron count distribution.

III. TRAINING AND TECHNOLOGY TRANSFER

A. Materials Management Course (N. Nicholson and P. E. Fehlau)

A session on "Personnel Monitoring and Vaults" was presented to the participants in this year's Materials Management Course conducted during the week of May 9. The topics included a description of the Real-Time Inventory system, the work done with the verification station on selected plutonium and uranium samples, the current status of the shelf system, and plans for the demonstration shelf system proposed for TA-55.

B. Delta Rate Meter Design (C. Henry, D. R. Millegan, and T. R. Capelli)

The design of a new hand-held rate meter was sent to several vendors in a request for quotation. We subsequently placed a purchase order with National Nuclear Corp., 3150 Spring Street, Redwood City, CA 94063, and CMS Inc., 1345 Norman Firestone Road, Goleta, CA 93017. Delivery is expected before October 1978, after which time the instruments should be commercially available.

PART 3

SAFEGUARDS SUBSYSTEM DEVELOPMENT AND EVALUATION

GROUP Q-3

Ronald H. Augustson, Group Leader

The DYMAC system has been keeping pace with Group CMB-11's progressive occupation of the Plutonium Processing Facility. During May-August, the advanced carbide fuels section of the plutonium facility (100 Wing) began sampling plutonium and made the corresponding DYMAC transactions. It begins processing plutonium in September. The metallography section, in the same wing, began using DYMAC in May when its transactions were ready. The metallography section measures subaccountable quantities of SNM; it uses special transactions that keep track of the amounts measured, even though they do not affect the station balance. The metal fabrication section, which occupies all of the 300 Wing, began processing in late April and has been making DYMAC transactions since then. In the 400 Wing, the oxide reduction and electrorefining sections began processing in mid-July. Other sections in the 400 Wing will start processing in September and October.

All of these processing sections use DYMAC to make transactions and to request reports. In addition, the NMO (nuclear materials officer) and his staff use DYMAC to make transactions for all shipments entering and leaving the facility; they alone have access to the vault. Count room personnel measure all shipments from the facility on an off-line basis and make the appropriate transactions. Maintenance personnel also use DYMAC in checking the precision and accuracy of NDA instruments in the facility.

CMB-11 occupied ~50% of the facility at the end of August, with DYMAC servicing all processing sections. Figure 54 shows the areas in the facility that DYMAC services and the terminals and NDA instruments in use. Not all the instruments shown are on-line (directly connected to the computer).

The major portion of Q-3's effort during the May-August period was devoted to Phase II activities, that is, installation of DYMAC instruments and software at the new facility. Two TNCs (thermal-neutron coincidence counters), one a barrel counter, the other a can counter, were installed in the count room in the 400 Wing. CMB-11 personnel are operating the TNCs manually until the THENCS (thermal-neutron coincidence counting system) logic unit is ready and the instruments can be brought on-line to the DYMAC computer. A PDP/11 computer is now coupled to the TNCs to compute the amount of plutonium from raw counting data; previously, DYMAC personnel performed the computation manually. The computer also provides printouts of the calculations. Another two TNCs are ready for installation in the 400 Wing as soon as the gloveboxes are ready.

DYMAC personnel moved an SGS (segmented gamma scanner) from DP Site into the new facility's count room. The SGS consists of a 55-gal barrel assembly and a can assembly, both supported by one set of electronics. Only one assembly can operate at a time. By the end of November a second set of electronics should allow the barrel and can assemblies to operate independently. The SGS is proving its worth in counting scrap material before the scrap leaves the facility. It detected more plutonium in one barrel of scrap than was thought to be inside and led to the discovery of a processing error. An FNC (fast-neutron coincidence counter) is located in the oxide-reduction process (400 Wing) for use on an experimental basis; it is not designed to work on-line with the DYMAC computer. Five SAIs (solution assay instruments) are planned, but the first will not be ready until early October. DYMAC personnel are dissatisfied with the SAIs' present design, but will install some to meet the schedule. They will be redesigned later this year. As of August 31, 18 DYMAC balances were on-line to the computer. All 5.5-kg balances with 0.1-g accuracy are performing reasonably well, but those with 0.01-g accuracy fail to meet specifications.

DYMAC personnel continue to install instruments in the new facility. The number of ports

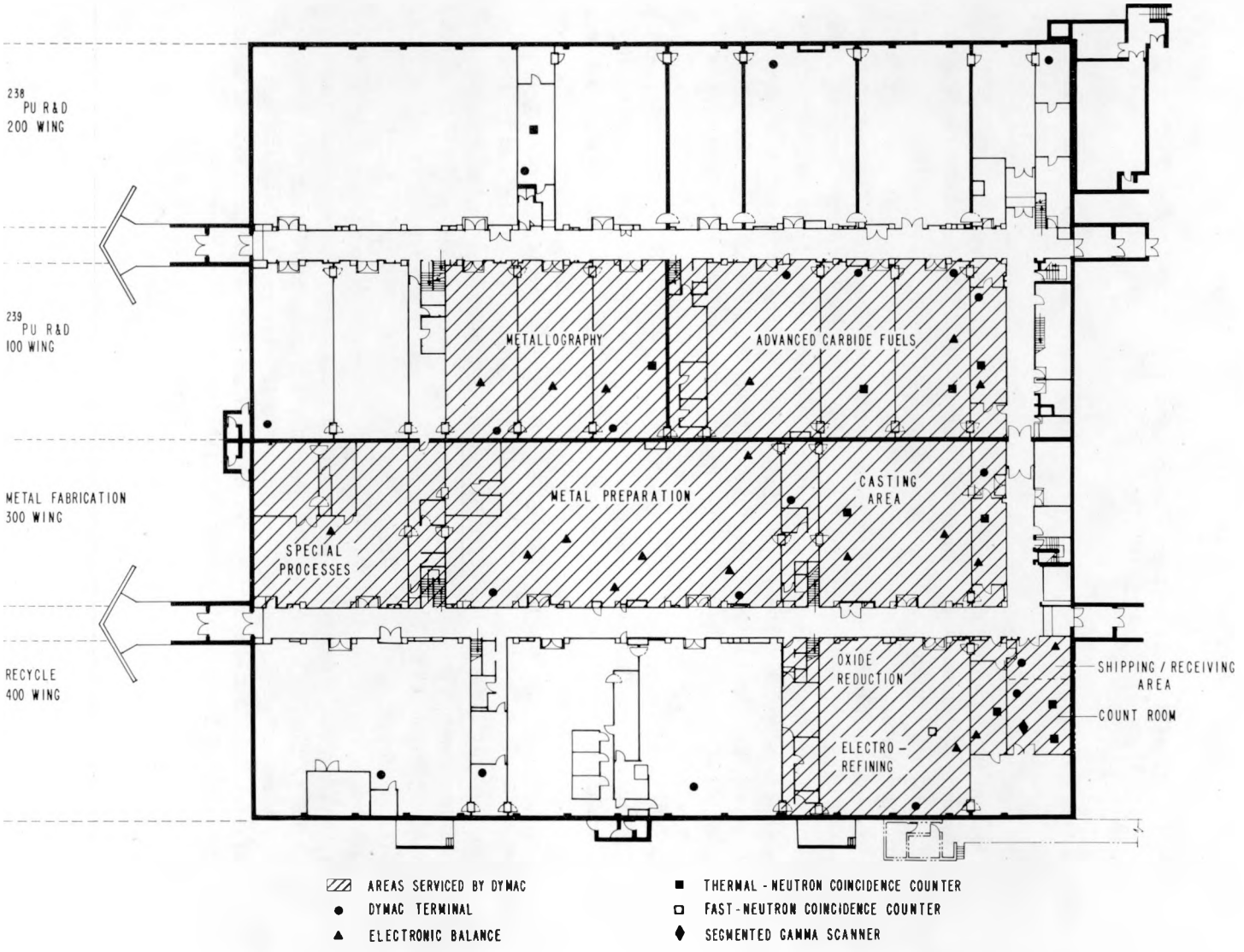

Fig. 54.
DYMAC activity and instrumentation on the main floor of the new facility.

TABLE XV

DYMAC INSTRUMENTATION

DYMAC Instrument	Number Installed	Number On-Line	Number Still to Be Installed	Location
Video terminal	34	34	7[a]	Facility and cold support building
Supervisory hard-copy terminal	7	7	---	Facility and cold support building
Label printer	2	2	3[a]	Vault and shipping/ receiving area
5.5-kg Arbor balance	21	12	14	Facility, all wings
15-kg Arbor balance	2	1	1	Facility, all wings
TNC	9	---	9[b]	Facility, all wings
SAI	---	---	5	400 Wing
SGS	1	---	1	400 Wing, shipping/ receiving area
FNC	1	---	0	400 Wing, oxide reduction

[a]To be ordered.
[b]Two have been ordered.

available to connect the instruments to the computer is a limiting factor. At present only 64 can be used although wiring exists for 128 ports. A software modification in the DYMAC system will double the number of available ports in November. Table XV enumerates the instruments already installed, as well as those remaining to be installed. Not all the instruments and terminals mentioned in Table XV appear in Fig. 54 because the figure shows only the main floor of the facility. DYMAC instruments and terminals are also located in the basement and mezzanine, as well as in the cold support building.

During the May-August period, the DYMAC programming team made the system faster and more responsive to the users and kept abreast of CMB-11's occupancy of the 300 and 400 Wings by supplying each section with specialized transactions. The DYMAC computer has been squeezed for logic space, although physically there is enough room. The programmers completely reorganized the logical structure of the data base and restructured the applications program to decrease response time. The restructuring provides the additional memory space to accommodate the other 64 ports. Transactions now run at a higher priority than inquiries, which means that a user making a transaction interacts more quickly with the system than does a user making an inquiry. DYMAC has increased the number of reports it produces. One new report is a mid-month archive of all transactions executed during the previous month. Account custodians can now request off-line printed reports of their accountable and nonaccountable holdings.

A second Eclipse C330, due to arrive in late October, will relieve the squeeze on computer time for software development and user training, which is now done outside regular processing hours. Of course, processing is of first priority. Software development and training cannot be concurrent with the processing because both must interact with the application programs and the data base; after hours a dummy data base is used. A larger capacity Zebra disk, on order for the present computer, will improve overall system response time.

The software code for the measurement control program was expanded to include additional calibration standards. The frequency of DYMAC instrument calibration was changed. Previously, technicians made daily precision checks; now they make them weekly and make accuracy checks (a much simpler procedure) on intervening days. The program now can print a comprehensive list of DYMAC standards for all on-line and off-line instruments of the measurement control program.

I. INSTRUMENTATION

A. Communications System (K. A. Lindsey and V. S. Reams)

The communications system is essentially complete. All the cables are installed and connected to the DYMAC computer, thereby increasing the number of available ports for terminals and instruments from 64 to 128. However, the additional 64 ports will not go into use until the code that services them is incorporated into the DYSS (DYMAC software system) in November.

The primary emphasis is now on maintaining the communications network. DYMAC personnel are on call to resolve minor problems. For example, a Teleray terminal was not transmitting to the computer; to put it back in service, we replaced a blown fuse at the Eclipse multiplexor chassis. Another maintenance call concerned a Texas Instruments hard-copy terminal that printed incorrect characters: we replaced it with another while it underwent repair.

Five supervisory terminal stations have been set up for the Plutonium Processing Facility. Each station consists of a Teleray 3711 CRT terminal and a Texas Instruments 733 hard-copy terminal (Fig. 55). The two are linked by the DYMAC computer. The supervisory station enables a supervisor to obtain a printout of a report, such as the inventory for a location, instead of a display on his video screen. Two of the stations are in the cold support building; the other three are in the plutonium facility.

Two Texas Instruments 810 printer-terminals were installed—one in the count room and the other at the vault entrance. Figure 56 shows the printer and a sample label. The NMO staff affixes a similar label to every can of an incoming shipment before placing the shipment in the vault. Printed labels are produced faster than handwritten ones, and there is less opportunity for error because the information comes from the DYMAC data base. Since installation, the printers have run at 300 baud, their slowest speed, because of malfunctions at the optimum speed of 1200 baud. Personnel from E-1 and Q-3 are resolving the problem.

B. Digital Electronic Balances (M. M. Stephens and C. C. Thomas)

The 5.5- and 15-kg electronic balances at the plutonium facility have 0.1-g sensitivity. Because of instability in their accuracy, none of the 0.01-g-sensitivity balances has been installed. We are examining modifications to rectify this.

Twenty-one balances were installed and interfaced to the DYMAC computer. Figure 57 shows a typical glovebox balance installation. The weighing portion of the balance is inside the glovebox and the readout portion is outside and beneath the glovebox. The two units are connected by a multiconductor cable. The operator controls the balance with three controls on the readout unit: TARE, HOLD, and RESET. The TARE lever enables the operator to zero the balance when the pan is empty. He can also tare the weight of an empty container or a partially filled container to which more material is to be added. The HOLD button locks the measured weight in the readout register and readies the interface for

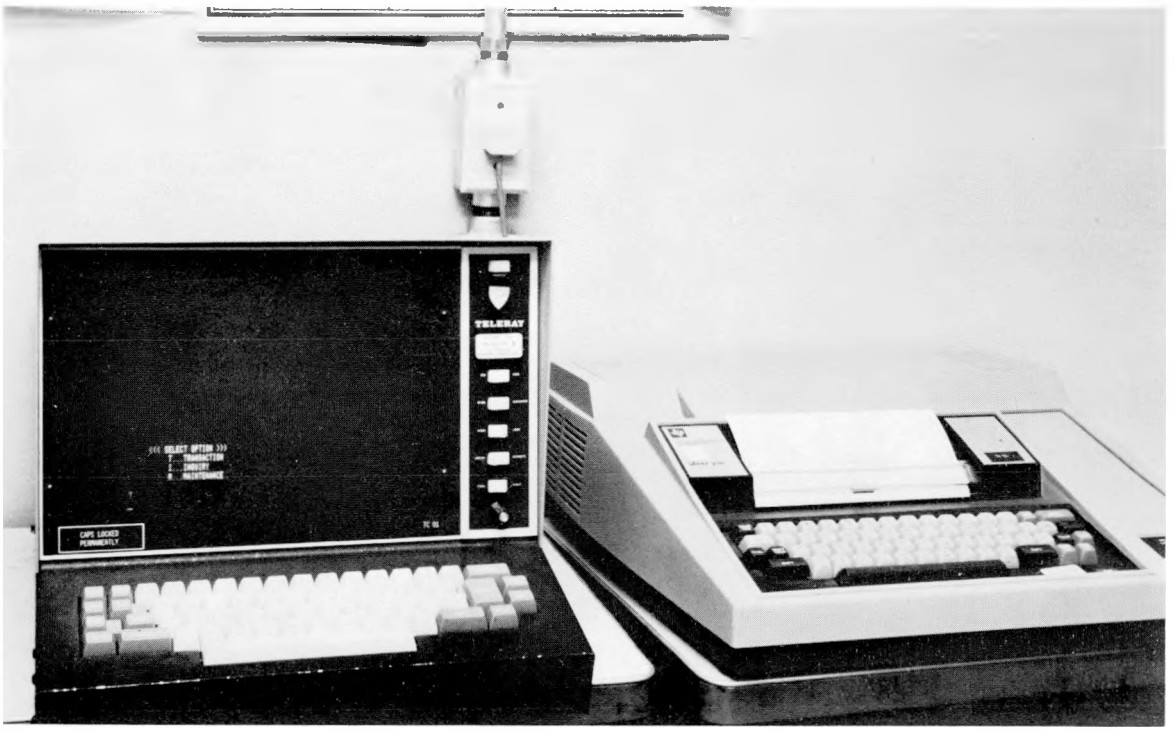

Fig. 55.
Supervisory terminal station.

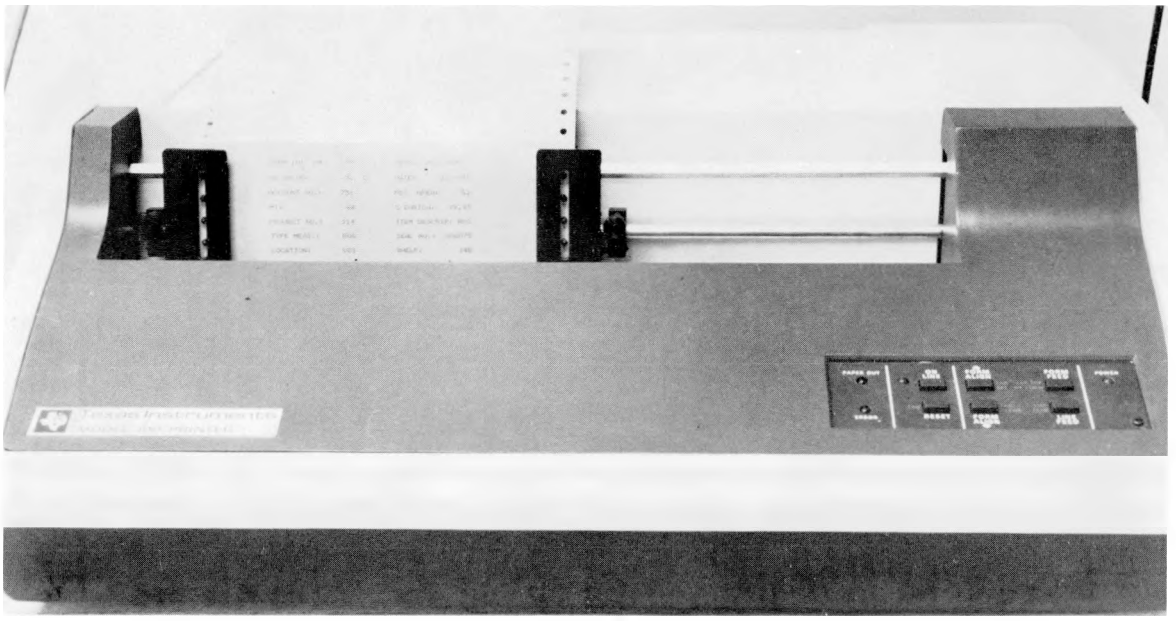

Fig. 56.
Label printer.

Fig. 57.
Operator weighs a can of material on an electronic balance.

weight transmittal to the computer. The RESET button unlocks the balance, freeing it for off-line use.

The interface is in the panel to the right of the readout unit and consists of three printed circuit boards, whose functional relationship appears in Fig. 58. The parallel-to-serial converter is on one board, the UAR/T (universal asynchronous receive/transmit) and optoisolator on the second, and the power supply, which provides 5 V at 1-A current to the other two boards is on the third.

The interface permits communication between the balance and computer. It converts the BCD data format of the balance to ASCII, which the computer expects, and then transmits those data to the computer. The computer initiates data transmission by a CONTROL X command, which the optoisolator relays to the parallel-to-serial converter. There the command is decoded, and a signal permits the parallel-to-serial converter to transmit data to the balance. Each data transmission is terminated by a RETURN character. The parallel-to-serial converter receives the parallel BCD data from the balance readout unit, converts them to serial ASCII format (digit parallel, word serial), and sends them to the optoisolator. The optoisolator transmits these data to the computer over optically isolated, 20-mA-current lines. The optically isolated lines provide direct electrical separation between the DYMAC computer and the balance electronics, thus avoiding ground loops and associated noise.

Between June 21 and August 1, 1978, the measurement control program generated check data for 17 balances, which DYMAC personnel have analyzed statistically. Two measurements were made for each balance by using 1-kg and 4-kg check weights. The data were pooled (that is, one value was obtained from several as a result of statistical analysis) on a weekly basis and for the total 6-wk period. Before the measurements were recorded, the balances were adjusted, if necessary. As a result, the balances exhibited their optimum behavior.

On examining the performance data for the one 15-kg balance, checked at 1, 4, and 8 kg, we found the optimum 1σ precision to be ~0.15 g, with a corresponding accuracy of ~0.2 and a positive bias of 0.1 g. The sixteen 5.5-kg balances exhibited optimum precisions of the order of 0.08 g and accuracies of the order of 0.15 g at the 1σ level. A majority of the balances had a bias at either or both of the weighing levels (1 and 4 kg). The bias is not included in the estimate of precision and accuracy because it is not always consistent among balances.

Figure 59 contrasts the performance of two 5.5-kg balances. Balance B16 exhibited the best precision and accuracy of the 17 balances under the measurement control program, whereas balance B42 exhibited the worst. The bias is determined by subtracting the reference weight from the observed weight. Each point is the bias to the nearest hundredth of a gram. As a *modus operandi*, we inserted 1σ precisions and accuracies of 0.08 and 0.15 g, respectively, into the measurement control program for performance evaluation. Balance B42 deviates as much as 1.1 g, and is not being used until

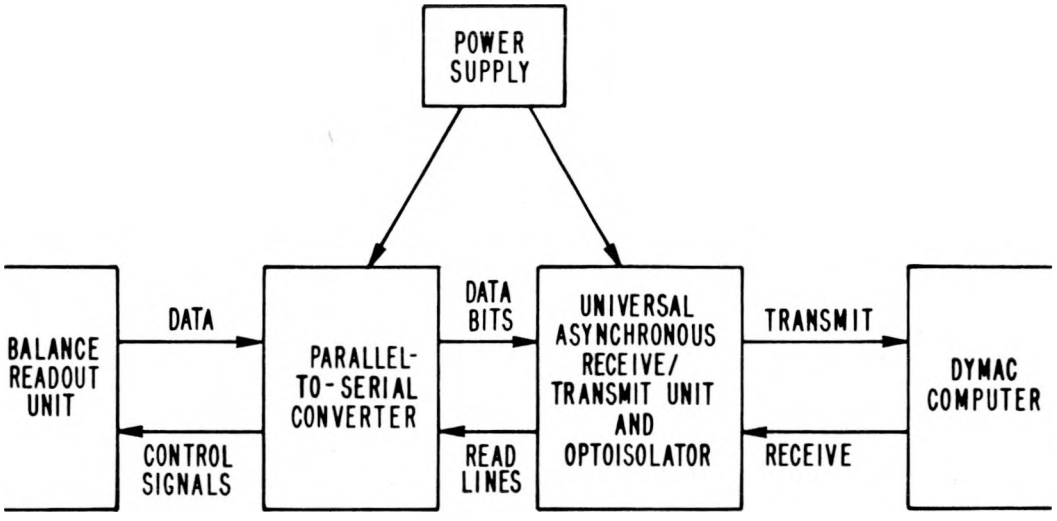

Fig. 58.
Relationship of the three printed circuit boards.

DYMAC personnel can solve the problem. This effect represents one of the first evaluations of the DYMAC system.

C. Solution Assay Instrument (D. G. Shirk and V. S. Reams)

Q-3 is fabricating five SAIs for the 400 Wing. Installation will begin in October. During the May-August period, DYMAC personnel fabricated two chassis and two complete sets of printed circuit boards for the SAI. The first SAI was assembled and thoroughly tested for software and hardware reliability. Certain design changes, particularly in the electronics, improved its reliability.

D. Shirk wrote two computer codes for the SAI. One allows both a calibration of the instrument and an assay for ^{239}Pu, ^{241}Pu, and ^{241}Am. The other code allows only the assay. The first code outputs diagnostic messages on a mobile terminal; the second outputs messages on a small printer in the operator console. Both codes include a measurement control program to monitor instrument performance.

Results from a solution assay may appear in two forms: concentration of ^{239}Pu, ^{241}Pu, and ^{241}Am expressed in grams per liter or grams per gram of sample. To determine grams of plutonium or americium per gram of sample, the SAI interrogates an electronic balance, checks the net mass for validity, and determines the grams of ^{239}Pu, ^{241}Pu, and ^{241}Am per gram of sample. If the net mass of the sample exceeds predetermined limits, the SAI issues a diagnostic message and terminates the assay.

D. Pressure-Transducer System (R. S. Marshall and W. R. Severe)

The SAI requires three measurements: (1) the plutonium concentration in a 25-ml sample drawn from the tank, (2) the mass of the sample, and (3) the mass of the solution in the tank. From these the SAI determines a mass ratio of the tank solution to the sample and multiplies that by the plutonium concentration in the sample.

Each SAI will have four to eight tanks affiliated with it. Each tank has its own pressure-transducer system (Ref. 1, p. 80). Figure 60 shows how the pressure-transducer system ties into the SAI. The pressure-transducer is mounted on a panel outside the glovebox that houses the associated solution tank. It senses the solution pressure in the tank via a dip tube that extends to the bottom of the tank. It transmits the pressure, which is directly related to the solution weight, to the associated, V/F (voltage-to-frequency) converter. On command, the converter relays it to an electronics package in the SAI.

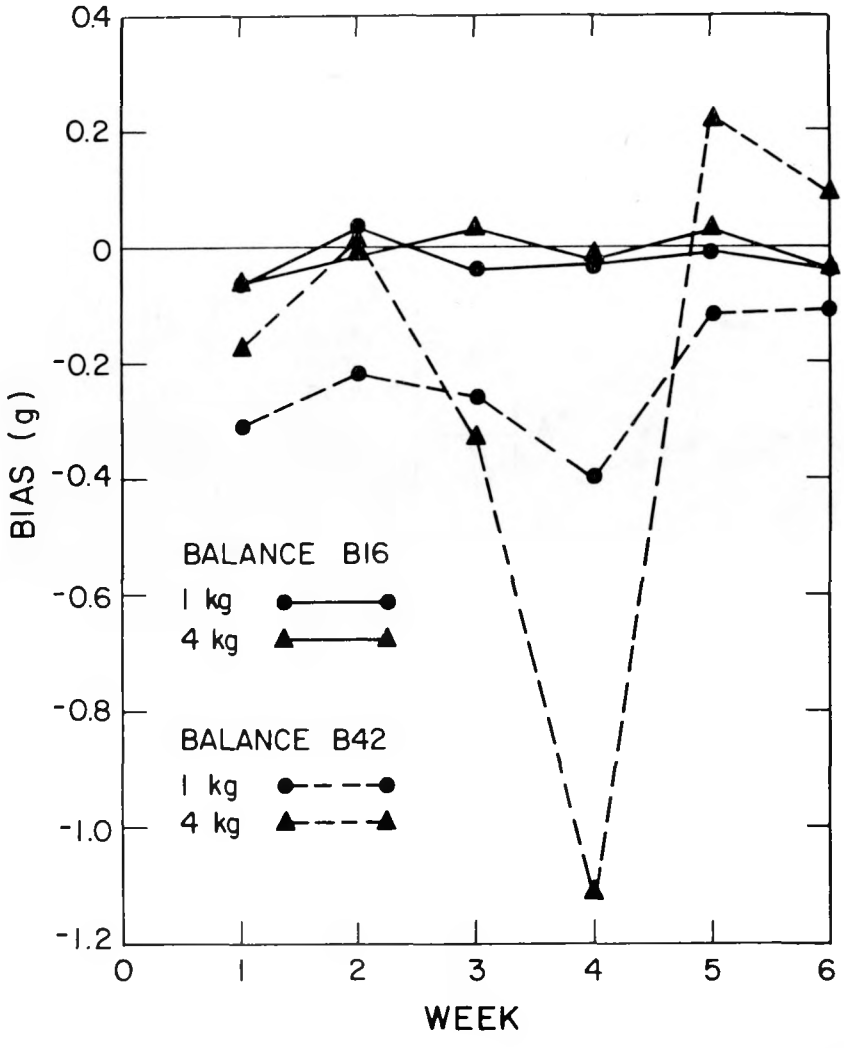

Fig. 59.
Relative performance of two 5.5-kg balances.

Q-3 awarded EG&G a contract to engineer, procure, assemble, and calibrate 42 pressure-transducer panels. Each panel contains a pressure manometer, an on-off valve, and a micrometering valve, as shown in Fig. 61. EG&G personnel have assembled all of the components for the panels and leak-tested them. Using a dead-weight pressure standard, they are testing the panels for millivolt output at five reference pressures.

Meanwhile, DYMAC personnel are assembling the SAI electronics packages. They have made the necessary glovebox to accommodate the pressure-transducer systems, such as making penetrations and mounting studs. Solution tanks were fitted with 6.3-cm-diam stainless steel dip tubes. Installation and calibration of the pressure transducers began in August and should be complete by mid-October.

E. Thermal-Neutron Coincidence Counters (R. S. Marshall)

During the May-August period, DYMAC personnel installed two TNCs beneath gloveboxes in the 400 Wing. One TNC, located in the material management room, is a large, 35-cm-diam unit that can be used to assay bulky items such as discarded equipment or rags. The other TNC, with a 16-cm well, is in a processing area where impure PuO_2 destined for FFTF fuel is dissolved and purified.

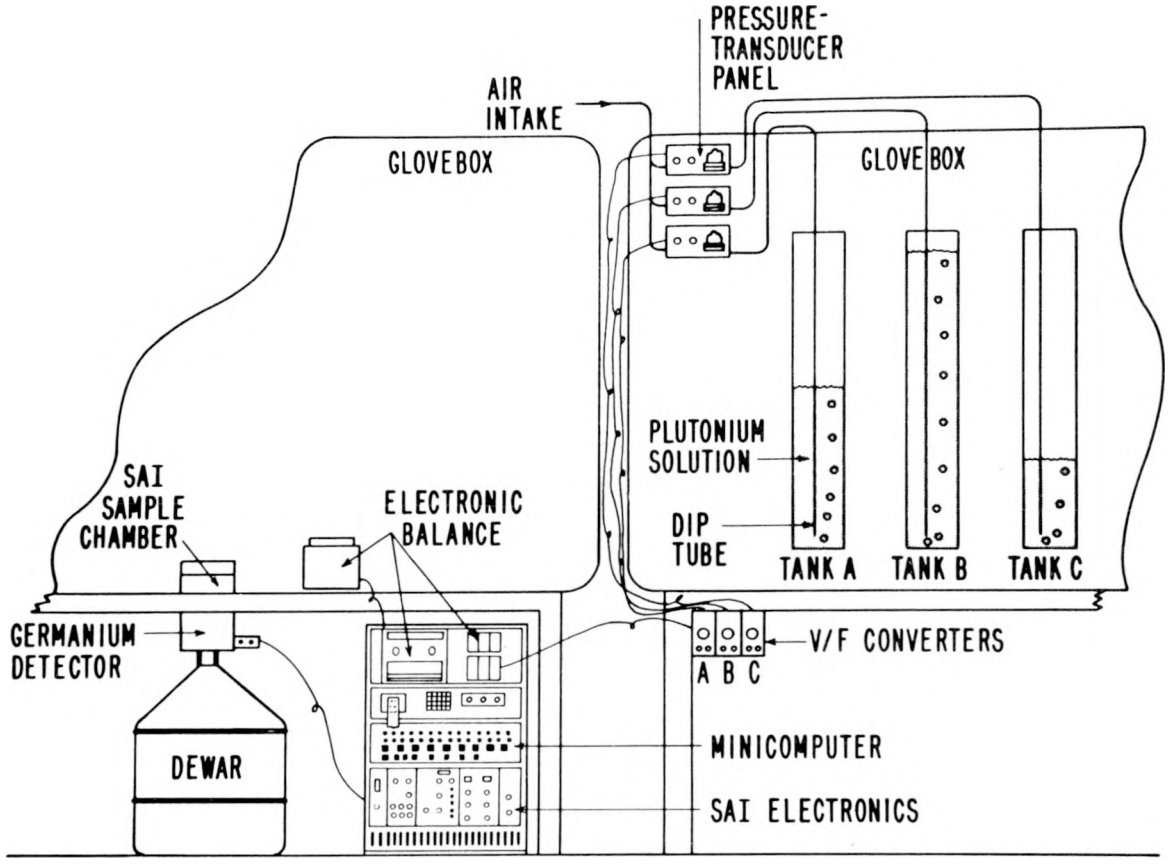

Fig. 60.
Schematic showing tie-in of the pressure-transducer system to the SAI.

Originally, four additional TNCs were to be installed in the 400 Wing by August, but delays in installing process piping, which must first be completed under the gloveboxes, has delayed our schedule.

The 400 Wing TNCs, similar to the one in Fig. 62, differ from those in other wings in that they contain two concentric rings of ^{3}He detector tubes instead of one. We expect the double ring design to provide a differential signal sensitive to neutron spectra shifts caused by matrix effects and moderation. This sensitivity should allow us to correct biases caused by different matrices and moisture content. Figure 63 shows the detector tube array and polyethylene moderator. Two quadrants are complete with detectors, and two quadrants await insertion of detector rings. The assembly is arranged in quadrants to facilitate installation around sample wells below gloveboxes.

In addition to the six double-ring TNCs planned for the 400 Wing, CMB-11 has requested two more. They will measure >100-g quantities of 85% ^{242}Pu isotopic material. The double-ring design may encounter excessive counting rates with such high isotopic material. We are trying to determine which instrument design will best accommodate a higher neutron flux.

F. Fast-Neutron Coincidence Counter (R. S. Marshall)

DYMAC and Q-1 personnel installed an FNC, also known as the random driver (Ref. 1, pp. 29-30; Ref. 9, pp. 23-27), beneath a glovebox in the 400 Wing metal preparation room. Figure 64 shows the instrument in place. Notice the two photomultiplier tubes between the wheels at the bottom of the photo, the dc motor controller for raising and lowering the sample chamber to the left center, assay-starting switches immediately above and to the right of the

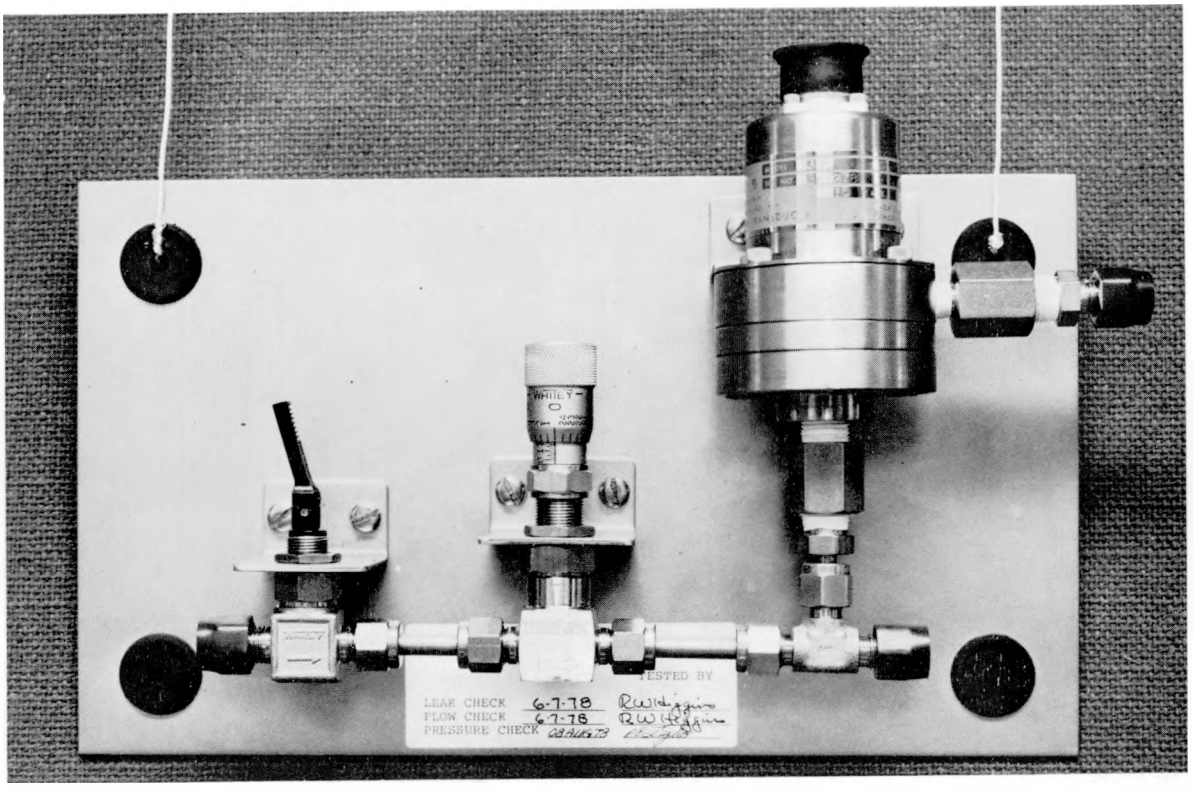

Fig. 61.
Pressure-transducer panel.

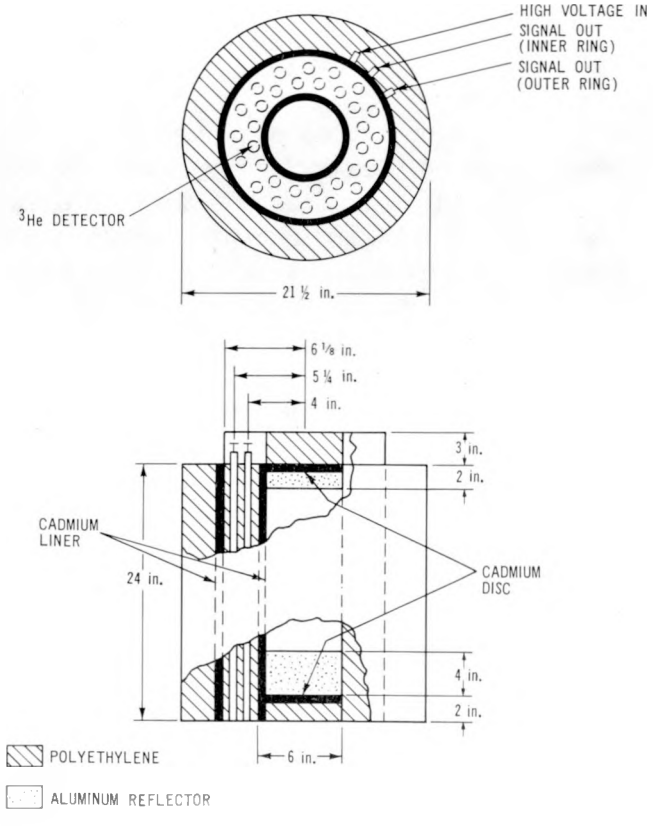

Fig. 62.
Double-ring TNC design.

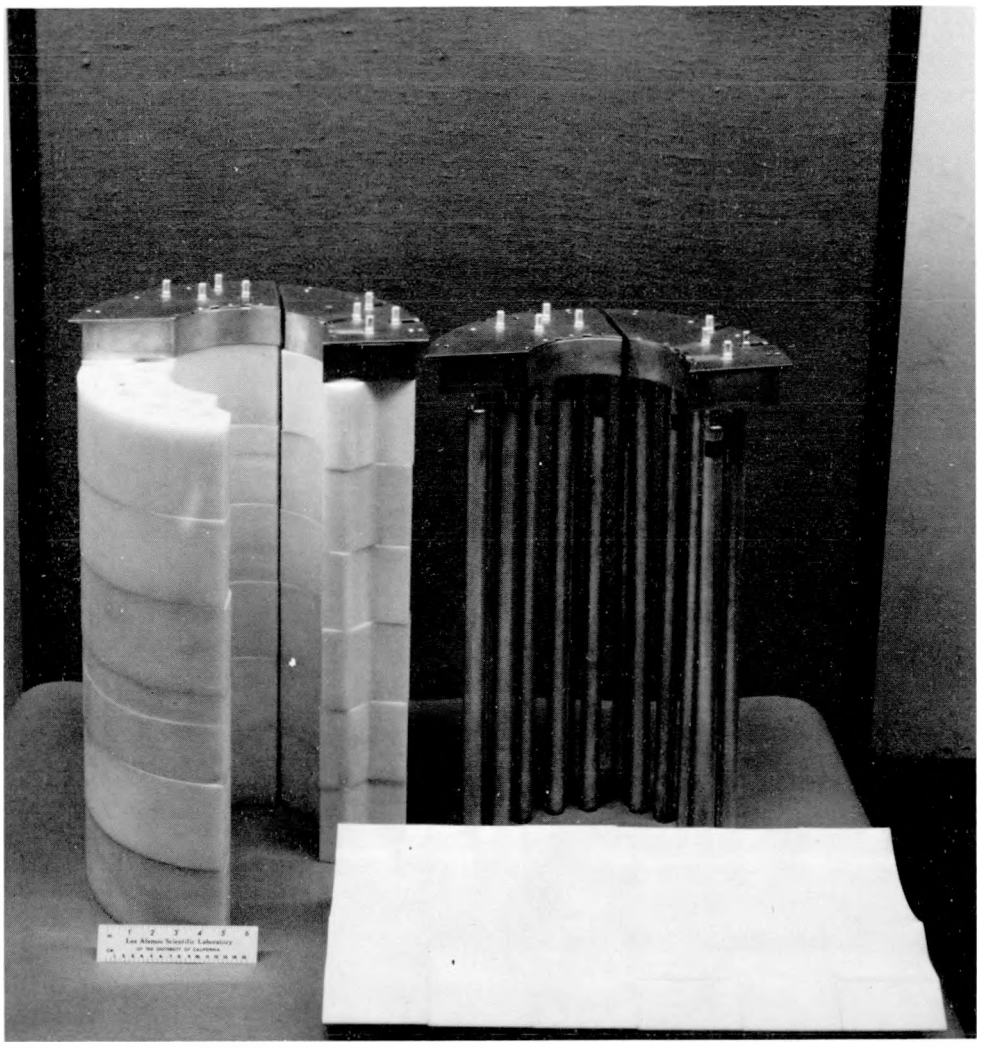

Fig. 63.
TNC detector tube array and polyethylene moderator.

motor controller, and the raised sample holder just inside the rectangular window cutout. Figure 65 shows in more detail the sample holder in the raised position. Notice the cylindrical opening of the sample well and the power cord for a rotating motor built into the sample holder.

During May-August the metal preparation section began operation of the plutonium oxide-to-metal reduction and the electrorefining processes. Taking advantage of materials flowing to and from these processes, Q-1 and Q-3 personnel performed many FNC assays of three types of material: plutonium metal, PuF_4 and electrorefining salts. They are now analyzing the measurement data to evaluate instrument performance and calibration.

The electrorefining salts are heterogenous materials containing NaCl, KCl, MgO, plutonium metal, PuF_4 and ^{241}Am. The quantity and chemical makeup of the plutonium in the salts is known only approximately. To evaluate the FNC's ability to assay these salts, we requested total dissolution and chemical analyses for six batches. We then counted the six batches in a TNC can counter, the counting room TNC barrel counter, and an SGS. Results of these analyses should appear in the next progress report.

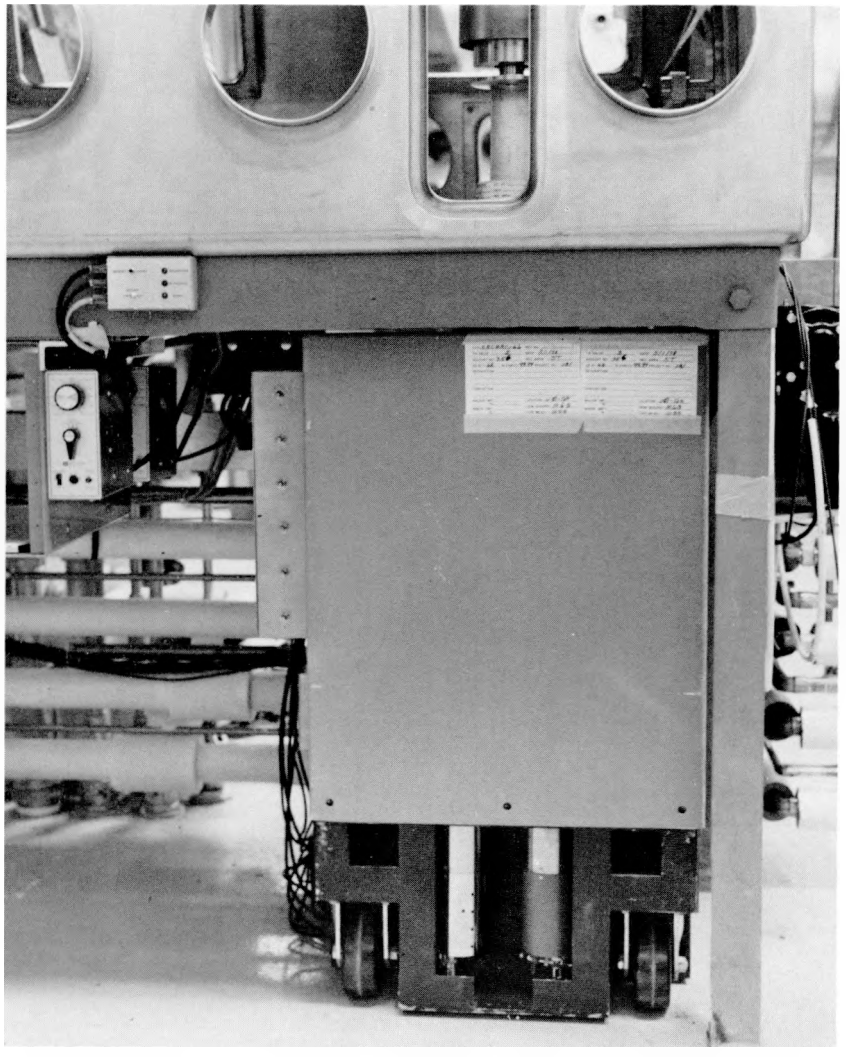

Fig. 64.
FNC installation beneath a glovebox.

G. Segmented Gamma Scanner (W. Ford)

The SGS measures the plutonium content in large barrels or small cans that contain low-density, inhomogeneous waste and scrap materials, such as incinerator ash, plastic, and paper. The container rotates during the scan to compensate for angular inhomogeneities. To compensate for vertical inhomogeneities, the detector looks at only one segment of the container at a time and sums the segments for total content. The SGS measures the passive gamma radiation from the various plutonium isotopes to determine the nuclear content of the container, and corrects for gamma-ray attenuation.

In July, DYMAC personnel moved the DP-Site SGS to the count room in the new facility. The instrument has electronics that can drive two scan tables, but not concurrently. The two scan tables accommodate a variety of container sizes for gamma-ray assay. The can table accommodates small cans, and the barrel table accommodates 55-gal barrels.

We are fabricating a second electronics unit that will permit the can and barrel scan tables to operate independently, thereby permitting greater throughput volume in the count room. Another advantage of interchangeable electronics units—one for each scan table—is that operation can continue if one electronic unit fails. With nearly identical units,

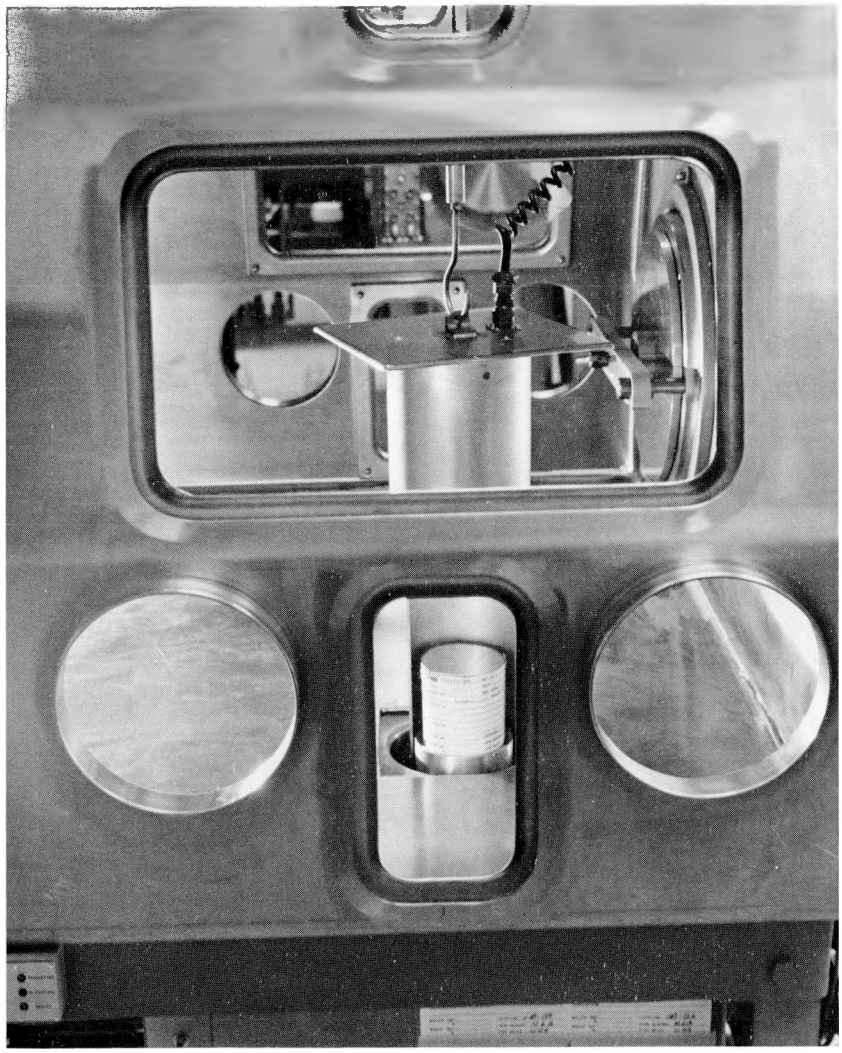

Fig. 65.
FNC sample holder.

we can trouble-shoot a down unit simply by interchanging components.

Fabrication of the second electronics unit is ~50% complete. All commercial components have arrived except the Keronix computer, which should arrive in early September. We should complete the electronics unit during October and then check it out for 2 wk.

H. Bar-Code Label Printer and Readers (W. Ford)

We are investigating for the DYMAC project the bar-code labels for containers of radioactive materials. Such labels are machine-readable and can significantly reduce the radiation exposure of an individual who is inventorying many containers in a storage vault having high ambient levels. Instead of verifying each label against an inventory list, the inventory-taker can quickly scan each machine-readable label with a wand and leave the vault. The computer can then verify the inventory. Another benefit is the quicker, more reliable readings compared to visual, manually recorded readings. Data on the label can be formatted for direct entry into a computer where they can be cross-checked and stored.

A Markem label printer and three label readers of different makes were purchased in December 1976 to

investigate the practical use of bar-code labels. At the urging of CMB-11, we resumed our investigation.

The label printer prints two lines: alphanumeric characters on top and bar code beneath. The bar code is a machine-readable progression of bars of equal length but differing width. Numbers appear immediately below the bars that contain the same information for easy visual inspection. The alphanumeric line appears only if programmed in the code; it may be part or all of the bar code or a totally independent message.

The printer has a serial EIA (Electronics Industrial Association) interface, which allows label generation from an external source such as a computer. Each label reader has (1) a buffer to store information read from a label and (2) provision for transmitting the data to a computer or similar device. It could print the information on a terminal, for example.

All of the equipment is configured for the CODABAR code, copyrighted by Monarch Systems. There was no overriding technical reason for choosing this code; rather, it seemed a reasonable code that was readily available in the equipment from several manufacturers. It includes 10 numeric characters, 6 control characters, and 4 start/stop characters. Each character is represented by four dark bars and three light spaces. If a wide space or bar is considered a binary 1 and a narrow bar or space a binary 0, each character is then made up of a 7-bit binary code. Each of the 10 numeric characters is made up of two 1s and five 0s. This is often referred to as a 2-of-7 code or, simply, code 27. The code patterns are bidirectional, that is, they may be read by scanning either left-to-right or right-to-left across the bars.

We have found that adjustments to the printer are critical in obtaining a quality label. One pass of the reader wand for any of the three readers is seldom sufficient to read a label, although all three reliably read preprinted sample labels produced on a printing press. The problem is not that the readers misread; rather, they don't read at all. Although the printer can be adjusted to produce better bar code, the quality of the alphanumeric line at the top suffers. We need to resolve this label quality problem or find an acceptable quality compromise between the lines of bar code and alphanumeric characters.

I. Holdup Measurements

1. Hot Gloveboxes (R. Siebelist and M. Hykel)

CMB-11 moved plutonium-contaminated gloveboxes from DP Site to the new facility. DYMAC personnel completed measuring the holdup and are now evaluating the measurements.

The measurement technique uses a collimated NaI detector coupled to a small, multichannel analyzer system. The instrumentation is mobile but not portable. We made as many measurements as practicable on all accessible sides of the glovebox. These measurements were later averaged, resulting in ~50 measurements of 100-s duration per glovebox.

On the whole, the gloveboxes were relatively clean. Despite low plant background, the counting rates were low, making statistical evaluation of the data difficult.

2. Filter Holdup Measurements (T. K. Li)

We have installed, calibrated, and begun operating a filter holdup monitor in the pellet area of the advanced carbide fuels laboratory to measure plutonium accumulation rates in the glovebox exhaust filter. Figure 66 shows the monitor package being installed next to the cylindrical column that houses the exhaust filter. The filter is shown in Fig. 67. The monitor, a well-shielded 50.8 x 50.8-cm NaI gamma detector, is on the top of the glovebox and 18 cm from the filter. The collimation was designed so that the detector views the whole filter. Absorbers of lead (~1.5 mm) and cadmium (~0.8 mm) are placed in front of the detector to attenuate the intense low-energy gamma rays and x rays.

A block diagram of the monitoring system electronics is shown in Fig. 68. An automatic gain control amplifier minimizes shift from counting rate variation and photomultiplier-tube aging. Three single-channel analyzers were used for setting the thresholds of the plutonium gamma-ray peak and adjacent background regions. The single-channel analyzer outputs, including output from the automatic gain control amplifier, are fed to counters and a printing unit. The printer is a digital printing accessory and program-control center for the data acquisition system. The data from each counter and

Fig. 66.
Filter holdup monitoring system being installed on top of a glovebox.

Fig. 67.
Filter for the holdup monitoring system.

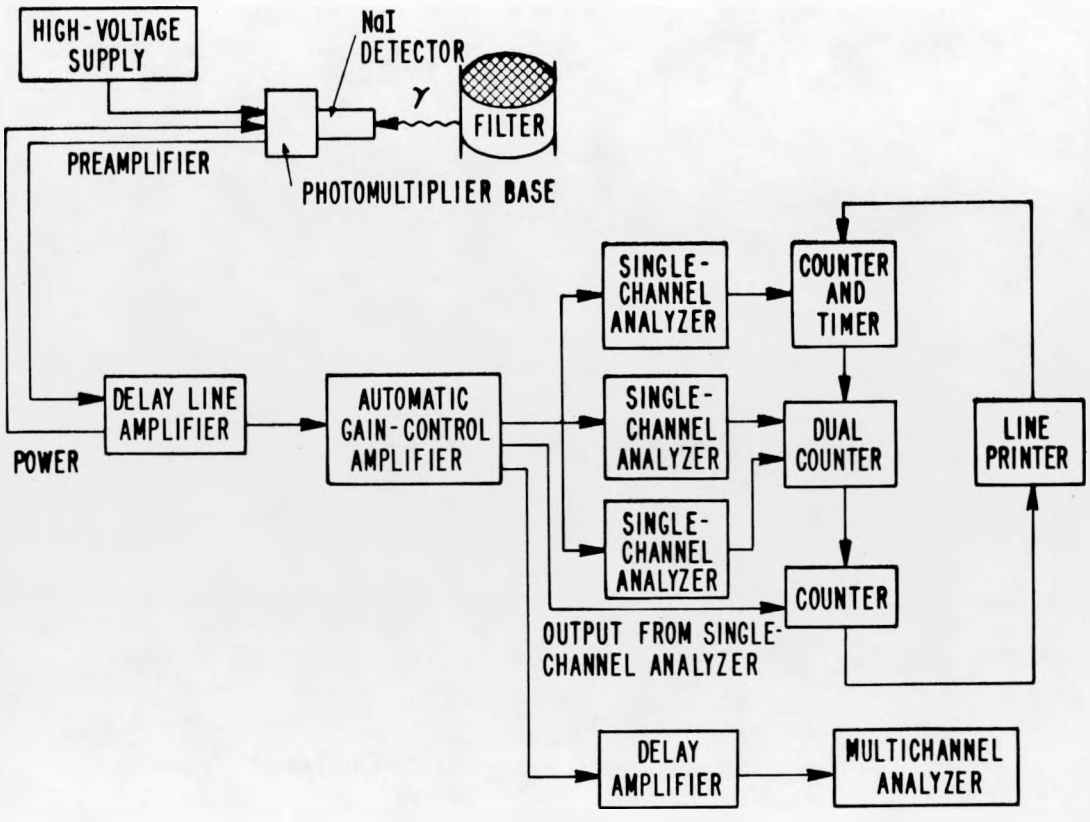

Fig. 68.
Block diagram of monitoring system electronics.

timer in the system will be printed in sequence with automatic paper-tape advance for each new data word. When the printer is preset on recycle mode, the system will reset automatically at the completion of the printing cycle and will start a new counting cycle for collecting new data. A 1-μCi ^{137}Cs source, which emits the 661-keV gamma ray, is used for the system deadtime and pileup correction as well as for stabilization.

The monitoring system was calibrated with three plutonium filter standards. CMB-1 prepared the standards by adding PuO_2 to glovebox filters of the same type actually used on the glovebox exhaust system. They sprinkled 1, 5, and 20 g of plutonium (reactor grade) in the form of PuO_2 powder evenly over the surface of each filter while drawing air through the filter to simulate the type of loading that might be observed on glovebox exhaust filters. The individual filters were then sealed with aluminium-foil covers and packaged in double plastic bags and in plastic boxes of 6.3-cm wall thickness. The calibration system setup (Fig. 69), including detector shielding and collimation, was the same as the in-plant setup at the new facility. Because all plutonium processed in this glovebox will be aged and of similar isotopic composition, we set the window width at 320 to 470 keV for the ^{239}Pu and ^{241}Pu gamma-ray complex. We used a 10-g plutonium standard source for the transmission correction.

No plutonium build-up has been detected in the filter we are monitoring. The only plutonium handling in the glovebox to date has been the sampling of a few containers of PuO_2, from which no more than microgram quantities of PuO_2 are expected to accumulate on the filter. Processing will soon begin in that glovebox, and then data can be collected from the holdup in the glovebox exhaust filter.

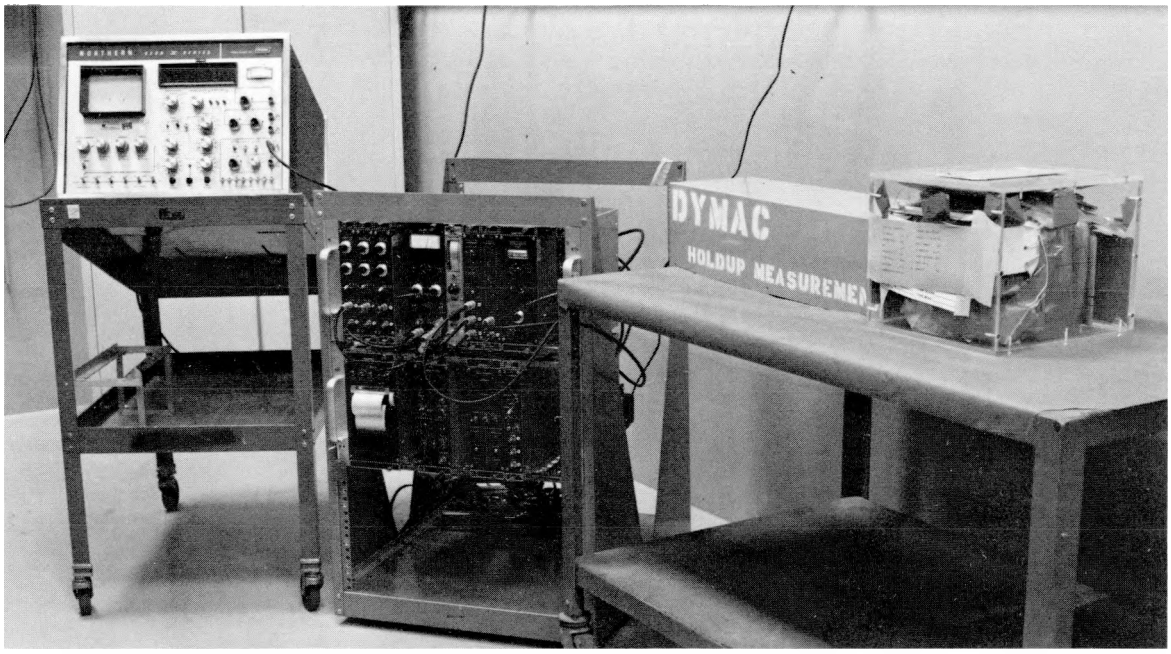

Fig. 69.
Calibration setup for filter holdup measurement.

II. ACCOUNTABILITY

A. Accountability Functions (W. R. Severe)

Unit-process accounting is a fundamental concept of the DYMAC accountability system. In its application at the new facility, the input, output, recycle, and scrap material for each batch are measured as the batch moves through predefined locations (unit-process areas). Material balances are drawn for each batch on the basis of these measured values. Zero material balances are not expected because complete cleanout of the unit-process area is not required. Indeed, there are three major components of the batch balance value: (1) unmeasured waste material, (2) holdup, and (3) measurement uncertainties.

Specific limits are set for both the individual batch balance and cumulative sum of these values for each unit-process area. Because the facility is new and little operating experience has been obtained, limits currently are based on the combined judgment of safeguards and production personnel. As we gain experience with operation of the unit-process areas, more exact limits can be set.

DYMAC produces a cumulative sum chart of batch balances for each unit-process area as a visual aid for evaluating batch balances. Figure 70 is an example of such a chart drawn for the casting unit process in the 300 Wing. The cumulative sum of batch balances is plotted against batch number; 1σ error bars for the cumulative sum are included. The balance for successive batches increases or decreases, depending on what the transaction added to it or took away from it. The transaction for batch 31 transferred 10 g from the balance to waste, resulting in a negative cumulative balance. The batch 32 transaction was a transfer from the machining area batch balance to the casting area balance and was attributable to a change in unit-process definition. Balance increase is the expected behavior until the unit process is cleaned out. Other fluctuations in the chart can be ascribed to instrument error, scrap or waste transfer out of the unit process, or cleanout. The error bars on each batch are cumulative and continue to grow regardless of the balance, except in the case of correlated errors. Currently, the cumulative sum charts are prepared

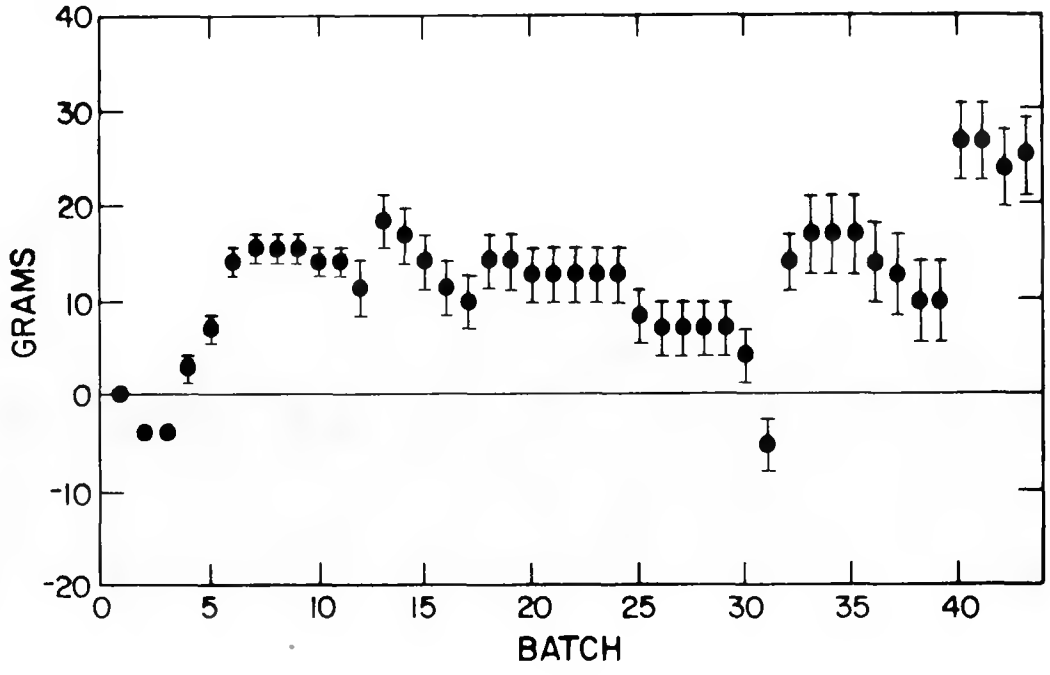

Fig. 70.
Example of a cumulative sum chart of batch balances.

by hand, but the methodology could be computer-implemented.

Because the new facility is not yet fully operational, it is too early to evaluate the effectiveness of this charting technique for all areas of the facility. However, for unit-process areas in current operation, the cumulative sum chart is a valuable indicator of performance for a unit-process area. Evaluation of current unit-process accountability techniques still continues, along with a program for test and evalution of advanced methods such as V-masks and Kalman filters.

B. Count Room at Plutonium Processing Facility (W. R. Severe)

The count room at the new facility became fully operational on July 24 with the installation of the last instrument to be transferred from DP Site. Count room equipment now consists of an SGS, a 2-ℓ TNC, a 114-ℓ TNC, and a 15-kg digital balance. Plans call for the addition of an FNC and a calorimeter.

Count room operations require a CMB-11 staff of three persons: two operators and a supervisor, all trained in the operation of NDA equipment. The primary function of the count room is the measurement of material (suited to NDA techniques), to determine shipper-receiver differences, and to verify, before shipment, both product and waste materials that have been measured elsewhere in the facility.

The measurement control program in effect for the count room is identical to that used in the DP-Site counting room.[80] At present, neither the measurement control program nor the measuring devices interact directly with the DYMAC computer. Ultimately, the count room instruments and the measurement control program will interact directly with the computer, eliminating the need for hand calculations and interim administrative procedures.

C. Nuclear Materials Officer (C. Nordeen)

During the May-August period, the NMO staff was responsible for ~55% of the transaction traffic

in the facility. The staff receives daily shipments from DP Site. As of August 31, approximately 2750 items were in the vault. As expected, the number of transactions between the vault and the operational areas of the plant increased as new sections began processing. The NMO staff makes all external shipments from the new facility to other LASL locations, as well as to non-LASL sites.

As of August 31, the new facility contained 3036 line items, each of which has an entry in the DYMAC data base. Transactions during the 4-month period averaged 2220 per month, with a total of 9317 for the reporting period.

III. COMPUTER PROGRAMMING

(J. Hagen, R. F. Ford,* J. W. Wooten,* E. P. Elkins,* W. H. Dorin,* and T. A. Cordova)**

During the May-August period DYSS operated for 85 processing days and handled 9317 transactions. As in the previous 4 months, no SNM discrepancies appeared between the DYSS inventory and that of the laboratory-wide accountability system.

A. Additional Hardware

A backup Eclipse C330 computer was ordered, with a scheduled delivery date of October 16, 1978. Seven additional CRT terminals and three additional printers were requested to accommodate supervisors' needs for on-line reports. Also on order is a larger capacity, faster responding Zebra disk to decrease system response time and provide storage space for CMB-11's increasing programmatic needs.

B. Transactions

1. Metal Fabrication (300 Wing)

The material management room and the remainder of the 300 Wing were combined into a single account, which was a major accountability change. The concept of the management room as a control area for all material entering or leaving a multi-account wing was dropped in this case because, unlike the other wings in the new facility, the 300 Wing has only one account, under a single custodian. The management room is now a receipt area within that account. This change eased the transaction-making procedure for moving material into and out of the wing.

The metal fabrication transaction sequence was altered to reflect a modification in the SEND/RECEIVE transaction concept. Previously the transaction was entered in two steps, SEND and RECEIVE, when an item moved in the conveyor system. Now, when the item remains within a single account, such as the 300 Wing, the user can advise the system of its relocation in tandem by making a processing transaction, such as COMBINE OR DIVIDE (option 4 in Fig. 71). Thus, as long as the item remains within a single account it does not apear in the in-transit file, even if it moves by conveyor.

The transaction menu (Fig. 71) was reordered, and some options were modified to be repetitive. For example, option 10, COMBINE TURNINGS, is used to collect metal turnings from different items in the machining area into a single item. The operator enters the material type and item identification of the new combined item only once, and the computer leads the operator through several transactions using that item. Time is saved because the operator no longer must return to the start-up menu each time, but may delay other users from gaining access to the system.

Transactions that affect the MIP (material in process) for a receipt area now direct the operator to enter remarks about the transfer. Suitable remarks might be SHIPPER/RECEIVER DIFFERENCE, HOLDUP, or GLOVEBOX CLEANED OUT. When a new on-line report is implemented, 300 Wing

*Group E-5.
**Group AADP-2.

```
<<< SELECT OPTION >>>
  1...RECEIVE FROM OUTSIDE 300 WING
  2...RECEIVE FROM WITHIN 300 WING
  3...SEND TO ANOTHER PERSON WITHIN 300 WING (W/ MEASUREMENT)
  4...COMBINE OR DIVIDE
  5...ADD ALLOY
  6...MEASURE SCRAP IN TNC
  7...WEIGH OXIDIZED SKULL
  8...VERIFY WEIGHT
  9...CHANGE LOCATION, SHELF, ITEM DES, OR REMARKS
 10...COMBINE TURNINGS
 11...SEND TO ISOPRESS ROOM
 12...RECEIVE IN ISOPRESS ROOM
 13...SEND FROM ISOPRESS ROOM TO 300 AREA
```

Fig. 71.
Metal fabrication transactions.

```
<<< SELECT OPTION >>>
  1...RECEIVE FROM MANAGEMENT ROOM
  2...TAKE SAMPLE
  3...RETURN FEED STOCK TO MANAGEMENT ROOM
  4...SEND SAMPLE OR SCRAP
  5...PREPARE NEW BATCH
  6...ADD CARBON AND UO2 TO PUO2 BATCH
  7...TRANSFER TO NEW RECEIPT AREA (WITH MEASUREMENT)
  8...REDESCRIBE BATCH
  9...WEIGH SCRAP
 10...REDUCE BRIQUETTES
 11...BLEND LOT
 12...WEIGH AND SEND FINISHED PELLETS
```

Fig. 72.
Advanced carbide fuels transactions.

supervisors can determine from these remarks what contributed to the MIP.

2. Advanced Carbide Fuels (100 Wing)

Transactions in the advanced carbide fuels process were simplified as a result of the modified SEND/RECEIVE concept. The transaction sequence is shown in Fig. 72.

3. Material Management Room (400 Wing)

The transaction sequence (Fig. 73) for the material management room of the newly operating 400 Wing is similar to that of the other management rooms. It has SEND and RECEIVE options for material leaving and entering the wing. The RECEIVE option asks for a seal number verification and allows the operator to break the seal. The SEND OUTSIDE 400 AREA option allows the operator to enter a new seal number. The management room also has SEND and RECEIVE options for moving material to and from 400 Wing processes. All transactions are repetitive; an operator can make a series of SENDS without returning to the start-up menu each time.

4. Oxide-Reduction Process (400 Wing)

The oxide-reduction section, which reduces plutonium oxide to metal, was the first to begin processing in the 400 Wing. Its transaction sequence appears in Fig. 74. The section receives oxide items and blends them (options 1 and 2). DYSS computes the blended item's new enrichment and isotopic content. The blended oxide is then weighed and moved to a furnace for calcining. WEIGH BLENDED ITEM AND TRANSFER TO CALCINING (option 3) is actually two transactions. The first uses the blended item's weight to compute the difference

```
<<< SELECT OPTION >>>
     1...RECEIVE FROM OUTSIDE 400 AREA
     2...SEND TO 400 AREA PROCESSING
     3...RECEIVE FROM 400 AREA PROCESSING
     4...SEND OUTSIDE 400 AREA
```

Fig. 73.
400 Wing material management transactions.

```
<<< SELECT OPTION >>>
     1...RECEIVE
     2...BLEND
     3...WEIGH BLENDED ITEM AND TRANSFER TO CALCINING
     4...TRANSFER CALCINED ITEM TO G411 AND REWEIGH
     5...TAKE SAMPLE
     6...DIVIDE AND TRANSFER TO OXIDE REDUCTION
     7...WEIGH PRODUCT METAL
     8...MEASURE CRUCIBLE OR SALT (WITH TNC)
     9...SEND
    10...TRANSFER STIRRER AND THERMOCOUPLE (MIPE-) TO PICKLING BOX
    11...MEASURE FILTRATE VOLUME AND TAKE SAMPLE
    12...MEASURE SOLID RESIDUE WITH TNC
```

Fig. 74.
Oxide reduction transactions.

between incoming and outgoing oxide for the blending receipt area, called MIPBB. The second transaction records the move to the calcining location. The item is calcined to remove impurities, then returned to the blending area and reweighed. The SNM value will not have changed but the bulk weight will be different. Option 4 documents the bulk weight change. The item is sampled (transaction 5) and sent away for analysis (option 9).

The calcined item is divided into appropriately sized batches, which are then transferred to an oxide-reduction glovebox (option 6). Each batch will generate product metal, which is weighed and recorded on DYSS (option 7). Crucible and salt waste products are measured with a TNC and recorded on DYSS (option 8). The difference between inputs and outputs in the oxide-reduction box is assumed to be material on the stirrer and thermocouple used in the process; this difference is called MIPXX (MIP for oxide-reduction, box XX). Several differences, or batch balances, may accumulate on one stirrer before it is pickled to remove the accumulation. CMB-1 samples and analyzes the resulting filtrate. The analysis is used to determine the SNM value of the filtrate (option 11). The resulting residue is measured in the TNC and entered into DYSS (option 12). SNM remaining on the books is considered MIP for the pickling process.

5. Electrorefining Process (400 Wing)

The electrorefining process removes impurities from plutonium metal to produce ultra-high-purity metal for weapons fabrication and is done in the same 400 Wing glovebox line as the oxide reduction. The electrorefining transaction menu appears in Fig. 75. A plutonium ingot is combined with NaCl-KCl and PuF_4 (option 2) and melted in an electrorefining furnace. Direct current passing through the cell dissolves plutonium at the anode and plates it at the cathode.

The process produces a ring of plutonium metal, with salt and crucible residues. The product is weighed and recorded (option 3). The anode heel generated in the process is plutonium metal containing much of the original impurities. Both the heel and the cathode used in the run are weighed (options 5 and 4). Salt and crucible residues are recorded (transaction 6). A single cathode may be used for several batches and then be transferred to the pickling glovebox (option 8). The pickling process and

```
<<< SELECT OPTION >>>
  1...RECEIVE
  2...WEIGH PUF AND COMBINE WITH CAST PART
  3...WEIGH PRODUCT RING
  4...WEIGH CATHODE
  5...WEIGH ANODE HEEL
  6...TRANSFER REMAINDER TO CRUCIBLE ID
  7...SEND
  8...TRANSFER CATHODE TO PICKLING BOX
  9...MEASURE FILTRATE VOLUME AND TAKE SAMPLE
 10...MEASURE SOLID RESIDUE WITH TNC
```

Fig. 75.
Electrorefining transactions.

transactions are similar to those in the oxide-reduction process.

6. NMO Transactions

As mentioned in Part 3, Sec. I-A, a TI 810 printer was installed at the vault to print labels for incoming items (see Fig. 77). It is used in conjunction with the vault options RECEIVE INTERNAL ITEM and GENERAL EDIT OF NON-NAME ATTRIBUTES, Fig. 76. After entering transaction information and approving it, the operator can decide whether to print a label. Because DYSS generates the label from information in the data base, the information on the label is current and free of transcription errors.

An option was added to the transactions for shipping/receiving account 770: RECEIVE EXTERNAL SHIPMENT (SIMILAR ATTRIBUTES) (see Fig. 78). Frequently, many items in a shipment will have similar attributes—the same project, receipt area, special designator, item description, and material type. The new option retains these attributes from one transaction to the next, so the operator need only answer the attribute questions once.

A temporary transaction option was added when personnel on the NMO staff discovered incorrect bulk values for >200 items received into the vault. They had entered the shipper's bulk values, which included the container weight. The new transaction subtracted the average container weight from current inventory bulk weight. The option was repetitive, allowing the NMO staff to enter the corrections quickly. The option was removed after the 200 items had been corrected.

7. Count Room Transactions

A minimal set of transactions was designed for the count room (see Fig. 79). None of the transactions involves on-line measurements. To access the count room options, the user selects from the list of 400 Wing processes, shown in Fig. 80, and then must enter the associated password.

C. System Refinements and Enhancements

During the May-August period the DYMAC programmers attended Data General courses in Los Angeles and Boston to learn more about INFOS, the data base management system, and enable them to make the system more responsive to the user. The memory was restructured to include more files in core and the data base was reordered to reduce inaccessible space and increase search speed. The operating system also was altered to handle more search requests. These changes made it possible to shorten the time for start-up and backup procedures at the beginning and end of the processing day.

The most obvious change to the user is a bell that rings when too many characters are entered. The keyboard input routine was modified so that a bell rings instead of an error message being displayed in the midst of the user's input.

As a major change, portions of the applications program were rewritten (using load-on-call virtual overlays) to free memory space. The additional space will increase the potential number of simultaneous users. It will also increase the potential number of software line handlers from 64 to 128.

```
<<< SELECT OPTION >>>
     1...RECEIVE INTERNAL ITEM
     2...SEND INTERNAL ITEM
     3...GENERAL EDIT OF NON-NAME ATTRIBUTES
     4...TRANSFER TO ACCOUNT 777 (NO PHYSICAL MOVE)
```

Fig. 76.
Vault transactions.

```
ITEM ID:  RAG  2951          TRANS. NO.:009D2

SS VALUE:        34.  G      DATE:      7/17/78

ACCOUNT NO.:     756         REC. AREA:      76

MT:               52         % ENRICH:    6.00

PROJECT NO.:     314         ITEM DESCRIP: D40

TYPE MEAS.:      G00         SEAL NO.:  005403

LOCATION:        V07         SHELF:          4A

REMARKS:GROSS WT. 2146.4 G
```

Fig. 77.
Sample label from label printer.

```
<<< SELECT OPTION >>>
     1...RECEIVE EXTERNAL SHIPMENT INTO TA-55
     2...SEND EXTERNAL SHIPMENT FROM TA-55
     3...ITEMIZE A SHIPMENT
     4...COMBINE ITEMS TO FORM A SHIPMENT
     5...CLEAR NON-PHYSICAL ITEM TO ACCOUNT 777
     6...SEND ITEM WITHIN TA-55
     7...RECEIVE ITEM FROM WITHIN TA-55
     8...EXTERNAL TRANSACTION CORRECTION
     9...RECEIVE EXTERNAL SHIPMENT (SIMILAR ATTRIBUTES)
```

Fig. 78.
Transactions for NMO shipping/receiving account.

Changes to the operating system increased the number of system buffers available to handle INFOS calls made by the application programs. Because more information can now be stored in main memory, data base searches are faster and more efficient.

Periodically, old transaction records must be purged from the data base to make room for more recent ones. In August all transaction records from January 1978 (when DYMAC first began operation) through June were deleted. Henceforth, transaction records will be retained in the on-line system for only 15 to 45 days. A tape archive of all purged transactions is maintained, from which off-line printouts are available. Transactions made during one month are purged at the middle of the following month: the first purge of January-June transactions required 6 h to delete ~6000 records. Subsequent system refinements, such as data base restructuring and an increase in system buffers, significantly reduced this

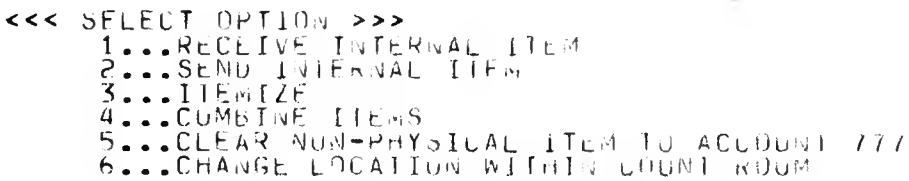

Fig. 79.
Count room transactions.

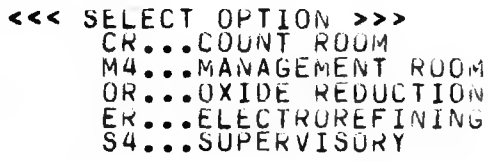

Fig. 80.
400 Wing processes.

time; a recent purge required 40 min to delete 4000 transaction records.

An off-line utility program was written to restructure the random data base organization on the disk. The utility program first writes each data base record to magnetic tape, creates skeleton data base files, then reads the magnetic tape and reinserts each record into the clean data base. Deletion of the January-June transactions left much free space scattered throughout the data base. The utility program compacted the data base, leaving no wasted, inaccessible space.

Another result of the data base reorganization is that similar records are written in a nearly contiguous fashion on the disk. This improves on-line search and update times as well as shortening off-line utility execution times.

A reorganization of data base files into separate logical partitions on the disk enabled us to shorten the time needed for daily tape backup of the data base. A faster tape-dumping routine allows us to write a backup tape in 6 to 7 min instead of the 20 it used to take. The time has been shortened similarly for loading the data base at the start of the processing day.

D. Measurement Control Program

By the end of August, 23 balances and 2 TNCs were part of the DYMAC system and under control of the measurement control program; 13 of the balances are on-line. Seventy-two standard weights are coded into the program for calibrating the balances. Each balance requires two standards (high and low range) for calibration. The program requires a daily accuracy check and a weekly precision check.

Instrument records, which the measurement control program maintains, were reduced in size and rearranged, giving a gain in disk space and on-line stack space. The option to report the calibration history on-line was deleted; instead, DYSS provides an off-line printout of calibration history.

Maintenance functions are semi-automated for on-line and off-line balances. The technician supplies the balance number, the standard identification, and the instrument reading. DYMAC compares the known standard weight in the data base with the instrument's output to determine whether the instrument is functioning within tolerances. Adjustments have been made to two maintenance utility programs. The off-line utility that edits the instrument file has been changed to delete instrument operating information that occurred before a given date. It prints out the information before deleting it from the on-line reporting system. A new option to the off-line utility that edits the standards file allows the user to print out a list of all the standards in the measurement control program. At present, the DYMAC system has implemented six maintenance functions:

- Instrument status,
- Calibration check,
- Accuracy check,
- Precision check,
- Display accuracy data,
- Display precision data.

E. On-Line Inquiries and Off-Line Reports

DYMAC's capability to provide information was enhanced. Available on-line inquiries and off-line reports are:

- Inventory by location,
- Inventory by account,
- Internal activity of item,
- External activity of item,
- Item status,
- Items in transit,
- Transaction lookup.

On-line inquiries are available in real time at video and hard-copy terminals. Off-line reports are available on an overnight basis and are printed on the line printer. These off-line reports can include information for all accounts in the facility or for accounts selected by the requestor:

- Current inventory, sorted by account, material type, and item ID;
- Activity, internal and external, sorted by account, material type, and item ID;
- Current inventory, sorted by account, material type, and item description;
- Transaction activity during last time period, sorted by account, material type, and item description;
- Inventory totals, sorted by account and material type;
- Inventory by location, sorted by location, shelf, and material type;
- Special designator report, sorted by special designator;
- General ledger, run on a daily basis.

The format of the off-line reports was changed to reflect the custodian's holdings in terms of accountable and nonaccountable holdings. The requestor can elect to store an off-line report on magnetic tape for reprinting.

We have improved on-line inquiries by adding a hard-copy capability. Supervisory terminals were installed in the facility and cold support building. A supervisor can obtain immediate printouts of information, such as an account inventory, without having to wait for an off-line report. He requests the report on his video terminal but, instead of having it appear on his display screen, he directs the system to print it on his hard-copy terminal.

The data base files on disk have greatly increased since the system began operation. To keep the disk files to a manageable size, we sorted all the transactions made from January through June, printed them as a report, then deleted them from the data base but created a backup archive tape. Thus, the several on-line reports dealing with activity will be reports on relatively current activity only. Users wishing to refer to transactions made before the last cutoff date must use printouts instead of making on-line inquiries at their terminals.

IV. OTHER FUNCTIONS

A. Training (D. C. Amsden)

During May-August, 47 DYMAC users from the metallography, advanced carbide fuels, and recovery processes attended 3-h introductory lecture sessions about the system. The first lecture was videotaped in early June and the second, in late August, was conducted from the videotapes. The viewers could ask questions after watching each tape. DYMAC personnel taught first-session participants how to use the video terminals by having them work with their own specialized transactions. August trainees will complete their terminal training in late September or early October.

The videotaped lectures will be useful in training CMB-11 personnel as they begin working in the new facility and in training new hires. (A DYMAC training person must show the tapes and answer questions.)

B. Technology Transfer

During May-August, DYMAC personnel met with 60 visitors, including 18 visitors from United Kingdom, Japan, the Republic of China, Belgium, and West Germany. Visitors from the US included representatives from private nuclear industry, the national laboratories, Congress, universities, and government agencies. Topics discussed were security at the new facility, DYMAC activities, diversion-path analysis, NDA instrumentation, and general safeguards considerations. Many of the visits involved a tour of the new facility and comprehensive briefings on the DYMAC program or an aspect of the program of special interest.

PART 4

INTEGRATED SAFEGUARDS SYSTEMS AND TECHNOLOGY TRANSFER

GROUP Q-4

R. J. Dietz, Group Leader

J. P. Shipley, Alternate Group Leader

A major effort of Group Q-4 is to establish design and performance requirements for cost-effective, integrated safeguards systems for typical nuclear fuel cycle facilities and to assess the impact of those requirements on process selection and plant design and operating criteria. Functions of the facilities include uranium enrichment, spent-fuel reprocessing, plutonium nitrate-to-oxide conversion, plutonium recycle-fuel fabrication, scrap recovery, and waste handling and disposal. Results of these studies provide working guides and performance criteria for materials control and accountability systems that can be integrated with physical protection and process control systems in conventional, as well as alternative, fuel cycle facilities.

By maintaining a high level of participation in measurement, analytical, and systems technologies through interactions with R&D organizations, industry, and government agencies, Q-4 staff members coordinate and disseminate safeguards technology throughout the national and international nuclear communities. By virtue of its overall cognizance of safeguards technology and needs, Q-4 also continues to provide technical information and assessments of both domestic and foreign fuel cycle facilities to DOE on a high-priority, as-needed basis.

During the past 4 months, Q-4 effort was divided between two line items: Safeguards Concept Definition for Fuel Cycle Facilities and Technology Transfer and Support to DOE/OSS, their subcontractors, the safeguards industry, and other interested government agencies.

In addition to program status reports, Q-4 efforts usually are reported in journals, papers, consultations, briefings, and topical reports at the conclusion of specific tasks. Publications issued during this report period are listed at the end of this status report.

I. SAFEGUARDS CONCEPT DEFINITION FOR FUEL CYCLE FACILITIES

The safeguards concept definition study, "Coordinated Safeguards for Materials Management in a Nitrate-to-Oxide Conversion Facility," is available.[81] The report is the third in a series that will treat each of the major processes characteristic of a complete fuel cycle. The mixed-oxide fuel fabrication and reprocessing facilities were addressed in LA-6536 (Ref. 32) and LA-6881 (Ref. 33), respectively.

Safeguards for enrichment plants continue to play an important part in the overall DOE/OSS program, and the Union Carbide Corp., Nuclear Division, has been assigned the management role for this effort. First priority is being given to development of a perimeter safeguards system for the GCEP at Portsmouth, Ohio. The current study will provide technical support for the decision on whether to offer the GCEP to the IAEA for international safeguards. Efforts of Q-4 in this area have consisted primarily of gathering the available facility and process design information necessary to evaluate proposed safeguards strategies.

The apparent advantages of LIS (laser isotope separation) for uranium enrichment make the safeguarding of facilities incorporating this technology a major international concern. The Arms

Control and Disarmament Agency has asked Q-4 to develop and evaluate safeguards strategies for commercial-scale enrichment facilities based on three LIS methods (atomic, molecular, and plasma), with particular emphasis on the goals and constraints of international safegurds as practiced by IAEA. The study will be based on reference facility designs being prepared as part of the NASAP (Non-Proliferation Alternative Systems Assessment Program). Q-4 is generating the process and facility design information required for the study.

II. SAFEGUARDS CONCEPTS FOR ALTERNATIVE FUEL CYCLE FACILITIES

In addition to the NASAP-related effort, Q-4 is supporting the DOE/NPD (Nuclear Power Development) Division's AFCT (Alternate Fuel Cycle Technology) programs, which are administered by the Savannah River Operations Office with the technical guidance of SRL.

The first alternative, investigated as a follow-on to the conversion process reported in LA-7011, is the coconversion of coprocessed, mixed uranium-plutonium-nitrate solutions via the General Electric COPRECAL process. A draft report, "Coordinated Safeguards for Materials Management in a Uranium-Plutonium Nitrate-to-Oxide Coconversion Facility," is nearly complete. It reports the first in a series of conceptual designs of advanced materials management systems for safeguarding SNM in alternative fuel cycle facilities. As in the previous studies, the conceptual design is based on measurement and control technology that has been demonstrated or that can be reasonably projected for the early 1980s.

Modeling and simulation of the COPRECAL process and the materials measurement and accounting system have been completed. The computer code COPSIM simulates normal process operation; the code COPMEAS simulates the materials accounting measurements that could be made on the results of COPSIM. Diversion sensitivities of several materials accounting strategies are being determined with the decision-analysis code DECANAL.

Work on safeguards concepts for reprocessing thorium-uranium fuels has continued in support of the TFTC (Thorium Fuel Cycle Technology) program sponsored by DOE/NPD. An overview of the process is given in Ref. 1; more detail is contained in LA-7411-MS, "Preliminary Concepts: Coordinated Safeguards for Materials Management in a Thorium-Uranium Fuel Reprocessing Plant."[34]

An associated report, "A Critical Review of Analytical Techniques for Safeguarding the Thorium-Uranium Fuel Cycle," has been published as LA-7372. These two reports complement each other and provide a framework for addressing safeguards-related process and measurement problems of the thorium fuel cycle.

The reports identify preliminary concepts for coordinated materials management in a generic thorium-uranium LWR fuels reprocessing plant. The reference facility recovers thorium and uranium from first-generation (denatured ^{235}U) startup fuels, first-recycle and equilibrium (denatured ^{233}U) thorium-uranium LWR fuels, and recovers the plutonium generated in the ^{238}U denaturant as well.

Conventional analytical methods applicable to the determination of thorium, uranium, and plutonium in reprocessing feed, product, and waste streams are reviewed. Separations methods of interest are discussed and recommendations are made concerning the applicability of various techniques to reprocessing samples. The process flow sheets for the reference facility were modified from conventional Purex, Thorex, and HTGR (High Temperature Gas-Cooled Reactor) reprocessing technology and may differ in detail from those finally adopted by the TFCT program.

Originally, thorium-uranium reactor designs relied on initial core loadings of high-enriched ^{235}U. Recycle cores would contain either ^{233}U produced from the thorium in the initial core or mixtures of ^{235}U and ^{233}U. Because both uranium isotopes are usable in nuclear weapons, diluting them with non-fissile ^{238}U to concentrations where they are no longer useful for weapons (12% for ^{233}U and 20% for ^{235}U) is probable. Consequences of this dilution are a loss in economic and neutronic efficiency and production of

significant quantities of weapons-usable plutonium that would not normally be produced in high-enriched thorium-uranium reactors. The ^{239}Pu, formed by parasitic neutron capture by the ^{238}U, is about one-third of that produced in an LWR operated on the plutonium-uranium cycle.

Although several alternate modes of operation are discussed in the draft report, safeguarding the reference facility is complicated by the need to maintain four component streams: (1) corecovery of ^{235}U from initial core loadings and ^{233}U generated from thorium; (2) thorium; (3) plutonium; and (4) fission products and other wastes. Thus, the facility combines features from two chemical separation plants, one based on the Purex process and the other on the Thorex process.

Because such a facility has never been demonstrated, the study relies heavily on extrapolations from extensive experience with plutonium-uranium reprocessing facilities and to a lesser extent from HTGR studies. The process and safeguards analogies for the thorium-uranium cycle are weakest in the areas of dissolving the refractory thorium-oxide fuels, disposing of the plutonium produced in the denatured fuels, and resolving problems from the greater induced radioactivity of the thorium recycle fuels. This hostile radiation environment will degrade most measurements.

Analytical capabilities for a thorium-uranium fuel reprocessing plant include precise measurements of both uranium and plutonium. The ^{233}U (and ^{235}U for first-generation reactor fuel) must be measured with the same care as plutonium. For fuels diluted with ^{238}U, the weapons-grade plutonium that is produced must also be measured accurately.

The high radiation fields in the samples will pose analytical problems from sample heat, radiolytic decomposition of reagents, polymerization, and radioactive sample decay, particularly at the dissolver end of the streams where high beta-gamma fluxes are present and at the product end where high alpha-radiation levels characterize the concentrated product solutions. The situation is further complicated by the high gamma-radiation levels from decay daughters in the case of ^{233}U and from reprocessed thorium. Reagent stability must also be considered in all analytical methods that are applied in high radiation fields. Isotopic decay results in plutonium loss in storage tanks and formation of impurities that may affect analytical results. Polymeric plutonium formed during reprocessing operations behaves erratically in analytical schemes. Problems in sampling and sample storage associated with high gamma fluxes will persist through the thorium and uranium storage areas for Thorex reprocessing.

Most analytical methods for thorium and uranium are based on the natural elements and, for plutonium, on the weapons-grade material. Their applicablity to reprocessed materials must be determined without significant loss of precision and accuracy under the radiation and remote operating constraints imposed by the thorium-uranium fuel cycle.

Further studies of thorium-uranium processes for the HTGR fuel cycle have been initiated with General Atomic Co., who will provide LASL with the design details of their proposed Youngsville, South Carolina, HTGR fuel fabrication plant. The Youngsville plant eventually will become the baseline facility for a conceptual safeguards systems design similar to that for mixed-oxide fuel fabrication.[82]

This activity will indirectly support Q-4's participation in the FRAD (Fuels Refabrication and Development) program, administered by Battelle-Pacific Northwest Laboratories for DOE/NPD. The FRAD program is to ensure the availability of fuel fabrication technology for both the AFCT and TFCT programs. Q-4 provided safeguards consultation and review in planning the FRAD program and will probably participate in subsequent safeguards activities.

III. INTERNATIONAL SAFEGUARDS

In support of IAEA we are tasked to: (1) define the materials accounting data required for safeguarding modern fuel cycle facilities; (2) review dynamic materials control concepts for IAEA personnel; and (3) develop techniques for materials control in critical assembly facilities. Q-4 also provides international safeguards concept development support to the DOE/OSS Safeguards Advisory Core Group and to the INFCE (International Fuel Cycle Evaluation) program.

Work continues on the development of materials accountability concepts for international safeguards in critical facilities.[15,35] "Concepts for Inventory Verification in Critical Facilities," will be issued as LA-7315 (Ref. 36), and supersedes LA-7028-MS (Ref. 35).

As a result of recommendations in the report, a program was initiated with Argonne National Laboratory to evaluate the use of reactivity measurements and supporting reactor-parameter measurements for *in situ* verification of critical assembly inventories. The program includes a series of calculations to determine the sensitivity of the techniques to various diversion threats, including the possibility of covertly making reactivity-compensating changes in the reactor core loading. A series of confirmatory experiments at Argonne's ZPPR (Zero Power Plutonium Reactor) facility will be made in FY-1979 under LASL sponsorship.

Several operational test and evaluation activities were recommended to DOE/OSS with regard to proposed inventory verification measurements and procedures for critical facilities.[37] These activities include evaluating reactivity, autoradiography, and NDA measurement techniques and proposed sampling procedures for reactor inventory verification.

A joint SLA/LASL report on critical facility safeguards is being prepared. A draft of the Q-4 contribution on inventory verification was transmitted to SLA.

Extensive support to the INFCE program has been provided. Safeguards sections were drafted for INFCE Working Groups Four and Five on LWR fuel reprocessing and fast breeder reactors, respectively. Q-4 also consulted on and reviewed other safeguards submittals to these working groups. Two meetings of the INFCE Safeguards Crosscut Group were attended in Washington. Much Q-4 effort has involved explaining the realities and potentialities of international safeguards and nuclear proliferation.

Toward this end, we initiated a study of international safeguards for an LWR fuel reprocessing plant. The baseline facility for the study will combine a reprocessing facility, based on the Allied-General Nuclear Services plant,[33] and a plutonium nitrate-to-oxide conversion facility, based on the SRL design studied in Ref. 31. The project will be pursued jointly by LASL and SLA; Q-4 will work on the materials accounting aspects and SLA will investigate the containment/surveillance problem. A joint draft report, "Preliminary Concepts: International Safeguards for a LWR Fuel Reprocessing Plant," will be issued on October 1, 1978. Its purpose is to define the problem in terms of diversion threats and types of countermeasures and to discuss the technical approach to the study. The result of the project will be a conceptual safeguards system incorporating ideas on both materials accounting and containment/surveillance and will include options for levels of effectiveness and systems tradeoffs.

Support for the Tokai Advanced Safeguards Technology Exercise, Task T-F, on dynamic materials accounting system began. Effort thus far has focused on providing Japanese representatives from the Tokai works and the Japan Atomic Energy Research Institute with information on the possible application of dynamic materials accounting to the fuel reprocessing plant at Tokai. Further systems support probably will be required soon.

IV. DEVELOPMENT OF SAFEGUARDS DESIGN AND EVALUATION METHODOLOGY

Development of systematic, efficient, and objective analysis methods for evaluating safeguards systems and the data they produce continues as a major effort. A novel and promising approach is to apply decision analysis techniques to assessing the diversion significance of materials accounting data.

Recent results of this approach are outlined in two papers, "Decision Analysis for Dynamic Accounting of Nuclear Material,"[38] presented at the May 1978 Am. Nucl. Soc. Topical Meeting, and "Efficient Analysis of Materials Accounting Data," presented at the June 1978 Annual INMM meeting.[39] Two sessions on decision analysis were presented at the Safeguards Systems Training Course at LASL on May 9-11, 1978. One session was a demonstration of the effectiveness of decision analysis in which course participants identified low-level diversion from a sequence of test results. The demonstration also provided experimental confirmation of the utility and correctness of our approach to diversion detection.

The diversion sensitivity of the decision tests is commonly evaluated by one or more reasonable diversion strategies, such as uniform diversion or single theft. Q-4 is developing a method of finding the optimal diversion strategy among all possible strategies for each decision test. This will allow independent determination of the worst-case detection probability of the particular diversion strategy.

Assessment of system security and reliability is important in the design and evaluation of safeguards systems. The extent to which data and computer security measures must be incorporated into the overall system depends strongly upon the specific installation, its fuel cycle type, and the threat environment. A series of simulation modules for security characteristics has been developed and a decision framework has been established to analyze the risk in terms of the value of what is to be protected.

The computer security simulation code SECSIM provides a set of methodologies and measurement criteria for determining security effectiveness.[40] Graded technological, administrative, and physical security strategies are modeled and evaluated repetitively as parameters are adjusted. This allows convergence toward a systems architecture having an acceptable level of security.

Current technology enables a full-time NRC or IAEA inspector with data processing and audit experience to insure that information-system security controls are in effect. He also can detect confidently (typically within one shift) any violations of safeguards controls at national and subnational levels.

The complex, distributed-access nature of computer-based information systems requires the development of new time-domain methods for predicting reliability. The broader concept of operational reliability includes timeliness of the system in responding to demands. Contributions to unreliability go beyond hardware failures into the areas of software failures, operator error, noise induction, source power outages, air-conditioning down-time, and machine loading. In multitransactions within the computer, a successfully completed task is one in which the system (including the operator) has functioned correctly within the time limit specified as the task allowable characteristic time. If the task cannot be completed during the first try, repeated attempts are permissible. Parameters pertaining to multitransaction computer systems performance are incorporated into a series of second-generation reliability simulation codes designated COMPTRANSIM, which model the system's architecture and predict operating effectiveness.

Systems reliability simulation and analysis were applied to the primary functions of the DYMAC system installed in TA-55. Individual module characteristics and systems architecture parameters were incorporated into the COMPTRANSIM code to predict system performance in an interactive, time-sequence-transaction mode of operation. Estimates of the expected yearly availability and down-time were tabulated for each module and for the number of incomplete or invalid computer transactions after the first, second, and third attempts. The process was repeated for maintenance functions and general data base inquiries. Results were related to actual operating environments through the use of

effective systems reliability parameters such as availability, mean time between failures, and mean time to repair, as contrasted to strictly hardware-reliability calculations provided by the manufacturer.

In complex digital systems, partial failures still allow for continued operation with some systems performance degradation. The hardware-reliability factors have been incorporated into the component reliability data used in the simulations. The results of the study show that DYMAC at TA-55 is a relatively robust system from a reliability viewpoint in that it is capable of carrying out its current and projected functional tasks. The expectation of repeating transactions more than three times is negligibly small. Systems upgrades to increase the transaction rates, to perform additional statistical and diagnostic computation, and to provide even greater reliability are available, when and if justified.

Estimation of in-process inventory in the various types of contactors required for fuel reprocessing was identified in Ref. 33 as a problem worthy of further effort. Q-4 is pursuing solutions to that problem with the help of the Fuel Operations Division of General Atomic and a multidisciplinary team at Clemson University. General Atomic will use their demonstration lines to investigate pulsed-column contactors for thorium-uranium fuel reprocessing. Clemson will work on mixer-settler contactors for uranium-plutonium fuel reprocessing with the experimental support of SRL. Clemson also will provide theoretical support for both programs. Results of these efforts will form the technical base for contactor model development by Q-4.

One of the most difficult, long-standing problems of safeguards system design is the coherent integration of materials accounting and physical protection (or international safeguards containment/surveillance) concepts. Fundamental to the solution is the ability to assess quantitatively the effectiveness of the integrated systems. Q-4 drafted some preliminary thoughts on the subject and briefly discussed them with SLA. The ideas will be developed more fully, with the joint LASL/SLA study on international safeguards for LWR reprocessing (see Part 4, Sec. III) serving as the vehicle for concept extension and verification.

V. TECHNICAL SUPPORT AND TECHNOLOGY TRANSFER

At the request of DOE/OSS, we reviewed several analyses of historical inventory-difference data from the NUMEC and NFS facilities for 1960-1976, as well as related material including reports of contemporary on-site inspections and surveys at NUMEC. A brief commentary was prepared describing and interpreting this material in layman's language for DOE/OSS. The materials accounting data showed no evidence of the need for procedural changes at NUMEC and NFS and no evidence of misappropriation of a sizable quantity of uranium from either facility.

Group Q-4 personnel participated in briefings, visits, and consultations with people from DOE/OSS, Brookhaven-ISPO, SLA, ORNL, Westinghouse, General Atomic, General Electric, SRL, SRP, DOE/NPD, NRC, Argonne National Laboratory, Battelle-PNL, the National Security Agency, ACDA, and IAEA, as well as with people from Japan, United Kingdom, West Germany, and the Republic of China. Q-4 also presented 10 sessions for the Safeguards Systems Training Course held at LASL on May 9-11, 1978.

As part of Q-4's responsibility for promoting safeguards developments, and as a result of information learned at the Am. Nucl. Soc. Williamsburg meeting, two proposals were written for funding of instrumentation research and development. One is to Mound Laboratory for an x-ray spectrograph to analyze dissolver solutions. The other is to Battelle-PNL for a passive-neutron leached-hull monitor.

Q-4 personnel participated in writing ANSI standards, and a member has been appointed chairman of INMM-N15 Standards Subcommittee INMM-9, Nondestructive Assay, which has the following six ANSI standards in various stages of completion: Material Categorization, Container Standardization, Physical Standards, Measurement Control, NDA Techniques, and Automation of NDA Data Acquisition.

In support of the LASL director's office, Q-4, with the assistance of Q-1, Q-2, and Q-3, prepared a 1-h

talk entitled "LASL and International Safeguards," outlining the history of international safeguards and giving an overview of LASL's participation in the relevant programs.

PUBLICATIONS

J. R. Phillips, S. T. Hsue, C. R. Hatcher, K. Kaieda, and E. G. Medina, "Nondestructive Assay of Highly Enriched Spent Fuel," Inst. Nucl. Mater. Manage. 19th Annual Meeting, Cincinnati, Ohio, June 27-29, 1978.

M. P. Baker, H. O. Menlove, and M. L. Evans, "Photoneutron-Based Assay Method for Direct Uranium Ore-Grade Determination," Am. Nucl. Soc. Annual Meeting, June 1978.

M. S. Krick, M. P. Baker, "Photoneutron Sources for the Assay of Fissile Material," Am. Nucl. Soc. Annual Meeting, San Diego, California, June 1978.

T. W. Crane, S. Bourret, G. W. Eccleston, L. G. Speir, "Enriched Uranium Measurements at the Savannah River Plant Fuel Fabrication Facility," Inst. Nucl. Mater. Manage. 19th Annual Meeting, Cincinnati, Ohio, June 27-29, 1978.

T. W. Crane, S. Bourret, G. W. Eccleston, H. O. Menlove, L. G. Speir (LASL); R. V. Studley (SRP), "Design of a ^{252}Cf Neutron Assay System for Evaluation at the Savannah River Plant Fuel Fabrication Facility," Am. Nucl. Soc. Topical Meeting, Williamsburg, Virginia, May 15-17, 1978.

M. Jain, D. A. Close, M. L. Evans, "Gamma-Ray Spectral Calculations for Uranium Well-Logging," Am. Nucl. Soc. Annual Meeting, San Diego, California, June 1978.

J. R. Phillips, B. K. Barnes, T. R. Bement, "Correlation of $^{134}Cs/^{137}Cs$ Ratios to Fast Reactor Burnup," to be published.

W. E. Kunz, C. N. Henry, and D. R. Millegan, "Effects of Background Gamma Radiation on the Sensitivity of Hand-Held Special Nuclear Materials Monitors," J. Inst. Nucl. Mater. Manage. **VII**, No. 2, 36-41 (Summer 1978).

R. H. Augustson, "Dynamic Materials Control Development and Demonstration Program," Proc. INMM Meeting, Cincinnati, Ohio, June 1978.

N. Baron, "A More Accurate Thermal Neutron Coincidence Counting Technique," Proc. ASM/ASTM/ASNT/ANS Int. Conf. Nondestructive Evaluation in the Nucl. Industry, Salt Lake City, February 13-15, 1978.

E. A. Hakkila, D. D. Cobb, R. J. Dietz, J. P. Shipley, and D. B. Smith, "Requirements for Near-Real-Time Accounting of Strategic Nuclear Materials in Nuclear Fuel Reprocessing," invited paper presented at Am. Nucl. Soc. Topical Meeting, Williamsburg, Virginia, May 15-17, 1978.

J. P. Shipley, "Decision Analysis for Dynamic Accounting of Nuclear Material," paper presented at Am. Nucl. Soc. Topical Meeting, Williamsburg Virginia, May 15-17, 1978.

D. D. Cobb, J. L. Sapir, E. A. Kern, and R. J. Dietz, "Concepts for Inventory Verification in Critical Facilities," Los Alamos Scientific Laboratory report LA-7315 (December 1978).

J. P. Shipley, "Structure of Safeguards Systems," Los Alamos Scientific Laboratory report LA-7337-MS (June 1978).

D. D. Cobb, J. L. Sapir, and E. A. Kern, "Inventory Verification in Large Critical Facilities," paper presented at Inst. Nucl. Mater. Manage. 19th Annual Meeting, Cincinnati, Ohio, June 27-29, 1978.

H. A. Dayem, D. D. Cobb, R. J. Dietz, E. A. Hakkila, J. P. Shipley, and D. B. Smith, "Coordinated Safeguards for Materials Management in Chemical Separations, Conversion, and Fuel Fabrication Facilities," paper presented at Inst. Nucl. Mater. Manage. 19th Annual Meeting, Cincinnati, Ohio, June 27-29, 1978.

J. P. Shipley, "Efficient Analysis of Materials Accounting Data," paper presented at Inst. Nucl. Mater. Manage. 19th Annual Meeting, Cincinnati, Ohio, June 27-29, 1978.

E. A. Hakkila, J. W. Barnes, H. A. Dayem, R. J. Dietz, and J. P. Shipley, "Preliminary Concepts: Coordinated Safeguards for Materials Management in a Thorium-Uranium Fuel Reprocessing Plant," Los Alamos Scientific Laboratory report LA-7411-MS (in preparation).

E. P. Schelonka, "Event and Effectiveness Models for Simulating Computer Security," accepted for presentation at IEEE Computer Conf. COMPCON FALL, Washington, D. C., September 7-8, 1978.

H. A. Dayem, D. D. Cobb, R. J. Dietz, E. A. Hakkila, J. P. Shipley, and D. B. Smith, "Dynamic Materials Accounting in Chemical Separation, Conversion, and Fuel Fabrication Facilities," accepted for presentation at IAEA Symp. Nucl. Mater. Safeguards, Vienna, Austria, October 2-6, 1978.

E. P. Schelonka, "SECSIM-A Computer Security Simulation Code," accepted for presentation at Am. Nucl. Soc. Winter Meeting, Washington, D. C., November 12-17, 1978.

D. D. Cobb, J. L. Sapir, and E. A. Kern, "Safeguarding Fast Critical Facilities," accepted for presentation at Am. Nucl. Soc. Winter Meeting, Washington, D. C., November 12-17, 1978.

E. P. Schelonka, "RELSIM-A Systems Reliability Simulation Code," accepted for presentation at 1979 Annual Reliability and Maintainability Symp., Washington, D.C., January 16, 1979.

REFERENCES

1. "Nuclear Safeguards Research and Development Program Status Report," Los Alamos Scientific Laboratory report LA-7439-PR (December 1978).

2. G. Charpak, "Evolution of the Automatic Spark Chambers," Ann. Rev. Nucl. Sci. **20**, 195-254 (1970).

3. D. M. Lee, S. E. Sobottka, and H. A. Thiessen, "A Bifilar Helical Multiwire Proportional Chamber for Position Sensitive Detection of Minimum Ionizing Particles," Nucl. Instrum. Methods **104**, 179-188 (1972); "Proportional Chambers with Monofilar Helical Cathodes for High Spatial Resolution," Nucl. Instrum. Methods **109**, 421-428 (1973); "Delay-Line Readout of Anode Planes in Proportional Chambers," Nucl. Instrum. Methods **120**, 153-156 (1974).

4. *Reactor Shielding Design Manual*, T. Rockwell, Ed. (Van Nostrand, New York, 1956), pp. 348, 360-364.

5. H. Goldstein and J. E. Wilkins, Jr., "Calculations of the Penetrations of Gamma Rays. Final Report," US Atomic Energy Commission report NYO-3075 (June 30, 1954).

6. J. H. Smith and M. L. Storm, "Generalized Off-Axis Distributions from Disk Sources of Radiation," J. Appl. Phys. **25**, 519-527 (1954).

7. G. R. Keepin, Ed., "Nuclear Analysis Research and Development Program Status Report, January-April 1974," Los Alamos Scientific Laboratory report LA-5675-PR (August 1974).

8. G. R. Keepin, "Nuclear Safeguards Research and Development Program Status Report, May-August 1971," Los Alamos Scientific Laboratory report LA-4794-MS (October 1971).

9. J. L. Sapir, Comp., "Nuclear Safeguards Research and Development Program Status Report, May-August 1977," Los Alamos Scientific Laboratory report LA-7030-PR (March 1978).

10. J. D. Brandenberger, "Calculation of (α,n) Neutron Production in Materials Containing Alpha Emitters," Los Alamos Scientific Laboratory Q-1 internal memorandum (May 23, 1978).

11. H. Liskien and A. Paulsen, "Neutron Yields of Light Elements under Alpha-Bombardment," Atomkernenergie **30**, 59-61 (1977).

12. J. K. Bair and H. M. Butler, "Neutron Yield from a Small High Purity $^{238}PuO_2$ Source," Nucl. Technol. **19**, 202-203 (1973); M. E. Anderson, and R. A. Neff, "Neutron Emission Rates and Energy Spectra of Two ^{238}Pu Power Sources," Nucl. Appl. Technol. **7**, 62-66 (1969); L. J. Mullins, "Preparation and Evaluation of Medical-Grade Plutonium-238 Fuels, July 1, 1967-June 30, 1971," Los Alamos Scientific Laboratory report LA-4940 (October 1972), p. 34.

13. J. K. Bair, private communication, 1976.

14. N. Ensslin, private communication, 1978.

15. J. L. Sapir, Comp., "Nuclear Safeguards Research and Development Program Status Report, September-December 1977," Los Alamos Scientific Laboratory report LA-7211-PR (August 1978).

16. M. M. Minor, private communication.

17. J. L. Sapir, Comp., "Nuclear Safeguards Research and Development Program Status Report, January-April 1977," Los Alamos Scientific Laboratory report LA-6849-PR (August 1977).

18. J. E. Foley (IAEA), unpublished data, 1978.

19. H. O. Menlove, R. A. Forster, J. L. Parker, and D. B. Smith, "^{252}Cf Assay System for FBR Fuel Pins: Description and Operating Procedures Manual," Los Alamos Scientific Laboratory report LA-5071-M (October 1972).

20. M. M. Stephens, J. E. Swansen, and L. V. East, "Shift Register Neutron Coincidence Module," Los Alamos Scientific Laboratory report LA-6121-MS (December 1975).

21. T. E. Sampson, "Neutron Yields from Uranium Isotopes in Uranium Hexafluoride," Nucl. Sci. Eng. **54**, 470-474 (1974).

22. W. H. Chambers, H. F. Atwater, P. E. Fehlau, R. D. Hastings, C. N. Henry, W. E. Kunz, T. E. Sampson, T. H. Whittlesey, and G. M. Worth, "Portal Monitor for Diversion Safeguards," Los Alamos Scientific Laboratory report LA-5681 (December 1974).

23. T. E. Sampson, Proc. ERDA Symp. X- and Gamma-Ray Sources and Applications, Ann Arbor, Michigan, May 19-21, 1976," US ERDA report CONF-760539 (1976), pp. 100-103.

24. H. F. Atwater, "Effect of Moderator Thickness on Neutron Detector Efficiency in R-2 Van," Los Alamos Scientific Laboratory internal memorandum.

25. R. E. Bobbett, A. R. Koelle, J. A. Landt, and S. W. Depp, "Passive Electronic Identification and Temperature Monitoring System," Los Alamos Scientific Laboratory report LA-6812-PR (July 1977).

26. W. E. Kunz, W. H. Chambers, C. N. Henry, S. W. France, D. R. Millegan, R. D. Hastings, and G. M. Worth, "Hand-Held Personnel and Vehicle Monitors," Los Alamos Scientific Laboratory report LA-6359 (September 1976).

27. W. E. Kunz, "Portable Monitor for Special Nuclear Materials," Los Alamos Scientific

Laboratory Mini-Review LASL-77-18 (September 1977).

28. W. E. Kunz, C. N. Henry, and D. R. Millegan, Nucl. Mater. Manage. **VII**, Summer 1978, pp. 36-41.

29. E. J. Dowdy, C. Henry, A. A. Robba, and J. C. Pratt, "New Neutron Correlation Measurement Techniques for Special Nuclear Material Assay and Accountability," paper prepared for presentation at IAEA Symp. Nucl. Mater. Safeguards, Vienna, Austria, October 2-6, 1978.

30. J. L. Sapir, Comp., "Nuclear Safeguards Research Program Status Report, September-December 1976," Los Alamos Scientific Laboratory report LA-6788-PR (June 1977), p. 39.

31. H. A. Dayem, D. D. Cobb, R. J. Dietz, E. A. Hakkila, E. A. Kern, J. P. Shipley, D. B. Smith, and D. F. Bowersox, "Coordinated Safeguards for Materials Management in a Nitrate-to-Oxide Conversion Facility," Los Alamos Scientific Laboratory report LA-7011 (April 1978).

32. J. P. Shipley, D. D. Cobb, R. J. Dietz, M. L. Evans, E. P. Schelonka, D. B. Smith, and R. B. Walton, "Coordinated Safeguards for Materials Management in a Mixed-Oxide Fuel Facility," Los Alamos Scientific Laboratory report LA-6536 (February 1977).

33. E. A. Hakkila, D. D. Cobb, H. A. Dayem, R. J. Dietz, E. A. Kern, E. P. Schelonka, J. P. Shipley, D. B. Smith, R. H. Augustson, and J. W. Barnes, "Coordinated Safeguards for Materials Management in a Fuel Reprocessing Plant," Los Alamos Scientific Laboratory report LA-6881 (September 1977).

34. E. A. Hakkila, J. W. Barnes, H. A. Dayem, R. J. Dietz, and J. P. Shipley, "Preliminary Concepts: Coordinated Safeguards for Materials Management in a Thorium-Uranium Fuel Reprocessing Plant," Los Alamos Scientific Laboratory report LA-7411-MS (October 1978).

35. D. D. Cobb and J. L. Sapir, "Preliminary Concepts for Materials Measurement and Accounting in Critical Facilities," Los Alamos Scientific Laboratory report LA-7028-MS (January 1978).

36. D. D. Cobb, J. L. Sapir, E. A. Kern, and R. J. Dietz, "Concepts for Inventory Verification in Critical Facilities," Los Alamos Scientific Laboratory report LA-7315 (December 1978).

37. D. D. Cobb, "LASL Contribution—Critical Facilities Safeguards Test and Evaluation: Materials Measurements and Procedures," Group Q-4 internal document, July 31, 1978.

38. J. P. Shipley, "Decision Analysis for Dynamic Accounting of Nuclear Material," presented at Am. Nucl. Soc. Topical Meeting, Williamsburg, Virginia, May 15-17, 1978.

39. J. P. Shipley, "Efficient Analysis of Materials Accounting Data," presented at Inst. Nucl. Mater. Manage. 19th Annual Meeting, Cincinnati, Ohio, June 27-29, 1978.

40. E. P. Schelonka, "Event and Effectiveness Models for Simulating Computer Security," accepted for presentation at IEEE Computer Conf. COMPCON FALL, Washington, D.C., September 7-8, 1978.

GLOSSARY

ACDA	Arms Control and Disarmament Agency
AFCT	Alternative Fuel Cycle Technology
AGNS	Allied-General Nuclear Services
BRP	Big Rock Point
BWR	boiling water reactor
CTF	Centrifuge Test Facility
DYMAC	dynamic materials control
DYSS	DYMAC software system
FAST	Fluorinel and Storage Facility
FCA	Fast Critical Assembly
FFTF	Fast Flux Test Facility
FNC	fast-neutron coincidence counter
FRAD	Fuels Refabrication and Development
GAT	Goodyear Atomic Corp.
GCEP	Gas Centrifuge Enrichment Plant
HEDL	Hanford Engineering Development Laboratory
HLNCC	high-level neutron coincidence counter
HTGR	high-temperature gas-cooled reactor
IAEA	International Atomic Energy Agency
INFCE	International Fuel Cycle Evaluation
LIS	laser isotope separation
LWR	light water reactor
NASAP	Non-Proliferation Alternative Systems Assessment Program
NDA	nondestructive assay
NEST	Nuclear Emergency Search Team
ORNL	Oak Ridge National Laboratory
PWR	pressurized water reactor
SAI	solution assay instrument
SGS	segmented gamma scanner
SLA	Sandia Laboratories, Albuquerque
SNM	special nuclear material
SRL	Savannah River Laboratory
SRP	Savannah River Plant
SSAS	small sample assay station
TC-XRF	transmission-corrected x-ray fluorescence
TFCT	Thorium Fuel Cycle Technology
THENCS	thermal-neutron coincidence counting system
TNC	thermal-neutron coincidence counter
ZPPR	Zero Power Plutonium Reactor

☆ U.S. Government Printing Office: 1979 — 677-013/72

Printed in the United States of America. Available from
National Technical Information Service
US Department of Commerce
5285 Port Royal Road
Springfield, VA 22161

Microfiche $3.00

001-025	4.00	126-150	7.25	251-275	10.75	376-400	13.00	501-525	15.25
026-050	4.50	151-175	8.00	276-300	11.00	401-425	13.25	526-550	15.50
051-075	5.25	176-200	9.00	301-325	11.75	426-450	14.00	551-575	16.25
076-100	6.00	201-225	9.25	326-350	12.00	451-475	14.50	576-600	16.50
101-125	6.50	226-250	9.50	351-375	12.50	476-500	15.00	601-up	

Note: Add $2.50 for each additional 100-page increment from 601 pages up.